Universidade de Aveiro
Departamento de Electrónica, Telecomunicações e Informática
2019

Rui Pedro
Castro Fernandes

Medium Access Control for Large Scale LoRa Networks

Acesso ao Meio em Redes LoRa de Grande Escala

Rui Pedro
Castro Fernandes

Medium Access Control for Large Scale LoRa Networks

Acesso ao Meio em Redes LoRa de Grande Escala

Dissertação apresentada à Universidade de Aveiro para cumprimento dos requisitos necessários à obtenção do grau de Mestre em Engenharia Eletrónica e Telecomunicações, realizada sob a orientação científica do Doutor Nuno Miguel Abreu Luís, Investigador Auxiliar do Instituto de Telecomunicações e co-orientação científica da Doutora Susana Isabel Barreto de Miranda Sargento, Professora Catedrática do Departamento de Electrónica, Telecomunicações e Informática da Universidade de Aveiro

o júri / the jury

presidente / president

Professor Doutor Arnaldo Silva Rodrigues de Oliveira
Professor Auxiliar do Departamento de Electrónica, Telecomunicações e Informática da Universidade de Aveiro

vogais / examiners committee

Professor Doutor Rodolfo Alexandre Duarte Oliveira
Professor Auxiliar com Agregação do Departamento de Engenharia Electrotécnica e de Computadores da Faculdade de Ciências e Tecnologia da Universidade Nova de Lisboa (Arguente)

Doutor Nuno Miguel Abreu Luís
Investigador Auxiliar do Instituto de Telecomunicações (Orientador)

agradecimentos / acknowledgements

Começo por agradecer às pessoas mais presentes na minha vida, e que tanto contribuíram para fazer de mim quem sou hoje. A conclusão deste ciclo é uma vitória tanto vossa como minha. Aos meus pais e irmã, Rui, Hermínia e Sofia, de quem apoio e carinho nunca me faltou, e à Reis, companheira de todos os bons momentos mas também das horas mais difíceis, tenho a agradecer especialmente pela enorme paciência que sempre tiveste, mesmo nos meus momentos de maior irracionalidade. És a melhor.

A todos os amigos que estiveram presentes neste período de 5 anos, tanto os de sempre como os adquiridos ao longo deste percurso, e que de alguma forma contribuíram para que estes anos fossem mais fáceis, ou pelo menos mais divertidos, um grande obrigado. Não teria sido a mesma coisa sem vocês.

Agradeço ao grupo de investigaçao do NAP, não só por estarem sempre dispostos a ajudar, mas também por criarem um excelente ambiente que ajudou imenso à realização deste trabalho.

Um agradecimento especial ao Professor Doutor Miguel Luís e ao Eng. Rui Oliveira, pelo seu enorme contributo e orientação dada na realização desta dissertação. Agradeço à Professora Doutora Susana Sargento por me ter guiado até este grupo e tema de dissertação, e pelo apoio providenciado de forma a que esta fosse concluída.

Agradeço ao Instituto de Telecomunicações e à Fundação Portuguesa para a Ciência e Tecnologia pelo suporte financeiro através de fundos nacionais e quando aplicável cofinanciado pelo FEDER, no âmbito do Acordo de Parceria PT2020 pelo projecto MobiWise através do programa Operacional Competitividade e Internacionalização (COMPETE 2020) do Portugal 2020 (POCI-01-0145-FEDER-016426).

Palavras-chave

LoRa, Low Power Wide Area Networks, Comunicações de Longo Alcance, Controle de Acesso ao Meio, Internet of Things

Resumo

A tecnologia *Long Range* (*LoRa*) tem vindo a ganhar bastante popularidade, tornando-se numa das tecnologias mais promissoras e frequentemente utilizadas entre as *Low Power Wide Area Networks* (*LPWANs*). Altamente compatível com aplicações da *Internet of Things* (*IoT*), LoRa permite comunicações de longo alcance, ainda que com baixas taxas de transmissão e restrições de *duty-cycle*.

O trabalho desenvolvido ao longo desta dissertação tem como alvo o acesso ao meio em redes *LoRa*, focando-se especialmente no seu desempenho em termos de entrega de dados em redes de larga escala. Para isto, são propostos: (1) um modelo probabilístico de colisões que estima a probabilidade de sucesso de duas ou mais transmissões simultâneas, com base numa avaliação exaustiva do efeito de captura da tecnologia *LoRa*; (2) uma adaptação ao protocolo de acesso ao meio *LoRaWAN*, através da inclusão de pacotes de controlo; e por fim, (3) um novo protocolo de acesso ao meio, denominado *LoRa Mode Adaptive Protocol* (*LoRa-MAP*), que permite manter a melhor ligação possível entre os dispositivos e o ponto de acesso ao variar os parâmetros de camada física do *LoRa*.

É realizada uma análise aos diferentes mecanismos de acesso ao meio, de forma a compreender como diferentes parâmetros e disposições de rede influenciam o processo de troca de informação. A avaliação realizada, que considera os resultados obtidos com a caracterização do efeito de captura, mostra que a solução proposta contribui para aumentar a escalabilidade das redes LoRa, tornando-a numa excelente candidata para ambientes IoT.

Keywords

LoRa, Low Power Wide Area Networks, Long Range Communications, Medium Access Control, Internet of Things

Abstract

LoRa technology has recently gained popularity, attesting itself as one of the most promising and widely adopted Low Power Wide Area Networks (LPWANs). Highly compatible with Internet of Things (IoT) applications and urban environments, this technology enables large range communications although with low data-rates and duty-cycle restrictions.

The work developed in this dissertation targets the medium access in LoRa, focusing on its performance in delivering data, especially in large-scale networks. To do so, it is proposed: (1) a probabilistic packet collision model that estimates the success delivery of two or more LoRa concurrent transmissions, based on an exhaustive evaluation of the packet capture effect; (2) an adaptation of LoRa's state of the art Medium Access Control (MAC) protocol, LoRaWAN, through the use of control packets; and lastly, (3) a new MAC protocol, denoted as LoRa Mode Adaptive Protocol (LoRa-MAP), that manages to maintain the best possible connection between end-nodes and the gateway by changing LoRa's physical layer parameters.

An analysis on different medium access schemes is conducted, aiming to perceive how different parameters and network layouts influence the information exchange process. The performed evaluations, that consider the results obtained from the real capture effect characterization, showed that the proposed MAC solution increases the LoRa network scalability, deeming it a great candidate for IoT environments.

Contents

Acronyms **xi**

1 Introduction **1**
1.1 Context and Motivation . . . 1
1.2 Objectives . . . 2
1.3 Contributions . . . 2
1.4 Document Organization . . . 3

2 State of the Art **5**
2.1 Low-Power Wide Area Networks . . . 5
2.1.1 Features . . . 7
2.1.2 Technologies . . . 7
2.1.2.1 Cellular-based LPWAN technologies . . . 8
2.1.2.2 Non cellular-based LPWAN technologies . . . 9
2.1.3 Long-Range (LoRa) . . . 11
2.1.3.1 Physical Layer . . . 11
2.1.3.2 MAC Layer - LoRaWAN Protocol . . . 14
2.2 Related Work . . . 16
2.2.1 LoRa Performance Studies . . . 16
2.2.2 MAC Protocols for LoRa . . . 18
2.3 Chapter Considerations . . . 20

3 Concurrent Transmissions in LoRa **21**
3.1 LoRa's Non-Destructive Property . . . 21
3.2 Characterizing Concurrent Transmissions . . . 22
3.2.1 Hardware Equipment . . . 22
3.2.2 Experimental Methodology . . . 24
3.2.3 Success Assessment of Concurrent Transmissions . . . 25
3.2.3.1 Two LoRa Concurrent Transmissions . . . 25
3.2.3.2 Three LoRa Concurrent Transmissions . . . 26
3.3 Probabilistic Model . . . 27
3.3.1 Probability of success with one interferer . . . 27
3.3.2 Probability of success with multiple interferers . . . 27
3.4 Chapter Considerations . . . 28

4 Medium Access Control in LoRa - The Use Of Control Packets **29**
4.1 The Importance of Control Packets . . . 29
4.1.1 Improving Network Throughput . . . 29

4.1.2 Increasing Network Fairness . . . 30
4.2 RTS-LoRa - Reservation based MAC protocol . . . 30
4.2.1 Overview . . . 30
4.2.2 Packet Structure . . . 32
4.2.2.1 RTS Message . . . 33
4.2.3 MAC Process . . . 33
4.3 Chapter Considerations . . . 35

5 Adaptive MAC Protocol for LoRa **37**
5.1 Protocol Description . . . 37
5.1.1 Motivations . . . 37
5.1.2 Characteristics . . . 39
5.2 Dynamic Medium Access . . . 40
5.2.1 Control Messages . . . 40
5.2.2 MAC Process . . . 42
5.2.2.1 Node side . . . 42
5.2.2.2 Gateway side . . . 44
5.3 Operation Mode Selection . . . 48
5.3.1 Ideal Mode of Operation . . . 49
5.3.1.1 Multi-mode connectivity tests . . . 49
5.3.2 Time allocation per Mode . . . 50
5.4 Medium Access Fairness . . . 52
5.5 Chapter Considerations . . . 52

6 Evaluation **55**
6.1 Simulation Environment . . . 55
6.2 LoRaWAN Single-Channel . . . 57
6.2.1 Network Capacity . . . 57
6.2.1.1 Different packet sizes and packet collision models . . . 57
6.2.1.2 The impact of different end-node distributions . . . 58
6.2.2 Channel Access Fairness . . . 58
6.3 RTS-LoRa vs LoRaWAN Single-Channel . . . 60
6.3.1 Network Capacity . . . 60
6.3.1.1 The impact of different packet sizes and packet collision models 60
6.3.1.2 The impact of different end-node distributions . . . 61
6.3.2 Channel Access Fairness . . . 62
6.4 LoRa Mode Adaptive Protocol . . . 62
6.4.1 The impact of different channel time distributions . . . 62
6.4.2 Calculating the duration of each mode . . . 67
6.4.2.1 Fairness Indicator . . . 68
6.4.2.2 Choosing the *best* combination . . . 68
6.4.2.3 Model validation . . . 69
6.5 Protocol Comparison . . . 73
6.6 Chapter Considerations . . . 77

7 Conclusions and Future Work **79**

Bibliography **81**

List of Figures

1.1 Internet of Things applications. 1

2.1 IoT requirements and challenges. 6
2.2 Growth in connected devices. 6
2.3 Required bandwidth vs range capacity of IoT technologies. 8
2.4 LoRa technology stack. 12
2.5 LoRa packet structure. 13
2.6 LoRa system architecture. 14

3.1 Example of a packet collision. 22
3.2 Hardware used. 23
3.3 Experimentation setup with one gateway and two end-nodes. 25

4.1 Summarized functioning of RTS-LoRa protocol. 31
4.2 Hidden terminals problem. 32
4.3 RTS message structure. 33
4.4 Packet time-on-air depending on payload size and operation mode. 34
4.5 Node backoff process after receiving a RTS message. 34
4.6 Medium access flow. 35

5.1 LoRa-MAP Operation. 39
5.2 Control Messages Structure. 41
5.3 Use of LoRa-MAP control messages. 42
5.4 Node backoff process. 43
5.5 Node medium access behaviour. 45
5.6 Node behaviour during backoff state. 46
5.7 Gateway medium access behaviour. 47
5.8 LoRa-MAP cycle. 51

6.1 Network Layout. 56
6.2 LoRaWAN capacity evaluation 1 57
6.3 LoRaWAN capacity evaluation 2 59
6.4 LoRaWAN fairness assessment 59
6.5 RTS-LoRa vs LoRaWAN: capacity evaluation 1 61
6.6 RTS-LoRa vs LoRaWAN: capacity evaluation 2 63
6.7 RTS-LoRa vs LoRaWAN: access fairness for different network layouts. 63
6.8 LoRa-MAP capacity evaluation 1. 64
6.9 LoRa-MAP access fairness evaluation. 64
6.10 LoRa-MAP performance evaluation 1. 66

6.11 LoRa-MAP performance evaluation 2. 66
6.12 LoRa-MAP performance evaluation 3. 67
6.13 Best *time_mid* for the several network scenarios. 70
6.14 Best *time_fast* for the several network scenarios. 70
6.15 Estimated ideal *time_mid* for non-evaluated scenarios (two different perspectives). 71
6.16 Estimated ideal *time_fast* for non-evaluated scenarios (two different perspectives). 71
6.17 LoRa-MAP, RTS-LoRa and LoRaWAN: network capacity analysis. 74
6.18 LoRa-MAP, RTS-LoRa, LoRaWAN: access fairness assessment. 75

List of Tables

2.1 LoRa compared to cellular-based LPWAN technologies 15
2.2 LPWAN technologies comparison 16

3.1 Raspberry Pi 3 Model B+ Specifications. 22
3.2 SX1272 Module Specifications. 23
3.3 SX1272 LoRa operation modes. 24
3.4 Relevant SX1272 functions. 24
3.5 PDR based on packets' strength, for two concurrent end-nodes. 26
3.6 PDR based on packets' strength, for three concurrent end-nodes. 26
3.7 Approximation of Packet Delivery Ratio for three concurrent end-nodes. . . . 28

4.1 LoRa Base Packet. 32

5.1 SX1272 module operation modes. 48
5.2 Time-on-Air and inherent duty-cycle restriction of each control message. . . . 49
5.3 Multi-mode connectivity results. 50
5.4 Adequate mode depending on the RSSI. 50
5.5 End-node list. 51

6.1 Range of RSSI values per group. 56
6.2 Fairness assessment example. 68
6.3 Scenario 1 network performance. 72
6.4 Scenario 2 network performance. 72
6.5 Scenario 3 network performance. 73
6.6 Average throughput per node in group 1. 75
6.7 Average throughput per node in group 2. 76
6.8 Average throughput per node in group 3. 76

List of Equations

2.1 Ratio between symbol rate and chirp rate in LoRa 12
2.2 LoRa useful bit rate 13
3.1 Packet Delivery Ratio in concurrent transmissions 28
4.1 Jain's Fairness Index 30
4.2 Backoff calculation in RTS-LoRa 34
5.1 Backoff calculation in MAP 44
5.2 Time on air depending on packet size in bytes for *standard* mode 48
5.3 Time on air depending on packet size in bytes for *mid-rate* mode 49
5.4 Time on air depending on packet size in bytes for *fast-rate* mode 49
5.5 Time in *standard* per cycle 52
5.6 Jain's Fairness Index adapted to LoRa-MAP 52
6.1 LoRa-MAP Fairness Indicator 68

Acronyms

3GPP 3rd Generation Partnership Project

ACK Acknowledgement

ADR Adaptive Data Rate

AES Advanced Encryption Standard

AFA Automatic Frequency Agility

BER Bit Error Rate

BLAST Bursty Light Asynchronous Stealth Transitive

BPSK Binary Phase Shift Keying

BW Bandwidth

CDMA Code Division Multiple Access

CF Carrier Frequency

CM Change Message

CR Coding Rate

CRC Cyclic Redundancy Check

CSMA Carrier Sense Multiple Access

CSMA/CA Carrier Sense Multiple Access with Collision Avoidance

CSS Chirp Spread Spectrum

CTS Clear to Send

dB decibel

dBm decibel miliwatt

DBPSK Differential Binary Phase Shift Keying

DL Downlink

DSSS Direct Sequence Spread Spectrum

FEC Forward Error Correction

FER Frame Error Ratio

FI Fairness Indicator

FSK Frequency Shifting Keying

GFDMA Generalized Frequency Division Multiple Access

GFSK Gaussian Frequency Shift Keying

GMSK Gaussian Minimum Shift Keying

GPS Global Positioning System

GSM Global System for Mobile Communications

GW Gateway

IEEE Institute of Electrical and Electronics Engineers

IM Intent Message

IoT Internet of Things

ISM Industrial, Scientific and Medical

JFI Jain's Fairness Index

LBT Listen Before Talk

LoRa Long Range

LoRa-MAP LoRa Mode Adaptive Protocol

LPWAN Low-Power Wide Area Network

LTE Long Term Evolution

LTE-M LTE for Machines

M2M Machine-to-Machine

MAC Medium Access Control

MIC Message Integrity Check

MoT MAC on Time

N/A Not Applicable

NB-IoT Narrow Band IoT

OFDMA Orthogonal Frequency Division Multiple Access

OQPSK Orthogonal Quadrature Phase Shift Keying

PER Packet Error Ratio

PDR Packet Delivery Ratio PHYPhysical

QPSK Quadrature Phase Shift Keying

RF Radio Frequency

RFID Radio Frequency Identifiers

RPMA Random Phase Multiple Access

RSSI Received Signal Strength Indicator

RTS Ready to Send / Request to Send

SC-FDMA Single Carrier Frequency Division Multiple Access

SF Spreading Factor

SIG Special Interest Group

SIR Signal-to-Interference Ratio

SNOW Sensor Network Over White Spaces

SNR Signal-to-Noise Ratio

ToA Time on Air

UL Uplink

UNB Ultra Narrow Band

WTS Wait to Send

WiFi Wireless Fidelity

WSNs Wireless Sensor Networks

Chapter 1

Introduction

1.1 Context and Motivation

The evolution and increasing integration of wireless communications in the everyday life of billions of people around the world has led to the emergence of the Internet of Things (IoT). This concept, formally proposed in 2005 [1], alludes to a network in which all objects can exchange information actively.

Since interaction between a large number of devices with different features is allowed, there is no shortage in applications for the Internet of Things (Figure 1.1). Whatever is the domain of interest, some stipulations are inevitable, regarding aspects like energy consumption and deployment/maintenance costs, especially given the massive and ever-increasing number of connected devices.

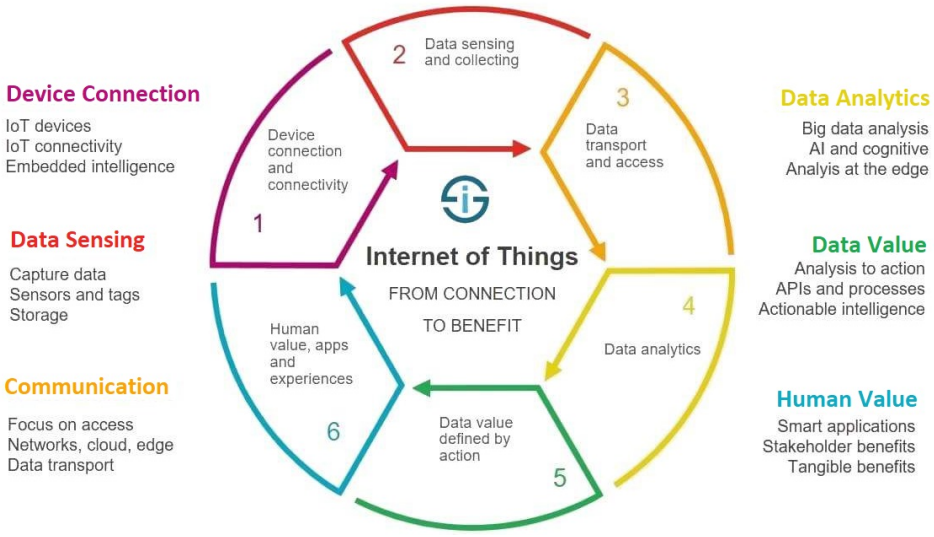

Figure 1.1: Internet of Things applications [2].

Low-Power Wide Area Networks (LPWANs) have recently emerged, as there is a need to develop and use technologies that can meet the IoT requirements. The LPWANs are a group of technologies that promise low cost and energy consumption while providing high coverage capabilities, making them excellent candidates for IoT applications.

One of the most promising and interesting LPWAN solution is LoRa (Long-Range), a versatile technology that can easily adapt to different environments and applications. Its proprietary modulation scheme, the use of unlicensed sub-GHz frequency bands and the non-destructive communication property are some of the features that make LoRa stand out from the remaining set of LPWAN technologies, while also making it a very attractive solution for IoT platforms.

The evaluation of LoRa technology, both by previous works and by new experiments, is of major importance for this dissertation, always with a critical look as to which impact LoRa's peculiar features would have in the information exchange in a real deployment. The main objective of this work is to, using LoRaWAN - the most adopted MAC protocol - as a starting point, study the enhancements that are needed to provide the use of LoRa in large scale environments, with high network capacity and fairness.

1.2 Objectives

The ultimate purpose of this dissertation, is to propose a MAC protocol for LoRa-based networks capable of overcoming some of the challenges that arise with the creation of IoT platforms. Having this goal in mind, the objectives of this dissertation are the following:

- Conduct a study on LPWAN technologies to comprehend the pros and cons of each of them, with special interest in LoRa;
- Validate and characterize the capture effect found in LoRa modulation, by forcing packet collisions under different circumstances;
- Perform LoRa quality tests using different combinations of physical layer parameters;
- Characterize a LoRaWAN, exploring the possibility of using control packets;
- Create a dynamic MAC protocol for LoRa networks capable of adapting to the network topology;
- Develop a parameterizable simulator to evaluate MAC schemes in large-scale LoRa networks.

1.3 Contributions

This dissertation has accomplished the following:

- Insights on how LoRa's capture effect behaves, by characterizing the probability of success of two or more concurrent LoRa transmissions;
- Characterization of the performance of a large scale single-channel LoRaWAN, by studying the impact of the characterization from the previous point;
- A study on the hypothesis of having control packets in the LoRaWAN medium access to improve the network performance;

- The creation of LoRa Mode Adaptive Protocol (LoRa-MAP), a new MAC protocol that resorts to changing LoRa's physical layer parameters cyclically in order to maintain the best possible connection between each device and the access point.

Part of the work presented in this dissertation, namely the study of LoRa's non-destructive communications presented in Chapter 3, resulted in a scientific paper already published in the Institute of Electrical and Electronics Engineers (IEEE) Communication Letters (IF 3.457)[3]. The work presented in Chapter 4 concerning the adaptation of LoRaWAN into a reservation-based protocol gave way to another scientific paper, currently under revision in IEEE Communication Letters. Finally, the adaptive MAC protocol presented in Chapter 5 will be submitted for peer evaluation in a scientific international journal.

1.4 Document Organization

The remaining document is organized as follows:

- **Chapter 2** presents the state of the art about LPWANs. At the end of this chapter some relevant works are explored, regarding the performance of LoRa technology in real deployments;
- **Chapter 3** characterizes the non-destructive property of LoRa through an exhaustive set of measurements;
- **Chapter 4** refers to LoRaWAN, exploring the possibility of having control messages in order to increase its performance;
- **Chapter 5** presents an adaptive MAC protocol for large-scale LoRa networks;
- **Chapter 6** evaluates the performance of the different protocols while considering networks with diverse characteristics;
- **Chapter 7** concludes the dissertation, enumerating directions for future work.

Chapter 2

State of the Art

The aim of this chapter is to provide the reader with a summary of some concepts that are crucial for the understanding of this dissertation, as well as some relevant existing work. Section 2.1 refers to the LPWANs, presenting a brief overview of the different technologies and common features, with a comparison between several LPWANs. Section 2.2 overviews the related work on LoRa performance studies and MAC protocols. At last, Section 2.3 summarizes the chapter contributions.

2.1 Low-Power Wide Area Networks

The term IoT refers to a network of interconnected things [4], and it extends to every object that can be connected to the Internet with the capability of transferring data using any kind of radio link [5]. With the goal of improving the efficiency of the human, natural and/or energy resource management, the applications of IoT [6] are numerous. Smart cities, home automation and environmental monitoring are some examples.

As there are countless possibilities for IoT applications, there are also different considerations and needs. In order to satisfy all requirements, a wide variety of technologies must be considered. Some traditional solutions are short-range wireless networks (e.g. Bluetooth, ZigBee, Z-Wave), wireless local area networks (e.g. WiFi), Radio Frequency Identifiers (RFID) and cellular networks (e.g.GSM), all capable of allowing the wireless connection of IoT devices in a network [7, 8, 9]. Most of these technologies are characterized by their short-range, and even though some of them recur to multi-hop techniques to enhance their range capabilities, this can quickly increase the network cost. In summary, they can usually suffer from having high cost, high energy consumption, high complexity and low reliability approaches.

For years there was the idea that, in order to provide ubiquitous coverage for IoT devices, the solution was to exploit the current and upcoming cellular technologies, but they were not conceived to provide machine-type services to a massive number of devices, which makes them unsuitable to fully support the envisioned IoT connectivity [7] (Figure 2.1).

Figure 2.2 depicts the foreseen number of connected devices over the years, dividing IoT devices into short-range (*i.e.* WiFi, Bluetooth) and wide-area segments (*i.e.* Cellular, LPWANs). The total number of connected devices has reached the 22 billion mark at the end of 2018 [10], and it is expected that by 2022 this figure is close to 30 billion, with Machine-to-Machine (M2M) connections contributing to more than half of this value [11, 12].

This is where LPWANs come in. To support the Internet of Things, recent developments

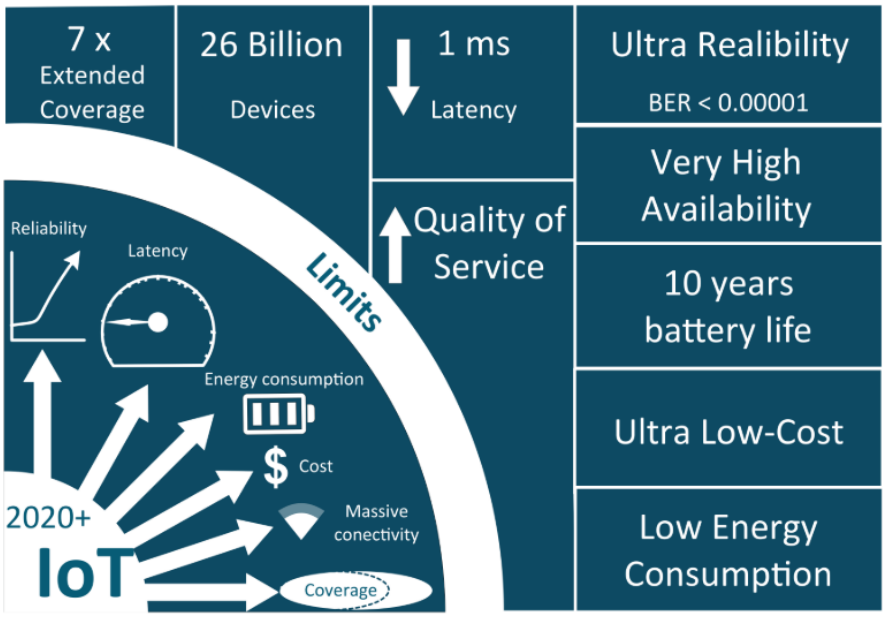

Figure 2.1: IoT requirements and challenges [6].

have given rise to LPWANs, an emerging network technology that successfully proposes wide area connectivity from a few to tens of kilometers for low data-rate, low power and low throughput applications. Similarly to cellular networks, LPWAN technologies typically have star network topologies in which the peripheral nodes connect directly to a concentrator that acts as a Base Station (Gateway).

The robust modulations used by LPWANs make them suitable to connect end-devices

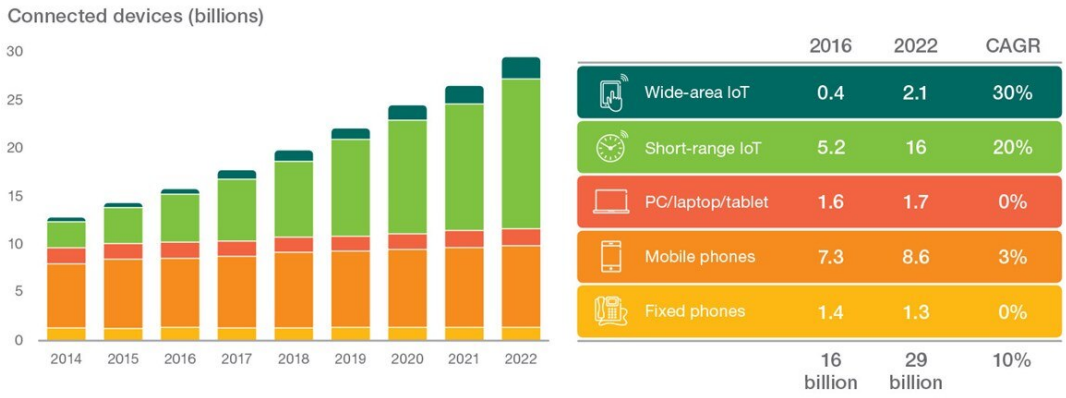

Figure 2.2: Growth in connected devices [11].

located in harsh environments, where cellular technologies may fail. Exploiting the unlicensed sub-GHz ISM band and sporadically transmitting small packets at low data-rates [13] are some of the characteristics of LPWANs that make them great candidates for IoT.

2.1.1 Features

The set of LPWAN technologies is very large (some of them will be explored further ahead), but some requirements are transversal to all of them [5, 6, 8]:

Long-Range: As the name indicates, LPWANs have the goal of offering coverage to a 'wide-area'. Lower frequencies provide longer communication range and have better propagation characteristics through obstacles, which causes most LPWAN technologies to operate in the sub-GHz band. This enables coverage from few kilometers in urban areas to tens of kilometres in rural areas.

Low-Power: It is crucial that IoT devices have long battery life in order to spare both economical and logistic expenses over the battery replacement, especially when talking about a huge amount of devices. Typically, LPWANs transmit small packets sporadically leading to a low power consumption, but there are several techniques applied to consume an even smaller quantity of energy, like using a star topology which eliminates the energy spent in multi-hop networks, keeping the node design simple (offloading complexities to the gateway) or using narrowband channels, decreasing the noise level and extending the coverage.

Low Deployment and Operation Cost: A major factor contributing to the rise of LPWANs is its low cost, as economic constraints are a strong driver. Low cost objects, easy network installation, minimun maintenance, limited hardware/software object complexity and simple protocols/architectures are some of the requirements to make LPWANs economically viable.

Reliability and Robustness: LPWANs are designed to provide reliable and robust communications, so most of them adopt robust modulation techniques and spread-spectrum techniques in order to increase the signal resistance to interference, and provide a level of security.

Scalability: The network needs to support a massive number of nodes due to the exponential increase of IoT devices. To efficiently use the limited spectrum, narrowband is used. Some factors that affect the scalability of a network are the underlying MAC protocol, duty-cycle restrictions and reliability requirement.

A comparison between the LPWANs and other technologies considered for IoT in terms of achieved range and required bandwidth is shown in Figure 2.3.

2.1.2 Technologies

There are two ways to approach the division of LPWAN technologies. Depending on the band adopted they can be broadly divided into [7]:

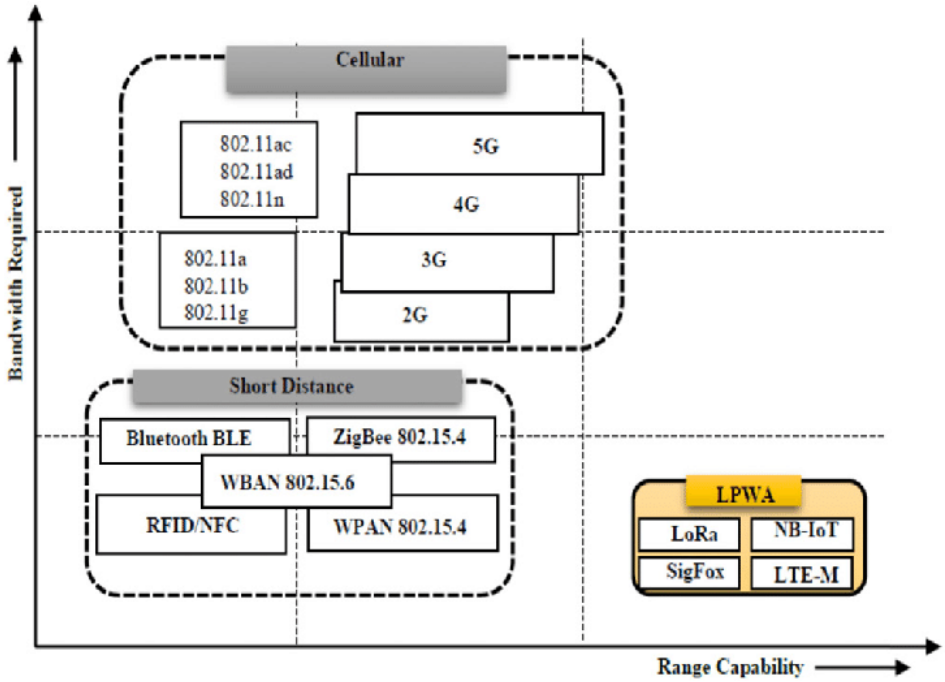

Figure 2.3: Required bandwidth vs range capacity of short distance, cellular and LPWANs [14].

Ultra Narrow Band (UNB): using narrowband channels with bandwidth of the order of 25kHz;

Wideband: using a larger bandwidth (125kHz or 250kHz) and employing some form of spread spectrum multiple access techniques to accommodate multiple users in one channel.

Other than that, the division can be done in terms of whether the technology is cellular-based or not (LoRa is the latest). An overview of some LPWANs is presented as follows, with the exception of LoRa, that will be detailed in subsection 2.1.3.

2.1.2.1 Cellular-based LPWAN technologies

NB-IoT is a narrowband LPWAN technology specified in Release 13 of the 3GPP in June 2016 [15]. It is based on the Long Term Evolution (LTE) protocol [16], reducing its functionalities to the minimum in order to achieve low-cost, ultra-low complexity and indoor improvement coverage. It uses the same frequencies as LTE (licensed frequency bands e.g. 700MHz, 800MHz and 900MHz), allowing its coexistence with GSM (Global System for Mobile communications) and LTE [4, 17]. NB-IoT occupies a frequency bandwidth of 200 KHz, which corresponds to one resource block in GSM and LTE transmission. Considering this frequency band selection, there are three possible operation modes [6]: *stand-alone operation*, that uses underutilized bandwidth, *guard-band operation*, using allocated bandwidth that is not utilized by LTE carriers, and *in-band operation* that uses LTE assigned carriers.

The uplink of NB-IoT is done using SC-FDMA (Single Carrier Frequency Division Multiple Access), in which multiple access among users is made possible by assigning different

sets of non-overlapping sub-carriers, and OFDMA (Orthogonal Frequency Division Multiple Access) for the downlink. It also employs quadrature phaseshift keying modulation (QPSK). The maximum payload size for each message is 1600 bytes.

NB-IoT supports a large number of devices per cell-site sector, low-power consumption, low data-rate and latency of less than 10 seconds. Those standards are developed to satisfy the needs of constrained IoT communication requirements. However, they almost consider exclusively static interconnected devices and pay less attention to the mobility of things.

LTE-M stands for LTE for Machines, and like NB-IoT, it is a licensed solution. The power consumption of conventional LTE end-devices is not acceptable for most IoT applications, this giving way to the creation of LTE-M, an evolution of LTE optimized for IoT in 3GPP Radio Access Network (RAN) [18]. LTE-M also shares with NB-IoT the objective of maximizing the re-use of existing cellular infrastructures and owned radio spectrum, providing cellular connectivity for a big number of end-devices with low power consumption and high interoperability in IoT networks.

2.1.2.2 Non cellular-based LPWAN technologies

Sigfox was the first LPWAN proposed in the IoT market [7]. It uses unlicensed ISM bands, for example 868 MHz in Europe, 915 MHz in North America, and 433 MHz in Asia [17] . The end-devices connect to the base stations using ultra-narrow band (100 Hz) Diferential Binary Phase Shift Keying (DBPSK) modulation.

The use of ultra-narrowband allows for an efficient use of the frequency bandwidth and low noise levels, which leads to a very low power consumption, high receiver sensitivity and low-cost antenna design. However, this comes at the cost of a maximum throughput of only 100 bps, a very low data-rate compared to other LPWAN technologies.

The MAC Layer is based on the unslotted ALOHA MAC Protocol [19], meaning that all devices can access the channel whenever they want. SigFox allows only 140 12-bytes message per day, each transmission taking 3 seconds [20]. To provide reliability, the message is transmitted multiple times, which increases energy consumption. Sigfox claims that each base station can handle up to a million connected objects, with a coverage area of 30-50km in rural areas and 3-10km in urban areas [7].

Weightless is both the name of the technology and the group developing it: Weightless Special Interest Group (Weightless SIG)[21]. Weightless technology delivers wireless connectivity for low power wide area networks specifically designed for the Internet of Things. It is a set of three standards, *Weightless-N*, *Weightless-P* and *Weightless-W*, in which they all work in the sub-GHz, but each of them has its own particularities [7, 8, 22]:

- **Weightless-W:** System with a star topology that operates in TV white space spectrum. It provides a wide range of modulation schemes, spreading factors and packet sizes. Weightless-W claims to achieve two-way data-rates from 1kbps to 10Mbps with very low overhead. These advantages come at the cost of a short battery lifetime for the end-nodes (limited to 3 years), and having the highest terminal cost of the three standards. The communication between the end-nodes and the base station can be established along 5 km, depending on the environmental conditions.

- **Weightless-N:** With a scheme based on nWave (which was donated as template for the Weightless-N standard), Weighless-N uses a class of low-cost technology very similar to that employed by Sigfox. It supports only unidirectional communication, in which ultra-narrowband (DBPSK) modulation is adopted, providing connectivity of up to 100kbps, exploiting ISM bands. Because of the simplicity of this solution, Weightless-N allows a battery duration of up to 10 years, very low cost terminals, and a long connection range similar to that reached by Weightless-W. The MAC protocol used is based on slotted ALOHA.

- **Weightless-P:** The most recent of the three, Weightless-P gathers the most proper characteristics of the previous two, claiming to be specifically focused on the industrial sector. The communication is bi-directional with support for acknowledgements, with an adaptive data rate from 200bps to 100kbps. It uses a narrowband modulation scheme, Gaussian Minimum Shift Keying (GMSK) and Offset Quadrature Phase Shift Keying (OQPSK). In comparison with the other two standards, Weightless-P provides a more limited range (2 km) and is a compromise in terms of battery life and terminal cost.

Regarding security, the three Weightless versions provide end-to-end network authentication and 128 bit AES encryption [22]. A summary of each Weightless variation can be found later in the chapter.

Ingenu, formerly known as On-Ramp Wireless, is a LPWAN platform currently beginning its deployment in the USA. The company developed and owns rights to the patented technology Random Phase Multiple Access (RPMA)[23], which is deployed in different networks. RPMA operates on the globally available 2.4GHz (which is unusual for LPWANs), exploiting the rules and regulations imposed by this band, such as minimum duty cycle, but thanks to a robust physical layer design it can still operate over long-range wireless links, and under the most challenging RF environments [7]. Ingenu claims to be able to scale in a truly unlimited way [24], and having an unheard-of amount of coverage in the order of the thousands of miles while using less than 20 access points. This technology is mainly targeted for metering and SmartGrid applications [7].

DASH7 is an open standard proposed by the DASH7 Alliance. It proposes a two-hops tree topology with hierarchical devices (endpoints, sub-controllers and gateways), ideal for wireless sensor and actuator networks [22]. The features of this technology can be described by the acronym BLAST [4, 25]:

Bursty: Transmission of short and sporadic sequences of data. Contents like video, audio or other isochronous forms of data are not supported;

Light: Small packet sizes, limited to 256 bytes. Transmission of multiple, consecutive packets may occur but should be avoided;

Asynchronous: Communication is command response based, which by design requires no periodic network hand-shaking or synchronization between devices;

Stealth: DASH7 does not use discovery beacons. End-nodes can chose to respond only to pre-approved devices;

Transitive: It supports mobility. A DASH7 system of devices is inherently mobile or transitional, allowing end-nods to move seamlessly between different gateways' coverage.

Some characteristics of this technology are: ultra low-power, seamless indoor and outdoor use, optimal RF performances and being a context-aware sensor and actuator data propagation system.

SNOW stands for Sensor Network Over White Spaces [26], and it uses the TV white spaces, exploiting them in order to achieve higher scalability for Wireless Sensor Networks, a common limitation for these networks.

Obtaining low data-rate, low cost nodes, scalability and energy efficiency are significant challenges for the SNOW technology [8, 26]. Scalability and energy efficiency are obtained through channel splitting, enabling simultaneous packet receptions at a base station with a single radio. The base station has a single transceiver that uses available wide spectrum from white spaces. The spectrum is split into narrow orthogonal sub-carriers whose bandwidth is optimized for scalability, energy efficiency and reliability. Narrower bands have lower throughput but longer range, and consume less power.

Despite its promise, SNOW has some limitations [15], such as not being able to implement bi-directional communications over different sub-carriers, not supporting per-transmission acknowledgments and using a modulation scheme that provides simplicity but not robustness (Amplitude Shift Keying).

Telensa is a proprietary LPWAN technology focused on the Smart Cities market. It pioneered the use of UNB operating in the unlicensed sub-GHz ISM band [8], and has also developed its own bi-directional ultranarrow-band technology.

Some specific applications for Smart Cities [22, 27] are Telensa PLANet (Public Lightning Active Network), the world's most deployed smart streetlight control system, and Telensa PARKet, for smart parking enhancement. Telensa claims to reach 23 km and 58 km ranges when in urban or rural environment, respectively. Solutions have already been deployed in different big cities worldwide [22].

2.1.3 Long-Range (LoRa)

Initially proposed by Semtech and currently being developed by the LoRa Alliance [28], LoRa, which stands for Long Range, is an infrastructure-less LPWAN technology [8]. Its focus is on the support of battery-powered devices that require a long life time, making energy consumption a primary requirement.

Two distinct layers can be referred: the physical layer, that uses a modulation scheme owned and patented by Semtech [29]; and a MAC layer protocol called LoRaWAN, an open standard being developed by the LoRa Alliance. The LoRa technology stack is presented in Figure 2.4.

2.1.3.1 Physical Layer

LoRa modulates the signals in sub-GHz ISM bands. Communication is based on a proprietary spread spectrum scheme derivative of the Chirp Spread Spectrum (CSS) modulation technique [7]. The innovation consists in ensuring the phase continuity between different chirp symbols in the preamble part of the physical layer packet, enabling a simpler and more accurate timing and frequency synchronization between transmitter and receiver.

The described scheme mantains the low power characteristics of FSK (Frequency Shifting Modulation) that many wireless systems use while increasing the communication range. Along

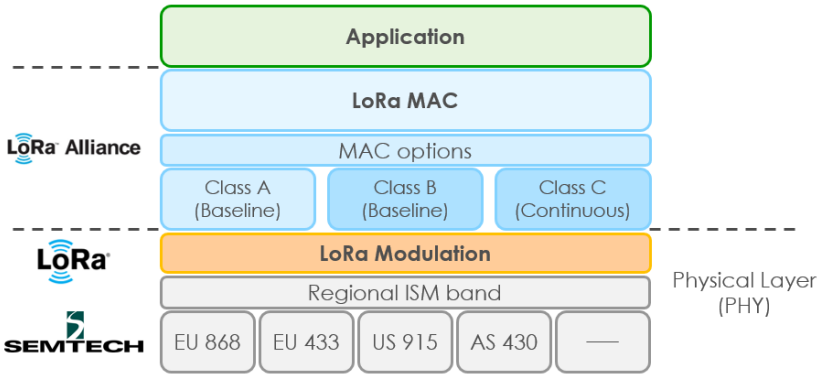

Figure 2.4: LoRa technology stack [14].

with this spread spectrum technique, FEC (Forward Error Correction) is implemented to further increase the receiver sensitivity.

Depending on the application it is possible to configure the LoRa modulation by customizing the following parameters [30, 31]:

- **Carrier Frequency (CF):** Center frequency used for the transmission band. It varies depending on the used transceiver;
- **Spreading Factor (SF):** Parameter that defines the tradeoff between the data-rate and communication range. It expresses the ratio between chip rate and symbol rate, as seen in Equation 2.1.

$$\frac{\#chips}{\#symbols} = 2^{SF} \tag{2.1}$$

  It can be chosen from 6 to 12, being SF6 (highest transmission rate) a special case, requiring special operations. A high SF guarantees longer range, higher SNR (Signal-to-Noise Ratio) and sensitivity, but also implies bigger Time on Air (ToA) of the packet, a lower data-rate, and increases energy consumption. Communications with different SF values are orthogonal to each other, meaning it's possible to perform network separation using different Spreading Factors for different channels;
- **Bandwidth (BW):** Range of frequencies in the transmission band. Typically with values of 125kHz, 250kHz and 500kHz, the Bandwidth value is equal to the chirp rate (one chirp per second per Hertz of BW). The outcome of changing the bandwidth is in some ways the inverse of changing the Spreading Factor, as a higher BW means higher data-rate and shorter ToA, but also lower sensitivity due to the integration of additional noise;
- **Coding Rate (CR):** LoRa performs Forward Error Correction (FEC), employing a cyclic error coding to offer protection against burst of interference. CR determines the rate of the FEC code. The higher this value the more protection it offers, but it also increases the ToA. $CR = \frac{4}{(4+n)}$, with n $\in [1, 4]$. Radios with different CR can communicate with each other as long as they maintain the same SF, BW and CF.

Different combinations of these parameters result in different values for the useful bit rate of a LoRa transmission [31] (Equation 2.2), as well as distinct trade-outs of throughput for coverage range, robustness and energy consumption.

$$Rb = SF \times \frac{CR}{\frac{2^{SF}}{BW}} \tag{2.2}$$

It is when two packets using the same parameters overlap in time that frame collisions occur, leading to packet loss. However, it is said that due to the capture effect found in LoRa modulation, or non-destructive property, it is possible for a packet to be decoded during a collision if the difference in received signal strength is big enough [32]. If not, the receiver keeps switching between the two signals, not able to decode any of them.

LoRa offers a maximum packet size of 256 bytes. Its structure is shown in Figure 2.5.

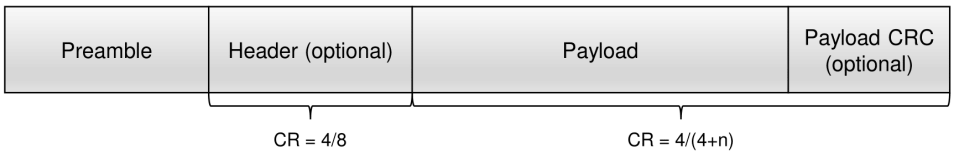

Figure 2.5: LoRa packet structure [33].

Packets are composed by the following fields [33]:

- **Preamble Field:** used for synchronization purposes. Receiver synchronizes with the incoming data flow;
- **Header Field:** It depends on which operation mode is being used:

  Default explicit operational mode: number of bytes in the header field specifies the FEC code rate, payload length(fist byte) and presence of CRC in the frame. The header field also contains a 2-byte CRC (Cyclic Redundancy Check) field. Together they are 4 bytes long and encoded with 1/2 coding rate, while the coding rate for the rest of the frame is specified in PHY header;

  Implicit operational mode: specifies that coding rate and payload length in a frame are fixed, so the frame does not contain this field, reducing transmission time;

- **Payload Field:** Varies from 2 to 255 bytes. Contains the following fields:

  MAC Header: defines frame type (data or ACK), protocol version and direction (uplink or downlink);

  MAC Payload: contains the data;

  MIC: used as the digital signature of the payload;

- **CRC:** Optional field. Comprises cyclic redundancy check bytes for error protection in the payload, allowing the receiver to discard packets with invalid header.

2.1.3.2 MAC Layer - LoRaWAN Protocol

Governed by the LoRa Alliance, LoRaWAN is a contention-based MAC protocol built to use the LoRa physical layer. Its characteristics make it suitable for Wireless Sensor Networks (WSNs), where data is exchanged occasionally and with low data-rates.

LoRaWAN defines the system architecture for the network, typically laid out in a star-of-stars topology, as seen in Figure 2.6, specifying the following components [7, 34]:

- **End-Devices:** Low-power sensors/actuators who are connected via single-hop LoRa to the gateways. These devices are not associated with a specific endpoint, enabling the data reception by multiple gateways;
- **Gateways:** Responsible for connecting all LoRaWAN nodes within their coverage, Gateways are powerful devices with powerful radios capable to receive and decode multiple concurrent transmissions. All of them are connected to a common NetServer, bridging all end-devices to the central element of the architecture;
- **NetServer:** Network Server that controls the whole network, with functions such as filtering redundant received packets, performing security checks, scheduling acknowledgements and performing adaptive data rate (distinguishing feature of LoRaWAN which allows to adapt the transmit rate of an end-device by changing the SF index, in order to find the best trade-off between energy efficiency and link robustness).

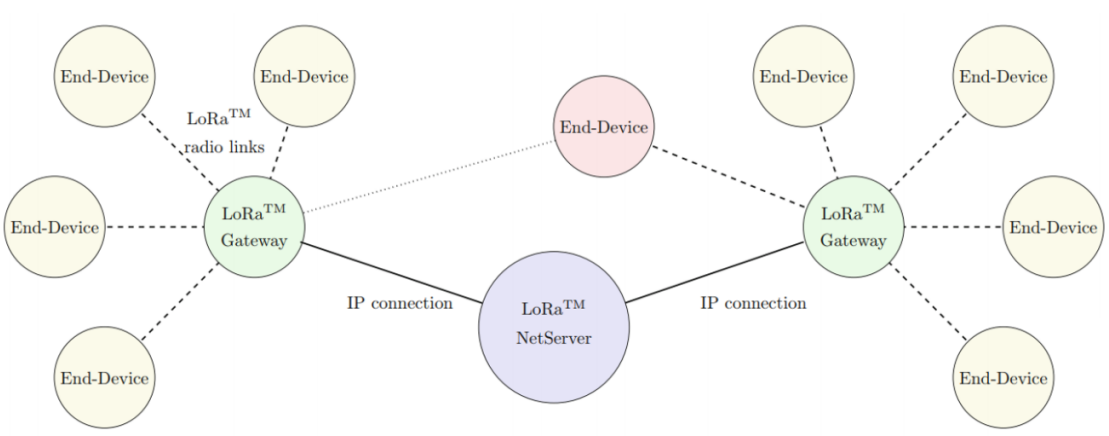

Figure 2.6: LoRa system architecture [7].

Increased network capacity is achieved by the use of this adaptive data rate and multi-channel transceivers in the gateways so that simultaneous messages can be received in multiple channels [14]. There are several factors that affect capacity, such as: number of concurrent channels, data-rate, payload length and how often the nodes transmit [35].

Nodes in LoRaWAN are asynchronous and communicate when they have data to send (ALOHA-based protocol) so unlike in other networks, such as cellular, there's no need for synchronization with the network, which gives LoRaWAN a battery lifetime advantage. On this subject, three different device classes are provided (A, B and C), each with a different operating mode, allowing a trade-off between performance (*i.e.* throughput and latency) and

energy consumption [5, 35, 36].

- **Class A (for All):** Bi-directional end-devices with scheduled uplink transmissions. After each uplink transmission, the device opens up two short downlink windows. This class has the lowest power consumption but the highest latency, and the least flexibility on downlink transmission;
- **Class B (for Beacon)**: Bi-directional end-devices with scheduled receive slots. These extra receive windows reduce the downlink latency and increase the power consumption. Devices must receive a time-synchronized beacon from the gateway, allowing the server to know if the end-device is in the listening windows;
- **Class C (for Continuously listening):** Bi-directional end-devices with maximal receive slots. These devices have no energy restrictions, having almost continuous reception windows. Because of this, Class C has the highest power consumption and the lowest latency.

Two layers of security are used, one for the network, which guarantees authenticity of the node in the network, and one for the application, ensuring the network operator cannot access the user's application data [5].

A key limiting factor that affects the performance of LoRaWAN is the duty-cycle regulations in the ISM bands [37]. For instance, the maximum duty cycle of the EU 868 ISM band is 1% for devices that do not implement Listen Before Talk (LBT) and Automatic Frequency Agility (AFA), allowing a maximum transmission time of 36 seconds per hour in each sub-band, for each end-device.

Tables 2.1 and 2.2 portray a summarized comparison between LoRa and the other technologies referred. The first contains the mentioned cellular-based LPWANs, and the second presents the remaining LPWANs: Sigfox, Weightless, Ingenu, DASH7, SNOW and Telensa.

Table 2.1: LoRa compared to cellular-based LPWAN technologies [6, 8].

	LoRa	**NB-IoT**	**LTE-M**
Band	Unlicensed Sub-GHz	Licensed Sub-GHz	Licensed Sub-GHz
Modulation	CSS	QPSK OFDMA (UL) SC-FDMA (DL)	SC-FDMA GFDMA
Max Range in Urban Scenario (km)	5	15	<11
Peak Data-rate	50kbps	250kbps (UL) 170kbps (DL)	<150kbps
Mobility	Yes	No	No
Battery Lifetime (years)	10	10	>10
Bi-directional Communication	Yes	Yes	Yes
Indoor Communication	Yes	Yes	Yes

Table 2.2: LPWAN technologies comparison [6, 8, 22].

	LoRa	SigFox	Weightless-W	Weightless-N	Weightless-P	Ingenu	DASH7	SNOW	Telensa
Band	Unlicensed Sub-GHz	Unlicensed Sub-GHz	Unlicensed TV White Spaces	Unlicensed Sub-GHz	Unlicensed/ Licensed Sub-GHz	Unlicensed 2.4GHz	Unlicensed Sub-GHz	Unlicensed TV White Spaces	Unlicensed Sub-GHz
Modulation	CSS	DBPSK GFSK	BPSK	DBPSK	GMSK OQPSK	DSSS CDMA	GFSK	BPSK	FSK
Max Range in Urban Scenario (km)	5	10	5	0-3	0-2	15	0-5	5	1-10
Peak Data-rate	50 kbps	100 bps	10 Mbps	100 kbps	100 kbps	80 kbps	166.766 kbps	50 kbps per node	65 kbps
Mobility	Yes	Yes	No	No	No	Limited	Yes	N/A	No
Battery Lifetime (years)	10	5	3-5	10	3-5	15	N/A	N/A	10
Bi-directional Communication	Yes	Yes	Yes	No	Yes	Yes	Yes	No	Yes
Indoor Communication	Yes	No	Yes	No	Yes	Yes	No	Yes	Yes

2.2 Related Work

2.2.1 LoRa Performance Studies

After delving into the characteristics of LPWANs and studying the different existing technologies, we realize that the LPWANs are indeed a promising solution when it comes to the future of IoT. LoRa, like the remaining technologies, is still at early stages of development, and there is still some debate about its coverage range, mobility and scalability.

Oliveira et. al [38] tested the LoRa coverage in three scenarios with different characteristics, one rural and two urban. Aveiro and Coimbra were the evaluated urban environments, the first presenting a flat profile and the second an uneven city with hills. The results showed that there are three scenario characteristics that influence the achieved results: distance, elevation difference and obstacles in the signal path. The maximum communication range achieved was 5660 meters for the rural scenario and around 2000 meters for the urban ones.

Andrei et. al [39] performed LoRa mobility and range tests in Bucharest, Romania. The authors configured the module with a 125 kHz BW, a SF of 7 and a CR of 4/8, achieving a measured distance of 4.3 km in urban area and 9.7 km in an open field, outside the town. They observed that moving the node during transmission affected the quality of the received packet (i.e. sometimes packets were so badly received it was impossible to reconstruct the location). The mobility problems increased with longer distances.

Sanchez-Iborra et. al [40] presented a performance evaluation of LoRaWAN under different environmental conditions, namely urban, suburban and rural, and tested different spreading factors. An end-node was equipped with a GPS chip and placed on the roof of a car, acting as periodic sender, in communication with a base station. First the tests were performed in a realistic dynamic scenario, with the vehicle speed being affected by real traffic conditions. In the most adverse scenarios (i.e. urban and suburban) a coverage range of around 6 km was attained, reaching 18 km in rural situations. After this, in order to evaluate the effect of mobility on performance, a nomadic test was performed, conducting a sampling campaign with the car stopped at different locations. The obtained results showed that there was not much influence from the vehicle motion when using low data rates, but the same could not be said for higher values.

Augustin et. al [34] did a similar study in Paris. A gateway was placed indoors, and

a mobile device was transmitting data packets to the gateway in an urban environment. Around 10,000 packets were sent using spreading factors of 7, 9 and 12, with the Received Signal Strength Indicator (RSSI) of the received packets being recorded. It was observed that for SF12, the Packet Delivery Ratio (PDR) was above 80% for distances around 3 km, whereas in the case of SF7, the same ratio was obtained for distances around 600m.

As previously referred, a fundamental feature of LoRa and LPWANs in general is scalability. The network should be able to support the exponential increase of IoT devices and the consequential incoming traffic volume. Such behaviour is very difficult to evaluate in real scenarios, as a very large amount of end-devices would be required. Georgiou and Raza [41] studied the scalability performance of a LoRa Gateway, providing a stochastic geometry framework to model the performance of a single channel network. Two conditions are studied: one is related to SNR (*i.e.* range) and another one is related to the same SF interference. It is argued that LoRa networks will inevitably become interference limited, as end device coverage probability decays exponentially with the increasing number of devices. The authors report that this is mostly caused by intra-SF interference.

Van den Abeele et. al [42] simulated a LoRaWAN network in ns-3, with the particularity of using a LoRa error model built from extensive complex baseband Bit Error Rate (BER) simulations. This model is combined with the LoRaWAN MAC protocol, adding some realism to the simulation. Some works have modeled LoRaWAN networks as pure ALOHA, which fails to capture important characteristics such as the capture effect, and effects of interference. For assignment of the SF, three strategies have been considered: *1) Random*, assigning SFs to end devices according to a uniform random distribution, *2) Fixed*, assigning the same SF to end devices, and *3) PER*, a strategy in which for every device, it is found the SF for which the Packet Error Ratio falls below a certain threshold. The latest strategy was proven to be the best for high scale networks, but for networks with under 100 nodes, the *Fixed* strategy with a high SF might suffice. When using the third strategy, it was obtained a packet delivery ratio of almost 100% in a network with 100 nodes, around 45% for 5000 nodes, and 30% with 10000 end-devices.

Bor et. al [32] developed a simulator, LoRaSim, describing LoRa communication behaviour in order to study its scalability, taking into account aspects such as the capture effect and communication range in dependence of the communication settings used. The simulations show that a typical smart city deployment can support 120 devices per 3.8 hectare, not considered sufficient for future IoT deployments. It is highlighted, however, the importance of using dynamic transmission parameter selection in order to achieve higher scalability.

The topic of LoRa's non-destructive property, though often ignored, has been the target of some research. This property is particularly relevant in future deployments with a high density of nodes due to the uncoordinated ALOHA-based random channel access of LoRaWAN.

Elshabrawy and Robert [43] determined a numerical approximation for the LoRa BER performance in the event of same SF interference as a function of both SNR and SIR (Signal-to-Interference Ratio). Simulations have shown that assessing coverage based on a threshold of 6 dB - as is conventionally done - is an underestimation of the coverage probability of LoRa signals with intra-SF interference.

Afisiadis et. al [44] have also studied the case of a gateway trying to decode the message of a user in the presence of an interfering LoRa device, showing that even for very low values of SIR, packet reception is possible as long as the SNR value is high enough.

The two previous works focus mostly in pure mathematical models. Haxhibeqiri et. al [45] performed real interference measurements, focusing the analysis on the impact of the

time shift between two concurrent transmissions. The tests demonstrated that, in the event of concurrent transmissions, one of the packets was received as soon as the last six symbols of preamble and header of the packet did not collide. This information was used to create a simulation model, and it was showed that one can send six-times more traffic with LoRaWAN than with pure ALOHA in a single-cell LoRaWAN network, for the same number of end devices per gateway.

2.2.2 MAC Protocols for LoRa

A MAC Protocol is essential for networks that work with shared medium and have a huge number of nodes. Different networks have different requirements in terms of medium access, so there is no standard protocol for WSNs. It is essential to ensure fair access to the channel and avoid packet collisions.

MAC Protocols can be divided into *contention based* and *schedule based*. Popular contention based protocols are ALOHA (and its variants) and Carrier Sense Multiple Access (CSMA) (and its variants). Because of the non-existence of scheduling, the major drawback of contention-based MAC protocols is low throughput, which is caused by packet collisions [46]. As packet delivery is not guaranteed, these protocols are rendered unsuitable for mission-critical applications [47]. On the other hand, schedule based protocols have minimal to zero collisions, making them theoretically more efficient. They have the advantage of avoiding collisions, overhearing and idle listening, achieving these features with scheduled transmissions and listen periods. This comes at the cost of constant re-synchronization.

As referred, in the case of LoRa, the adopted MAC behaviour is LoRaWAN. Being ALOHA-based, this protocol results in low channel utility under high traffic load due to packet collisions. Most of the research on LoRa has been focused on either improving or studying LoRaWAN. Meanwhile, other LoRA-based MAC layer protocols has had far less scrutiny due to the limited research on using LoRa with MAC layer protocols other than LoRaWAN [48]. There are, however, some proposed alternatives.

Bor et. al proposed LoRaBlink [30], that aims to support multi-hop communication, low energy, enabling high message delivery and low-latency. However, these requirements are met only with the assumption that the network has a low density, low traffic volume and contains a limited number of nodes, something that cannot be expected given the increase of IoT devices.

Oliveira et. al [49] proposed a MAC protocol based on the Carrier Sense Multiple Access with Collision Avoidance (CSMA/CA), with a Request To Send (RTS)/Clear To Send (CTS) message exchange to control the medium access by the devices. In order to take advantage of the LoRa non-destructive communication property, a Wait To Send (WTS) packet was created.

Hassan et.al [47] proposed MoT (MAC on Time), a hybrid scheduling-based protocol that aims to guarantee the delivery of all uplink packets in the network and addresses most of the important parameters required by mission-critical applications, such as PDR, bandwidth and data-rate, battery life, range, latency and throughput. Packet collisions are eliminated by precise time-slot scheduling, and MoT claims to improve the bandwidth capacity four times beyond that of LoRaWAN. A Base Station coordinates the channel access time-slots in a semi round-robin manner. The authors then proceeded to evaluate the energy performance of contention-based versus scheduled-based protocols [48], with LoRaWAN as the leading contention-based class and MoT as the candidate for schedule-based protocols. It was con-

cluded that the energy performance of MoT is unaffected by the number of nodes in the network, making this protocol highly scalable compared to contention-based protocols.

Deng et. al [50] proposed ADC-MAC, a protocol that also takes into account the energy efficiency. The basic idea of ADC-MAC is to adjust the node duty-cycle dynamically. The duty-cycle selection is based on three indicators: *1) residual energy*, *2) node load* and *3) network congestion rate*. It was seen that, for small-scale networks the PDR was lower, when compared to the standard duty-cycle limitation. However, when increasing the size of the network, ADC-MAC gets better results.

One of the reasons why LoRa is so promising is its flexibility, being possible to choose from over 6500 transmission parameter combinations [51]. In recent years it has been a challenge to determine which settings can meet the required communication performance while minimizing the transmission energy cost. Some proposed protocols have made use of this possibility to select the transmission parameters, opting for an adaptive configuration that best suits the characteristics of the network at the time.

Flabicki et. al [52] developed FLoRa, an open-source framework for LoRa simulations that implements the physical and medium access control layers of LoRa and supports bi-directional communications. FLoRa allows to configure all the parameters in the LoRa physical layer, with different configurations being used depending on the distance of the node to the Gateway - Adaptive Data Rate (ADR). The authors claim that, using the ADR technique, a better network performance is achieved when the variance of the channel is null or very low but, for highly varying channels, additional mechanisms are needed. Also, for dense networks, a link-based adaptation is not sufficient, making it necessary a network-aware approach wherein the link parameters are configured based on the global knowledge of the network.

Reynders et. al [53] proposed a way to improve the reliability and scalability of LoRaWAN through lightweight scheduling - RS-LoRa. In this new MAC, the scheduling is done in a two-step process, in which first the Gateway schedules nodes, specifying the allowed transmission powers and spreading factors on each channel. Then, based on the scheduling information, a node determines its own transmission power, spreading factor, when and in which channel to transmit. Scalability is obtained by guiding the nodes to select different spreading factors. RS-LoRa was tested in NS-3, and the results showed improvements in terms of packet error ratio, throughput and fairness, at a reasonable energy efficiency.

Sartori et. al [54] proposed a protocol to allow multi-hop over LoRa devices, RLMAC. Based on the IPv6 Routing Protocol for Low-Power and Lossy Networks (RPL) [55], the idea is to allow the node to act as a router, able to select the optimal SF per link. Being capable of selecting the optimal routing path improves both time on air and power consumption.

Lee and Jeong [56], proposed a scheduling algorithm to improve the scalability of LoRaWAN. This algorithm proposes the scheduling of spreading factors, frequency channels and time slots for wireless links connecting the end-devices to the gateways. It also employs GACK (group acknowledgment), a message that aggregates acknowledgements of uplink transmissions received simultaneously in order to improve channel efficiency. The algorithm runs when a message indicating a request of scheduling is received from the device. The first step is the allocation of the spreading factor, considering the received signal power from the device. Afterwards, a frequency channel and time slot is scheduled. If other links have already been scheduled prior to receive the request message, the network server allocates time slots and frequency channels so that multiple uplink messages on links assigned to the same spreading factor can be delivered simultaneously. When compared to ALOHA, used in the uplink transmissions for LoRaWAN, the results obtained were very positive, with simulations

showing that the proposed algorithm provides more than 60% increase in the number of end devices connected to a gateway. The simulation also showed that it is possible to maintain a PDR of 90% in a network with around 8,000 devices.

Polonelli et. al [57] regulated the communication of LoRaWAN by using a Slotted-ALOHA variant on the top of the common pure-ALOHA approach used by the standard. To assure the slots were aligned in all end-devices, a lightweight synchronization methodology tailored for LoRaWAN end nodes was used. This solution showed a very low impact on the power consumption of the equipment, while achieving a theoretical value of doubling the network throughput and reducing packet collisions by 26% in a real deployment using 24 nodes.

2.3 Chapter Considerations

This chapter presented an overview of the LPWANs, referring its main features as well as their advantages for the IoT market in comparison with more traditional technologies. Several LPWAN technologies were explored, with special attention to LoRa , both Physical and MAC layer, the LPWAN technology under evaluation in this dissertation.

At the end of the chapter, related work on topics that are relevant to this dissertation were presented. On the subject of LoRa performance, special attention was given to the communication range achieved depending on environment conditions, scalability of LoRa networks and characterization of LoRa packet capture effect in the presence of multiple transmissions. The remaining related work tackles previously proposed MAC protocols with similar characteristics as the one developed in this work, or presenting relevant considerations.

The next chapter explores LoRa's non-destructive property and the tests performed in order to characterize it.

Chapter 3

Concurrent Transmissions in LoRa

This chapter refers to a very unique characteristic of LoRa's physical layer, its non-destructive property, focusing mainly in characterizing the success of concurrent transmissions. Section 3.1 provides an explanation on what this property consists of, and under what conditions it occurs. Section 3.2 details the hardware used and tests performed in order to characterize the behaviour of a LoRa gateway upon receiving overlapping packets. Section 3.3 demonstrates a probabilistic model obtained by an exhaustive evaluation process, that estimates the success of a transmission in the event of concurrent interference. Finally, Section 3.4 presents a chapter summary and considerations.

3.1 LoRa's Non-Destructive Property

As detailed in the previous chapter, as long as the emitter and receiver have the same configuration, LoRa transmissions can be configured via customization of four parameters. From these, three are relevant in terms of characterizing the packet collision behaviour: Carrier Frequency (CF), Bandwidth (BW) and Spreading Factor (SF). Two transmissions that overlap in time but use a different CF do not interfere with one another [32] (if a tolerable frequency offset is respected, dictated by the bandwidth), and both can be decoded if the receiver has the ability to be listening at both frequencies.

The same can be said for SF: transmissions with distinct SF values are orthogonal to each other which enables multiple signals to be transmitted at the same time. Modulated signals at different SFs appear as noise to the target receiver and can be treated as such [31]. There are, however, studies [58, 59] that show that inter-SF collisions can indeed cause packet loss if the interference power received is strong enough.

The term *concurrent transmissions* alludes to when two or more packets coming from devices configured with the same parameters overlap in time, as illustrated by Figure 3.1, leading to frame collisions and consequently to packet loss. However, it is referred that, due to the capture effect found in LoRa modulation, or non-destructive property, it is possible for a packet to be decoded during a collision if the difference in the received signal strength is higher than a certain threshold value [32]. If this difference is not big enough, the receiver keeps switching between the two signals not being able to decode any of them, leading to the loss of both packets.

The possibility of a LoRa gateway decoding the message of a user in the presence of an interfering device is of major importance, especially in deployments with a high density of

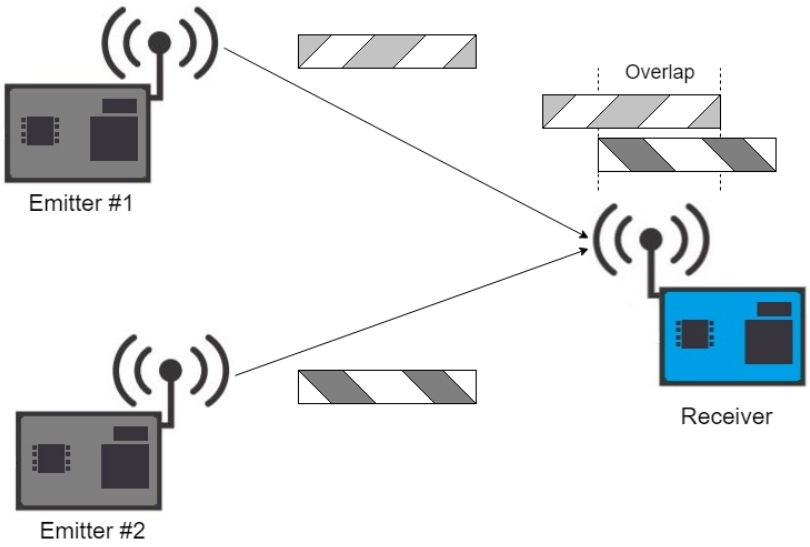

Figure 3.1: Example of a packet collision.

nodes, and therefore high amount of collisions. Such property leads to an increase on the network capacity instead of assuming that all overlapping packets are lost, as it happens when LoRaWAN is modeled as a pure-ALOHA network.

3.2 Characterizing Concurrent Transmissions

To evaluate and characterize the non-destructive property, experimental tests were performed where synchronized nodes, configured with the same modulation parameters, transmit packets to a receiver at the same time.

3.2.1 Hardware Equipment

To perform communication by LoRa, the transmitters and the receiver are composed of a Raspberry Pi Model 3B+ allied with a SX1272 LoRa module [60], and a Multiprotocol Radio Shield that bridges the previous two. Connected to the SX1272 module, a 4.5dBi, 868 MHz SMAM-RP antenna is used.

Figure 3.2 presents the hardware described, showing how the components connect to form the network elements used. Some characteristics of the Raspberry Pi 3B+ and LoRa module used can be found in Tables 3.1 and 3.2, respectively. In addition to changing the transmission power of the emitters, attenuators were used, with attenuation values of 30dBm, 10dBm and 6dBm.

Table 3.1: Raspberry Pi 3 Model B+ Specifications [61].

Processor	RAM	Networking	Operating System
1.4GHz 64-bit quad-core ARMv8 CPU	1 GB	2.4GHz and 5GHz IEEE 802.11.b/g/n/ac Wireless LAN Bluetooth 4.2/BLE	64-bit Raspbian GNU

(a) Antenna, SX1272 module (left) and Multiprotocol Radio Shield (right)

(b) Raspberry 3B+ equiped with material in Fig 3.2a

Figure 3.2: Hardware used.

Table 3.2: SX1272 Module Specifications [60].

Dual Frequency Band	**Transmission Power**	**Sensivity**	**Channels**	**Range**
863-870 MHz (Europe) 902-928 MHz (US)	0,7,14 dBm (adjustable)	-134 dBm	8 (Europe frequency band) 13 (US frequency band)	LOS = 21km NLOS = +2km

The module can be configured with 10 different predefined modes, each consisting of a different combination of the LoRa physical layer parameters, as shown in Table 3.3. Mode 1 privileges distance, having the higher range and the most sensitivity, while Mode 10 is the fastest, with the lowest transmission time-on-air. The remaining Modes combine the parameters resulting in a set of communication ranges and data-rates (bit rate increases with the Mode number while the transmission range decreases).

The SX1272 module counts with a library that is mandatory to include when using it, of which are part a wide range of functions. The relevant ones to carry out the experimental evaluation are presented in Table 3.4.

Table 3.3: SX1272 LoRa operation modes.

Mode	Bandwidth (Hertz)	Coding Rate	Spreading Factor	Sensitivity (dB)
1	125	4/5	12	-134
2	250	4/5	12	-131
3	125	4/5	10	-129
4	500	4/5	12	-128
5	250	4/5	10	-126
6	500	4/5	11	-125.5
7	250	4/5	9	-123
8	500	4/5	9	-120
9	500	4/5	8	-117
10	500	4/5	7	-114

Table 3.4: Relevant SX1272 functions.

Function	Description
ON()	Opens the SPI and switches the SX1272 module ON.
OFF()	Closes the SPI and switches the SX1272 module OFF.
setMode()	Sets the BW, CR, and SF of the LoRa modulation.
setChannel()	Sets the indicated frequency channel in the module.
setNodeAddress()	Sets the node address in the module.
setPower()	Sets the signal power indicated in the module.
getSNR()	Gets the SNR value in LoRa mode.
getRSSI()	Gets the current value of RSSI from the channel.
getRSSIpacket()	Gets the RSSI of the last packet received in LoRa mode.
sendPacketTimeout()	Sends a packet to the specified destination before a timeout expires.
sendPacketTimeoutACK()	Sends a packet to the specified destination before a timeout and waits for an ACK response.
receivePacketTimeout()	Receives information before a timeout expires.
receivePacketTimeoutACK()	Receives information before a timeout expires and responds with ACK.

3.2.2 Experimental Methodology

For the characterization process, it was created a network topology with one gateway and two end-nodes (or three later on), with all elements composed by the assembly represented on Figure 3.2b and operating at the same Mode, to force packet collisions. Synchronization between the end nodes was accomplished by the use of sockets, with one computer acting as a server.

Several studies on LoRa performance in city scale environments [62, 38, 39] have showed that, in real case scenarios, the RSSI of transmitted packet ranges between around -90 and -120dBm. This being said, the interval [-120,-95]dBm was chosen as the range of interest.

Needing to receive packets with a minimum signal strength of -120dBm, Mode 7 (BW = 250Hz, CR = 4/5, SF = 9) was selected, to ensure the required sensitivity to receive such weak signals, while also minimizing the time-on-air of each transmission as much as possible.

Since even using the lowest power settings in the module was proven insufficient to achieve the low signal strength of the range of interest, the use of attenuators was necessary, as can be seen in the setup illustrated in Figure 3.3. Altogether 12 attenuators were used, with the following attenuation values: 4 of 30dBm, 6 of 10dBm and 2 of 6dBm, with different combinations being made to achieve the values of interest.

The synchronized transmissions were performed in a controlled environment, an anechoic chamber, without external interference. Even though such environment is no way similar to a real case scenario in which LoRa is used, this place was chosen to keep the RSSI values as

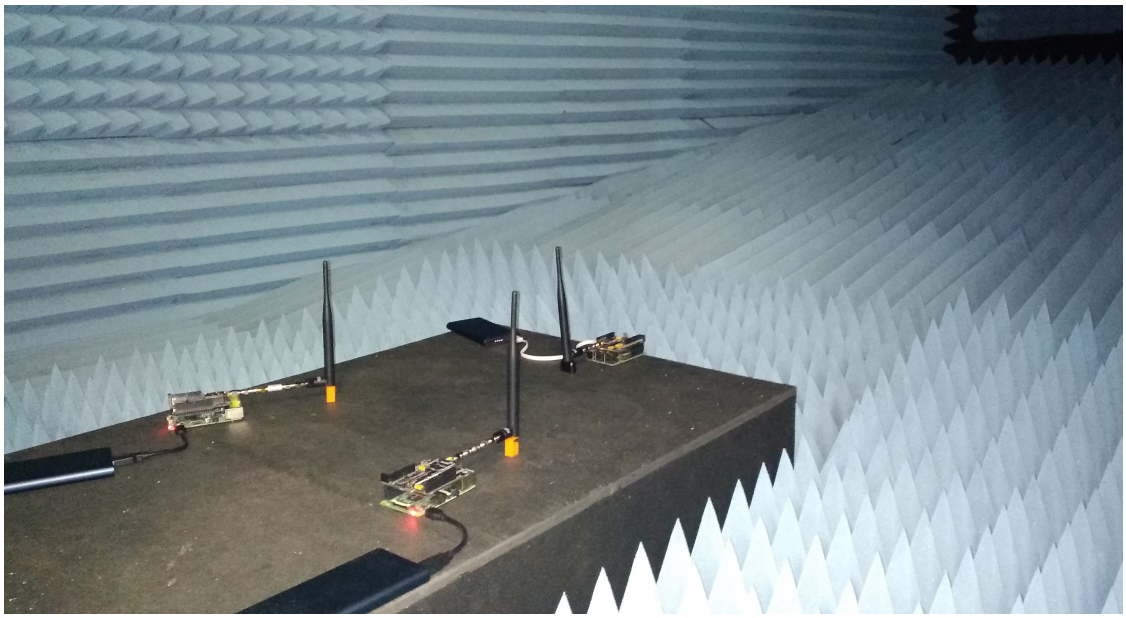

Figure 3.3: Experimentation setup with one gateway and two end-nodes.

much stable as possible over the course of successive transmissions, ensuring the validity of the characterization.

Each test started with the gateway being put on listening state, and having only one of the end-nodes sending packets continuously until the RSSI was stabilized on a desired value. An important aspect was attaining this value by adding/removing attenuators instead of changing the distance to the receiver, so that the results were not affected by a difference in the propagation time. When this was achieved, the procedure was repeated for the remaining end-node(s).

Only after the described setup phase the characterization was ready to begin. This procedure was repeated several times and for a different set of RSSI values, with 600 packets being sent per node in each scenario.

3.2.3 Success Assessment of Concurrent Transmissions

These tests aim to characterize the success of LoRa transmissions in the event of collisions, by representing the PDR obtained through realistic measurements.

3.2.3.1 Two LoRa Concurrent Transmissions

For the first round only two emitters were used, and the PDR values obtained are represented in Table 3.5. Tests were started with an RSSI gap of 5 dBm between the two transmissions. After realizing that this discrepancy was big enough so that the stronger transmission could be received with an average probability of 96% for several combinations of RSSIs with a gap of 5dBm, the RSSI gap was reduced.

The results show that the PDR of the strongest transmission decreases with the RSSI gap reduction until it reaches the average value of 29%, obtained when two concurrent transmissions arrive at the gateway with the same RSSI. When both emitters are on the same

Table 3.5: Packet Delivery Ratio based on packets' strength, for two concurrent end-nodes.

RSSI gap [dBm] / RSSI of weakest node [dBm]	5	3	2	1	0
-100	96%	96%	79%	62%	25%
-105	100%	98%	80%	64%	26%
-110	94%	98%	83%	62%	32%
-115	94%	96%	81%	57%	30%
-120	98%	98%	86%	59%	34%
Average	96%	97%	82%	61%	29%

conditions *i.e.* when the transmissions of both end-nodes are received with the same RSSI, for all packets received by the gateway, 43% were transmitted by one end-node and 57% by the other.

Given the experimentation conditions there is no reason for one node to have supremacy over the other, being safe to assume that for a higher number of repetitions these values would tend for a 50/50 situation. In all remaining scenarios, with an RSSI gap of 1dBm or higher, all received packets belonged to the node that had the stronger connection during the setup phase.

An important consideration to be taken from Table 3.5 is that the absolute RSSI value of each packet is not relevant to determine the success probability, being the discrepancy between the two the actual decisive factor.

3.2.3.2 Three LoRa Concurrent Transmissions

The characterization tests were repeated for a network topology with one receiver and three emitters. Since the absolute values of RSSI were shown to be irrelevant, for the three emitters test the only requirement was to keep the values within the range of interest, *i.e.* [-120,-95].

Table 3.6 presents the PDR depending on the gap between each of the interfering emitters and the reference one (dominant node).

Table 3.6: Packet Delivery Ratio based on packets' strength, for three concurrent end-nodes.

RSSI gap of end-node #2 [dBm] / RSSI gap of end-node #1 [dBm]	0	1	2	3
0	8%	18%	24%	24%
1	-	41%	50%	55%
2	-	-	73%	78%
3	-	-	-	92%

3.3 Probabilistic Model

The characterization described in the previous section, following a rigorous and exhaustive evaluation process, allows for the estimation of the probability of success of a given transmission, as a function of the strength of both the emitter and the interferer to the receiver.

3.3.1 Probability of success with one interferer

Summarizing the information from Table 3.5, when two concurrent LoRa transmissions exist, the following holds:

- When both transmissions have the same RSSI: 71% chance of losing both packets, 29% chance of one arriving (with the same probability for each of them);
- With an RSSI gap of 1 dBm: 39% chance of losing both packets, 61% chance of the strongest packet arriving;
- With an RSSI gap of 2 dBm: 18% chance of losing both packets, 82% chance of the strongest packet arriving;
- With an RSSI gap of 3 dBm or higher: 3% chance of losing both packets, 97% chance of the strongest packet arriving.

These approximations are inline with many works on the subject, like [58], which presents a Frame Error Ratio (FER) of approximately 70% for a scenario with SIR equal to 0. It also states that, if the power of the reference stream is at least 3 dB higher than the interferer, the FER obtained is below 2%, which is very close to the 3% verified in the tests performed.

The work in [43] claims that, depending on the placement of the nodes and channel conditions, the coverage probability obtained is within 25% to 48% when dealing with the same SF interference, and [44] admits a FER higher than 50% in synchronized concurrent transmissions with the same SF, scenario adopted for this experimentation as well.

Modeling collisions this way contradicts however the common mention [63, 64] that one transmission can be successful over the other if received with a least more 6dB of difference, showing that considering this threshold value is pessimistic modeling.

3.3.2 Probability of success with multiple interferers

When overlapping with multiple interfering signals, the likelihood of a successful signal decoding at the gateway decreases, in comparison to the scenario with one single interferer.

From the results represented in the previous two tables one could assume that the probability of success when dealing with multiple interferers can be calculated by multiplying the PDR values obtained in the characterization with a single interferer scenario, *i.e.*, a packet arriving at the gateway at the same instant as two other weaker packets, one with 2dBm gap and the other with a 1dBm gap, would have a probability of being decoded equal to $61\% \times 82\% = 50\%$, which is coincident with the PDR obtained experimentally for that exact same situation. Extending this assumption for all the RSSI combinations tested with 3 concurrent transmissions, the values from Table 3.7 can be obtained.

By comparing the approximated values with the ones obtained experimentally, it is seen that the error introduced by this estimate is considerably small.

Table 3.7: Approximation of Packet Delivery Ratio for three concurrent end-nodes.

RSSI gap of end-node #1 [dBm] \ RSSI gap of end-node #2 [dBm]	0	1	2	3
0	8%	18%	24%	28%
1	-	37%	50%	59%
2	-	-	67%	71%
3	-	-	-	94%

Assuming that this behaviour is similar when the amount of overlapping packets is higher than three, it is possible to estimate an approximation for the Packet Delivery Ratio of any number of concurrent LoRa transmissions, which is given by

$$PDR \approx \prod_{j \in J} PDR_j, \tag{3.1}$$

where J is the set of weakest end-nodes transmitting at the same instant as the reference end-node, and PDR_j is the PDR between the reference end-node and end-node j. Expression (3.1) is written from a network standpoint, meaning that in the event of more than one dominant node (interferers with the same connection strength as the reference), the probability of success obtained is divided equality among them. For simplicity, this model assumes that it is irrelevant which device started the transmission or how big the time overlap is, since all tests were performed with completely overlapping packets.

3.4 Chapter Considerations

This chapter detailed one of the main achievements of this dissertation, obtaining a probabilistic model that characterizes the success of concurrent transmissions in LoRa due to the capture effect verified in its modulation. Both the setup and methodology used for characterization the process are described, as well as the results presented in terms of PDR.

Later, the results are transposed into a probabilistic model. Throughout the remainder of this document, the derived packet collision model will be used to verify the impact that this distinct aspect of LoRa modulation, often overlooked, has on the performance of LoRa networks with different characteristics, on parameters such as capacity or fairness.

The next chapter focuses on Medium Access Control in LoRa, proposing some improvements to LoRaWAN, which is the state of the art MAC Layer adopted for the technology.

Chapter 4

Medium Access Control in LoRa - The Use Of Control Packets

This chapter concerns the medium access in LoRa networks, using LoRaWAN as a starting point, proposing as an alternative, a reservation based MAC protocol using control packets. Section 4.1 lists some reasons as to why the use of control packets for medium access in LoRa networks would be beneficial. Section 4.2 proposes an adaptation of the simple pure-ALOHA scheme used by LoRaWAN, creating the RTS-LoRa. The operation mode of RTS-LoRa is explained and some comments are made from an energy consumption standpoint. The chapter ends with Section 4.3 presenting the chapter considerations.

4.1 The Importance of Control Packets

It is a well known fact that, allowing many users to use the same radio channel without coordination, inevitably leads to packet collisions. LoRaWAN deals with collisions by adding a random backoff time for the end-node after each communication (in addition to the mandatory duty-cycle restriction), so that nodes involved in a collision have a chance to deliver its packet on the next transmission. The LoRaWAN specification [65] does not specify a maximum value for the backoff, leaving it at the user's discretion. Naturally, allowing random access to a high number of users will still lead to a high collision count.

This issue, even if not fully resolved, can be alleviated by the inclusion of a control packet sent as broadcast preceding every data message, in order to warn the remaining nodes that a data transmission is about to take place and for how long. Control packet collisions, although possible, are much less likely due to smaller packet size, and consequently less time-on-air.

4.1.1 Improving Network Throughput

Contention-based protocols such as ALOHA or CSMA suffer from low throughput due to packet collisions (*i.e.* the maximum throughput achieved in pure-ALOHA is 18% [57]). Even if, as shown in the preceding chapter, overlapping transmissions in LoRa can frequently lead to the successful reception of one packet at the gateway, the event of a collision will always imply an unnecessary delay in the delivery of information by the node that has lost the access.

This delay is aggravated by the fact that LoRaWAN operates in the ISM Frequency Bands, whose regulations regarding maximum duty-cycle obligate devices to include an interval of

silence between successive transmissions. Limitations correspond to 1% duty-cycle, which taking into account the typical LoRa low data-rates, can in some cases lead to minutes of wasted time because the message did not reach its destination. This being said, packet collisions should be avoided at *all costs* in order to make a good use of the channel and maximize the network throughput.

4.1.2 Increasing Network Fairness

The previous subsection referred to the throughput of the network as a whole, ignoring possible discrepancies between end-devices, occurrence that affects the network fairness.

In pure ALOHA networks the channel access is considered completely fair because, from the channel access management point of view, each end-node has the same probability of having a successful transmission. For LoRaWAN however, even when all nodes behave in the same way (considering all of them in the same power consumption class and using equal physical layer parameters), this cannot be stated, as the capture effect found in LoRa's modulation privileges nodes with a stronger connection to the gateway(s).

In densely populated scenarios, it cannot be expected that all devices maintain similar signal quality when transmitting data, which can lead to the nodes in the most adverse conditions (whether long distance, current moving speed or obstacles in the path to the gateway) having little to no channel access opportunities. It can be anticipated that fairness decreases as the network scale grows, and with it the occurrence of collisions. By broadcasting a control packet before each data transmission this issue could be mitigated, providing nodes in disadvantaging situations with a higher likelihood of successful transmissions.

In this work fairness will be assessed in terms of throughput comparison, by using Jain's Fairness Index [66], an expression that evaluates the network based on the individual throughput of each node, and given by

$$\jmath(x_1, x_2, ..., x_n) = \frac{(\sum_{i=1}^{n} x_i)^2}{n \times \sum_{i=1}^{n} x_i^2}. \tag{4.1}$$

In this expression, n is the total number of nodes in the network, and x_i is the channel access opportunity for the ith node. The result of this expression ranges from $\frac{1}{n}$ (worst case scenario) to 1 (completely fair network, with every user receiving the same allocation time). A situation with a total of n nodes where k users equally share the resource and the remaining $n - k$ are totally deprived of it would result in $\jmath = \frac{k}{n}$.

4.2 RTS-LoRa - Reservation based MAC protocol

4.2.1 Overview

The proposed protocol adopts a typical LoRa network topology with a single gateway and multiple end-nodes. It aims to improve the performance of a pure-ALOHA scheme by including a Ready-to-Send (RTS) packet, notifying neighbors that a transmission will take place. This way, the remaining nodes are able to readjust their access time window to try to access the channel, avoiding collisions.

When not transmitting, devices are in one of two states: *Listening State*, so that it is possible to receive RTS messages coming from other nodes, and *Sleeping State*, for when the

channel is known to be occupied or the end-node is forbidden to communicate for duty-cycle reasons. *Sleeping State* is used as much as possible in order to save energy.

The protocol characteristics can be summarized as follows:

- End-nodes decide whether or not to send data based on the overheard RTS messages;
- Does not use burst transmissions, a single packet is sent at each instant;
- Acknowledgement packets are not used;
- Packet retransmissions are never used;
- RTS messages contain information regarding the size of the following data packet, allowing neighbours to calculate the minimum backoff time;
- Backoff time is composed of both sleeping periods and listening periods.

Figure 4.1 exemplifies the use of Ready-to-Send messages according to the aforementioned considerations, in a scenario with three end-nodes competing for channel access.

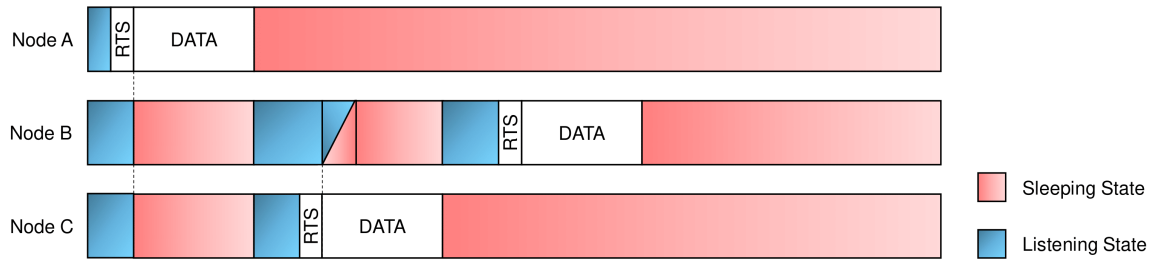

Figure 4.1: Summarized functioning of RTS-LoRa protocol.

Node A first gains access, forcing nodes B and C to backoff for at least the duration of the transmission. For this amount of time, calculated according to the data message size, B and C have no need to be listening since the channel will be occupied, so both enter *Sleeping State*. A random extra backoff time is calculated to prevent end-nodes from attempting to send RTS at the same time afterwards, period in which devices must listen to the medium to assess its availability.

The random backoff time added to node C is smaller than the one calculated by node B, which grants access to node C. The reception of the RTS message causes node B to readjust its backoff time, abandoning the *Listening State* earlier than predicted, entering *Sleeping State*. Later, unopposed this time, Node B is able to transmit its packet.

The shown behaviour is possible by assuming that at all times the end-devices are capable of hearing each other's messages. However, even with the long range achieved by the technology, this scheme can still suffer from the hidden terminal problem [67], meaning two devices in communication range to the gateway might not be in range of each other (Figure 4.2), thus being unable to communicate among themselves. This inconvenience will be addressed on the next chapter.

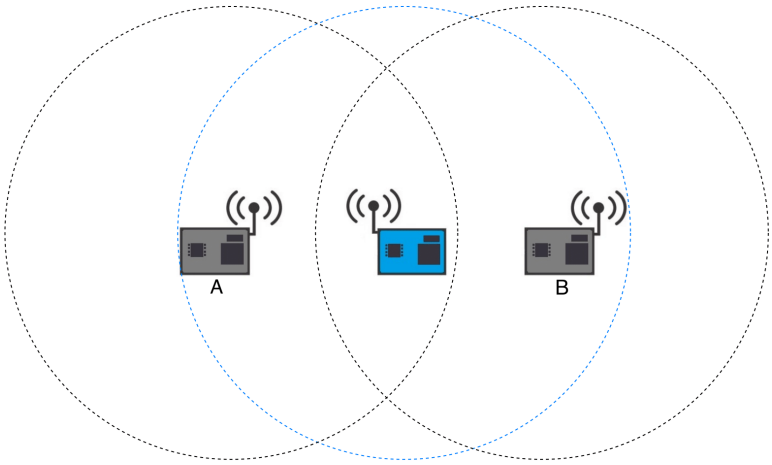

Figure 4.2: Hidden terminals problem.

4.2.2 Packet Structure

The packet structure adopted is the one defined by the SX1272 LoRa module support library, shown in Table 4.1. This structure has many fields to be filled by the user or the application:

Table 4.1: LoRa Base Packet, from [60].

dst	src	packnum	length	data	retry
(1 Byte)	(1 Byte)	(1 Byte)	(1 Byte)	(Variable Bytes)	(1 Byte)

dst - Destination node address: this parameter is indicated as an input in the function used by the user;

src - Source node address: this parameter is filled by the application with the module's address (previously set by the user);

packnum - Packet number: this parameter indicates the packet number and is filled by the application. It is a byte field, so it starts in 0 and reaches 255 before restarting. If the packet is trying to be retransmitted, the packet number is not incremented;

length - Packet length: this parameter indicates the total packet length and is filled by the application;

data - Data to send in the packet: It is used to store the data to send to other nodes. All the data to send must be stored in this field. Its maximum size is defined by MAX_PAYLOAD, a constant defined in the library;

retry - Retry counter: this parameter is filled by the application. It is usually equal to 0. Only when we use the retries feature, this value is incremented from 0 to the maximum number of retries stored in the global variable _maxRetries which value is 3 by default. If the packet is sent successfully, or if the maximum number of retries is reached without success, the retry counter is set to 0.

4.2.2.1 RTS Message

As referred, the single purpose of the RTS message is to warn neighbours that a node is in fact ready to send information to the gateway so they can postpone their upcoming transmissions. The efficiency of this method depends greatly on the ratio between data and control packet lengths. This, along with the 1% duty-cycle restrictions, makes it of major importance for the network performance that the control message used is as small as possible.

Figure 4.3 details the structure of the RTS message. In addition to the 5 bytes required by the LoRa library a header is included (which allocates 4 bytes), composed only of essential information:

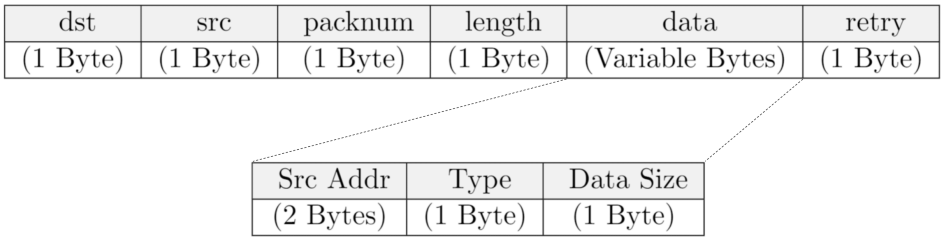

Figure 4.3: RTS message structure.

Source Address - With a size of 2 bytes, this field contains the source node identification;

Type - Single byte field that identifies if this is a MAC packet or a data packet;

Data Size - This field contains information regarding the size of the following data packet, so that the other nodes can calculate the minimum backoff time necessary accordingly.

This division allows 246 out of 255 bytes to be used for data transport.

4.2.3 MAC Process

When a node is ready to send a data packet, it starts by broadcasting a RTS message. By containing the amount of bytes of the following data packet, this message allows the remaining nodes to estimate the time the transmission will take.

Tests performed in [68] using the SX1272 LoRa module showed that the time-on-air of a packet varies linearly with its size. This relation, for each of the 10 operation Modes, is presented in Figure 4.4. From the information presented it is possible to obtain a linear regression for every Mode, allowing for an estimation of the time-on-air using the packet size in bytes and the operation Mode as inputs.

This calculated time-on-air corresponds to the *obligatory backoff time* represented in Figure 4.5, period in which nodes have no need to listen to the medium and are allowed to sleep in order to save energy. When this time is fulfilled, the devices are obligated to switch to and remain in *Listening State* for a random amount of time. To maximize the probability of success this additional time is divided into n slots, with one slot corresponding to the time-on-air of a RTS message.

Thus, each node calculates its own backoff time according to

$$backoff = ToA(Data\ Size, Mode) + randi([0\ n]) \times ToA(RTS\ Size, Mode), \tag{4.2}$$

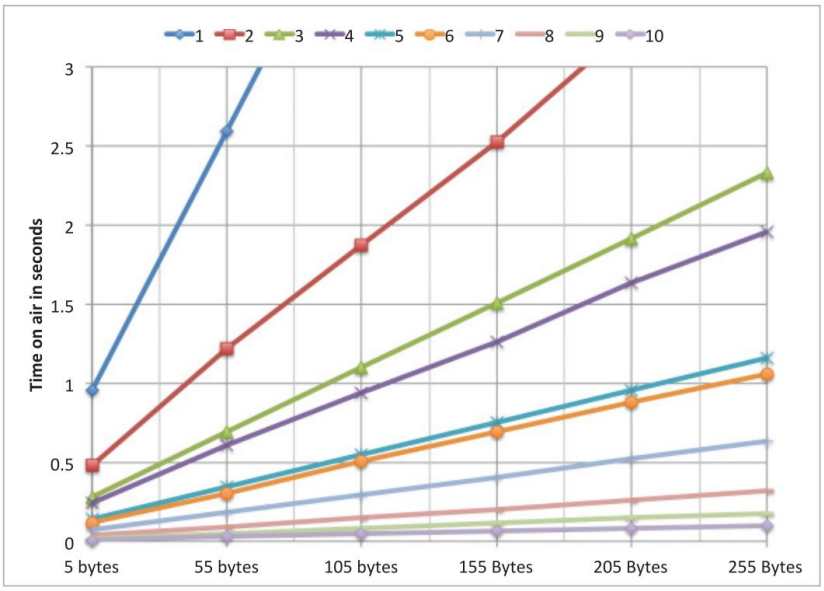

Figure 4.4: Packet time-on-air depending on payload size and operation mode, from [68].

where $randi[0, n]$ outputs a random integer between 0 and the maximum number of slots.

In the event of another RTS being heard while the node is in *Listening State*, the backoff time is adjusted accordingly. If nothing is received two things may occur: either the node accesses the medium, or if at the moment it has no information to send, goes into *Sleeping State*. The amount of time spent sleeping is chosen depending on the packet generation periodicity to maximize efficiency, but it is crucial that before it tries to access again some time is spent in *Listening State*, checking the channel availability. The described medium access flow can be seen on Figure 4.6. Next to it the behaviour of LoRaWAN end-devices is also presented.

RTS-LoRa takes into account the energy expenditure of the end-nodes by allowing them to be in *Sleeping State* whenever possible. Even so, devices have a higher consumption than Class A LoRaWAN end-nodes - the least energy consuming class due to limited downlink

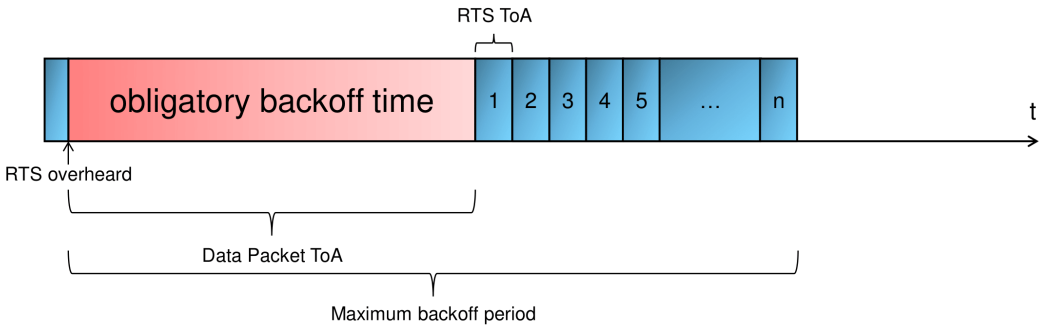

Figure 4.5: Node backoff process after receiving a RTS message.

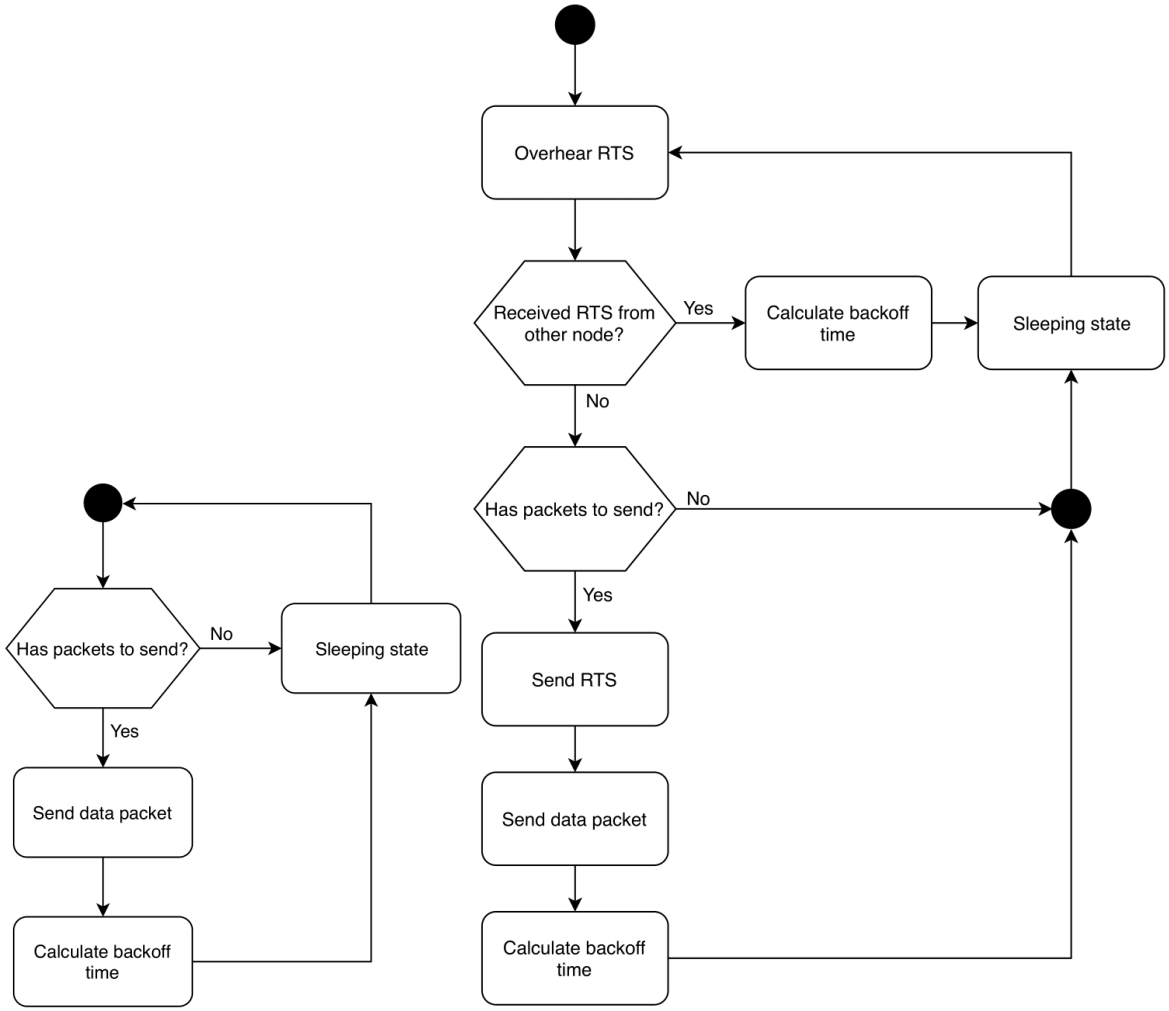

(a) Pure-ALOHA medium access.

(b) RTS-LoRa medium access.

Figure 4.6: Medium access flow.

windows - due to the constant need to listen to the channel, waiting to receive RTS messages.

Therefore, a shorter battery lifetime is the price to pay for the introduction of the RTS packet, in comparison to the simple scheme detailed in Figure 4.6a. However, it should be noted that this MAC protocol differs from LoRaWAN Class B, since synchronization with the gateway is not necessary.

4.3 Chapter Considerations

This chapter addressed the Medium Access Control in LoRa, and analysed the current standard protocol used by the technology, as well as its main drawbacks.

A simple solution - RTS-LoRa - is proposed and explained: a MAC protocol whose base idea is the inclusion of a broadcast message to reduce the high collision count inherent to pure-ALOHA schemes. The structure of the created control message is presented, as well as

the behavior of end-nodes in the medium access.

Some considerations from this chapter are crucial for the final protocol proposed in this dissertation, with RTS-LoRa serving as a halfway point to the LoRa Mode Adaptive Protocol (LoRa-MAP) to be presented in the next chapter.

Chapter 5

Adaptive MAC Protocol for LoRa

This chapter describes, in detail, LoRa-MAP, a MAC protocol for LoRa networks designed to be adaptive to network characteristics. Section 5.1 presents an overview of the protocol, listing both characteristics and the main reasons for its development. Section 5.2 explains the multi-mode medium access scheme, as well as its specific messages. Section 5.3 provides an explanation on how end-nodes compute their ideal operation mode and, from the gateway point of view, it is described which information is stored and constantly updated, and the process of mode switching. Section 5.4 concerns the impact of using different transmission configurations on the fairness of the network. Section 5.5 concludes the chapter.

5.1 Protocol Description

LoRa-MAP, which stands for LoRa Mode Adaptive Protocol, is a medium access control protocol that explores the idea of adapting the LoRa physical parameters (i.e. SF, BW) according to the strength of the connection of each end-node to the gateway.

5.1.1 Motivations

Medium Access Control is a crucial aspect in high-dense networks, as stated in the previous chapter. A MAC protocol must exist in order to maintain the network reliability and ensure that the information is exchanged successfully. LoRa-MAP was created not only to prevent packet losses, but also to improve other aspects of the network, such as having a more efficient time allocation, crucial for scalability purposes, and a lower power consumption per device, aiming to increase their battery lifetime.

The two medium access schemes detailed in the previous chapter do not account for the use of different physical layer parameters. Although this brings simplicity, some problems arise. As it is important to offer coverage to a wide-area, the parameters chosen must provide a high sensitivity. If not, only devices in close proximity to the gateway would be able to communicate with it, nullifying the purpose of even using a LPWAN.

In LoRa, configurations that allow robustness and long distance communications are known to have the slowest data-rate and highest energy consumption, meaning that the use of LoRaWAN or RTS-LoRa with a single mode of operation will lead to most devices having an unnecessarily shorter battery lifetime and throughput. The introduction of the Adaptive Data Rate (ADR) technique in LoRaWAN deals partially with this problem, modifying the

transmission power and SF over time when necessary. If an end-node notices that a certain amount of consecutive transmissions are not followed by a downlink response, connectivity loss is assumed and the transmission power is gradually increased. Afterwards the same is done for the SF until the connection is restored. The opposite occurs when the link quality calculated from recent transmissions is much higher than the receiver sensitivity, in order to enable faster and less energy consuming transmissions.

However, this mechanism reportedly requires a number of hours to days to converge to a reliable and energy-efficient communication state [69], being specially slow when the link quality degrades and the end-node needs to regain connectivity by increasing the value of SF and the transmission power. The lack of agility of this model leads to a high number of packet losses.

Other than the aforementioned considerations, this scheme has some inconvenient obligations, such as the necessity of downlink messages in order to acknowledge the delivery of packets to the gateway, which greatly limits the gateway's duty-cycle. In order to use the ADR technique described, it is also required that the gateway is able to listen in multiple SFs, since end-nodes are allowed to freely increase and decrease its SF value without pre-coordination. Since the solution proposed is aimed to be used with single-channel gateways (devices that are not LoRaWAN compliant), it is impossible to use a similar strategy.

The mechanism proposed consists on using three different predefined configurations, called modes, each one providing a different tradeoff between data-rate and sensitivity. The gateway must switch between these three modes of operation as Figure 5.1 suggests, alternately, thus allowing an appropriate connection to a certain group of devices.

One of the modes, *standard*, exists for transmissions made by nodes under the most adverse conditions, privileging sensitivity. There is a mode used for devices with very good connection to the gateway, *fast-rate*, capable of transmitting data at a high bit rate. Finally, a third mode exists, *mid-rate*, which is a compromise between the previous two (*i.e.* not as slow as *standard*, but with a higher sensitivity than *fast-rate*).

Such system enables connectivity to mobile nodes moving at high speed, stations located far away from the gateway or with numerous obstacles located in the transmission path, by using *standard*, but does not force the inherently long time-on-air from this mode to devices with a better connection, as it happened with RTS-LoRa. Using the same parameters for the communications of every node, together with the mandatory 1% duty-cycle restriction, would greatly affect the network capacity. The idea is to use more appropriate modes whenever possible, reducing the waiting time imposed by regulations.

By having end-nodes divided by operation mode, at the time of transmission each device will only compete with those using the same mode. For large-scale networks, this is determinant to reduce the packet loss due to collisions, providing network separation (in the time domain).

The optimal mode calculation for a device is done taking into account its connection quality to the gateway, which means that there is a decrease in the occurrence studied in Chapter 3, of packets received with higher RSSI having supremacy over weaker ones in the event of a collision. This contributes positively to the fairness of the network.

Through the prioritization of modes with lower time-on-air whenever possible, LoRa-MAP is expected to achieve higher capacity and lower energy consumption than protocols that always maintain the same physical parameters.

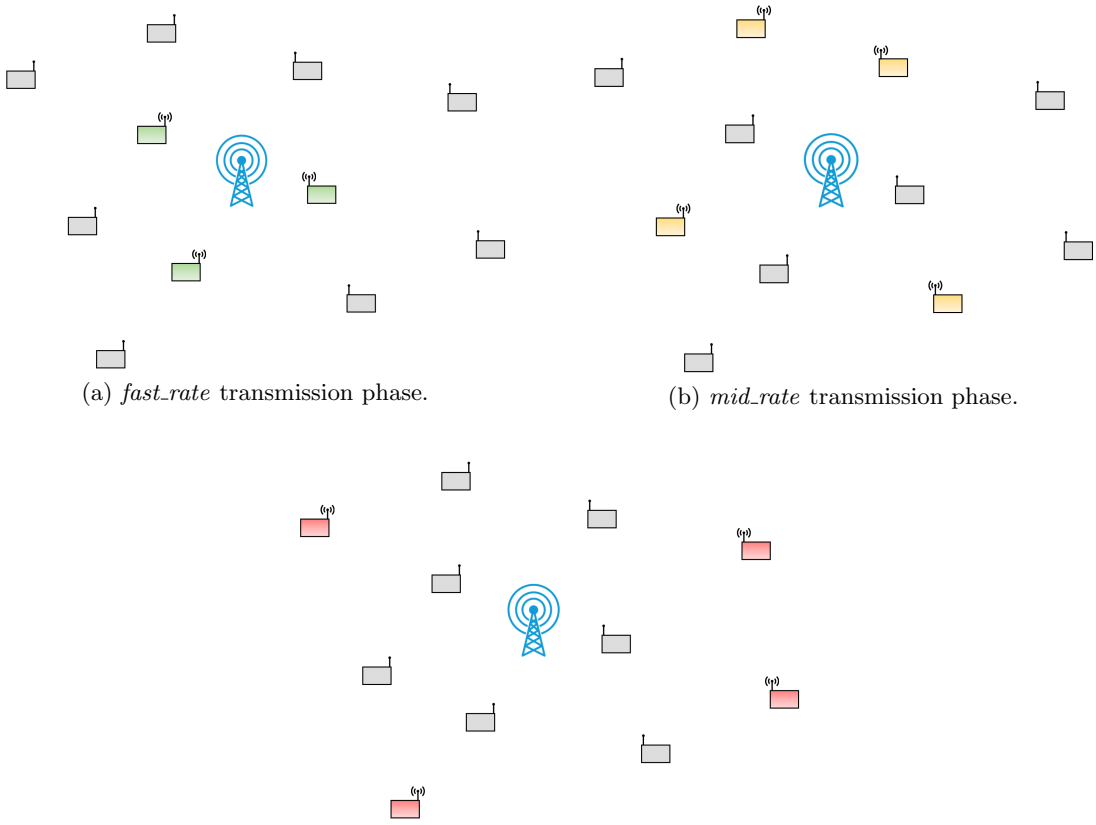

(a) *fast_rate* transmission phase.

(b) *mid_rate* transmission phase.

(c) *standard* transmission phase.

Figure 5.1: LoRa-MAP Operation.

5.1.2 Characteristics

The protocol works cyclically, with the gateway alternating between the 3 modes dynamically to allow fair access to every element of the network. The gateway keeps and constantly updates information (exchanged in control messages) on the intervening devices, in order to decide the amount of time assigned to each of the modes at a time. This makes the network scalable and of easy adaptation to different scenarios.

An overview on the characteristics of LoRa-MAP is presented:

- Considers only single gateway scenarios;
- Nodes decide whether or not to send data based on the overheard control messages;
- Does not consider burst transmissions, a single packet is sent at each instant;
- Acknowledgement packets are not used;
- Packet retransmissions are never used;
- Every data packet is preceded by a control message;
- Downlink messages are used for the sole purpose of the gateway announcing a mode change;

- *Standard* is, as the name shows, the default mode of operation, and each mode change must go through it first (*i.e.* it is not allowed to switch from *fast-rate* to *mid-rate* directly, or vice-versa);
- The gateway sends messages only when using the default mode, *standard*;
- End-node's backoff time is composed of both sleeping periods and listening periods.

5.2 Dynamic Medium Access

Looking at any of the modes separately, the medium access works in a similar way to RTS-LoRa, described in the last chapter. A simple scheme is used with nodes broadcasting a control message when they have data to send, warning neighbors that a transmission is about to take place. The complexity of the proposed protocol is in the mode change phase and not in the data exchange process.

Two LoRa devices cannot communicate with each other without using the same configuration, so in order to implement a multi-mode scheme, it is required a bi-directional exchange of control packets. The gateway must be able to communicate to the entire network which mode will be used and for how long, while end-nodes need to provide the gateway with information on what mode would be ideal for their data transmissions.

5.2.1 Control Messages

Two specific control packets have been created to handle the MAC process, one used by the gateway (downlink) and another used by the end-devices (uplink):

Intent Message (IM) - Broadcast sent by a node that is ready to transmit data. If the current gateway operation mode is the appropriate one, this message serves the same purpose as a Ready-to-Send, warning neighbors with the same configuration that a data packet is about to be transmitted. However, if the gateway is set to *standard* and a faster mode is beneficial, this message serves a mode change request. The node then waits for a response from the gateway, signaling that the request was attended (Change Message).

Change Message (CM) - Message sent by the gateway as a response to an IM, announcing that a mode change is about to occur. It is broadcasted so that all nodes can either adapt their configurations, or sleep if the advertised mode is not favorable. As mode change requests are always emitted in *standard*, this is the only mode in which the gateway transmits. Mode changes from other modes to the default are not advertised, as all the end-nodes know when it will happen because this information is present in the CM.

Following an approach similar to that of the RTS-LoRa, the control packets were kept as small as possible in order to minimize their transmission time. The structure of the messages created is shown in Figure 5.2.

Type - This field identifies the packet as data or a MAC message, and if the latest, which type of message it is. Six different identifiers are needed: data, two for CM (each

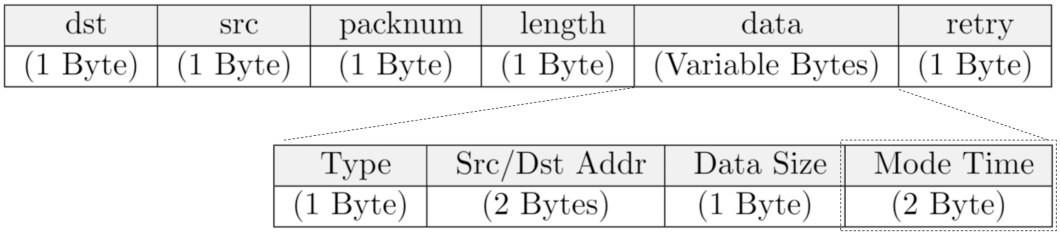

Figure 5.2: Control Messages Structure.

advertising a non-default mode), IM with no request to change the mode, and two for IM requesting a mode change, also one for each non-default mode;

Source/Destination Address - Composed by two bytes, this field contains either the source or destination of the message. It is possible to use it for both purposes alternately because the protocol was developed taking into account scenarios with only one gateway. In CMs it represents the address of the node that successfully requested the change, indicating that it can adapt its configuration and send the packet. For the remaining messages, it represents the source node's address;

Data Size - The Data Size field provides information regarding the size of the next data packet to be transmitted, so that the other nodes can calculate the minimum backoff time necessary accordingly;

Mode Time - Exclusively used in CMs, the Mode Time field expresses how long the gateway will remain configured for the advertised mode. This information is crucial, allowing every node to either adjust their sleep/backoff time, or to know how much time it will be spent in their ideal operation mode. After this time passes, the gateway returns no *standard*.

Figure 5.3 details a use case of LoRa-MAP control messages, with four end-devices competing for medium access.

Nodes A and C have *mid-rate* as the ideal mode of operation, whilst node B is able to use a faster bit-rate, with *fast-rate* being preferable. Node D has the weakest connection to the gateway, so it needs to resort to the long transmissions inherent to using the *standard* mode.

With the gateway currently in the default mode, node C sends an IM requesting a mode change to *mid-rate*. As the gateway confirms this change, node D enters the sleeping state for the advertised time (in the Mode Time field). Node B, due to preferring a non-default mode different than the requested, will enter sleeping state for a longer period of time, because changes from *mid-rate* to *fast-rate* and vice-versa never occur, as the gateway must return to *standard* first. Finally, node A sleeps only for the duration of the transmission, adjusting its access window to transmit afterwards.

In the previous chapter, the hidden terminals problem was pointed out, since RTS-LoRa relies on end-devices being able to hear each other in order for the medium access scheme to work properly. In LoRa-MAP this problem also exists, but as the IMs are also supposed to be received by the remaining nodes (while some are unreachable), CMs sent by the gateway are supposed to reach the entire network, guaranteeing a periodic coordination of every participating end-node.

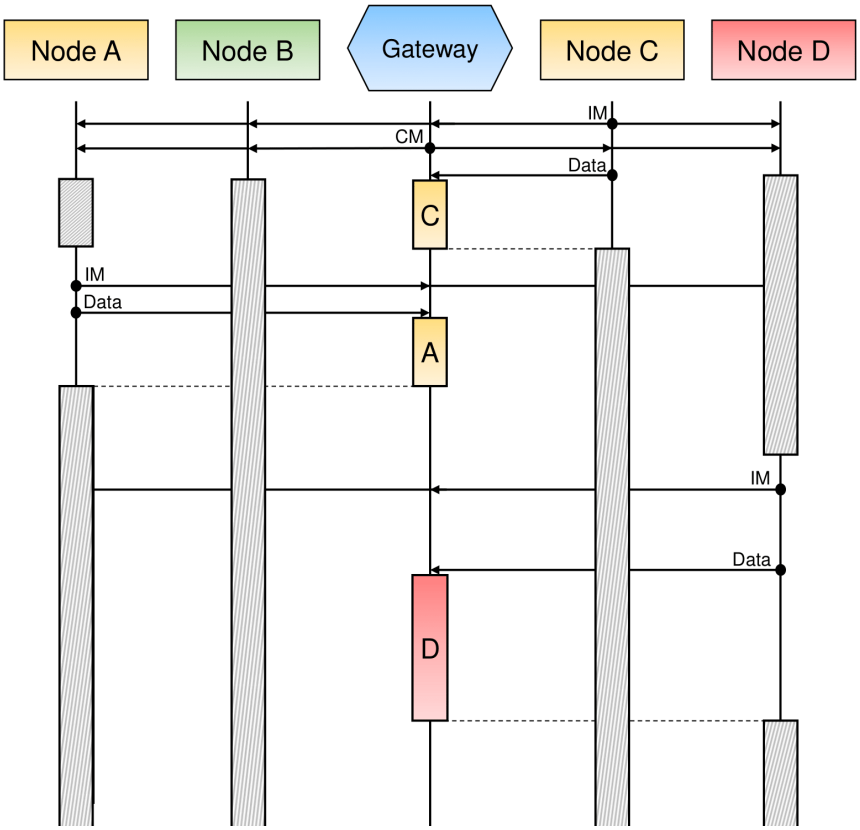

Figure 5.3: Use of LoRa-MAP control messages.

5.2.2 MAC Process

This section describes how the proposed MAC works.

5.2.2.1 Node side

When a node has data to send and the channel is available (indicated by an absence of recent Intent and Change messages), it starts by assessing its situation in terms of operation mode. To decide which IM needs to be sent at the moment, three variables are taken into account:

current_mode: indicates the node's configuration at each instant;

ideal_mode: shows which operation mode is ideal for the node at the moment. This value is updated with every CM received, based on the RSSI value;

gw_mode: represents the gateway's current operation mode, announced in the CMs. The Mode Time field also lets nodes know when the gateway returns to the default mode, *standard*.

When the gateway is operating in one of the fastest modes, *fast-rate* or *mid-rate*, all the end-devices in the network are either using that same mode or in backoff state, waiting for *standard* to be used again. This being said, only two situations can occur:

Node and Gateway using the same mode

In this situation, the node behaviour is exactly the same as in RTS-LoRa, sending an IM serving the purpose of a Ready-to-Send, followed by the data packet. After the transmission, the node enters a backoff stage, going into *Sleeping State*.

The decision to not include downlink messages in this scenario is due to the duty-cycle restrictions that the gateway would have to comply with. While a node being forced to stay sleeping over a long period of time does not affect the remaining devices in any way, if the gateway is unable to send messages that are essential to the reception of data (*i.e.* a RTS/CTS mechanism), frequent restrictions periods would lead to fewer packets arriving.

Node requesting a new mode while Gateway in *standard*

When an end-node is able to communicate with the gateway using one of the faster modes, it expresses its intention by sending an IM requesting a mode change. For the data transmission to take place, the node is dependent on the reception of a CM announcing that its request has been answered. If nothing arrives, the node backoffs and tries again later, after fulfilling the duty-cycle restriction due to sending the IM.

Upon reception of the expected CM, the node finally changes its mode to the one it requested. Since it is possible that more than one end-node requested a change to a given mode at the same time, the gateway indicates in the *DstAddr* field which device has permission to transmit immediately after the mode change. If the destination address of the CM packet does not correspond to the node's identifier but the mode is ideal, the node must backoff for a short amount of time, adjusting its access window to communicate at least when it is certain that the data transmission from the addressed end-node is complete.

If the mode announced by the CM is not the one intended, the node can backoff for a higher amount of time. A long period will be spent on sleeping state, since it is known that after using the announced mode, the gateway will need to remain in *standard* for some time, allowing connectivity to devices that need to use this configuration.

As described, there are several scenarios in which a node goes into backoff state. They can easily be divided into three situations: a backoff caused by the reception of a broadcast control message, a backoff calculated after transmitting a data message, and finally, a backoff due to an unanswered mode change request. All these scenarios have a minimum *obligatory backoff time* dictated by the specific situation (*i.e.* how long a data packet will take to transmit). However, in order to prevent future collisions, an extra amount of time must be added. This added time is divided into slots, as shown in Figure 5.4.

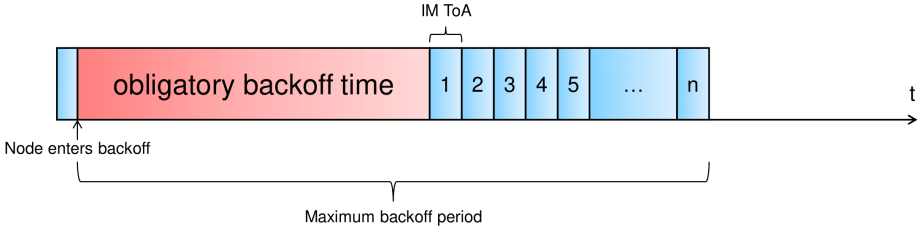

Figure 5.4: Node backoff process.

Each communication to be performed by the end-nodes starts with the transmission of an IM, which means that, when the end-nodes backoff and adjust the access window, they postpone the transmission of their next IM. This way, to minimize the likelihood of control message collisions, each time slot corresponds to the time-on-air of an IM transmission, in the current mode.

The random added backoff time for a node that finished transmitting data serves to prevent that two or more nodes, that sent colliding packets, from doing so again in their next attempt, with the same backoff scheme being utilized.

In this protocol, nodes calculate their own backoff time in a way similar to the described in the RTS-LoRa.

$$backoff = obligatory\ backoff\ time + randi([0\ n]) \times ToA(IM\ Size, current\_mode), \quad (5.1)$$

with n being the total number of slots.

The channel access flow is presented in Figure 5.5.

Node backoff state

The channel access flowchart details all the situations in which a node is prohibited from transmitting information. When this prohibition lasts for a long time, there is no need for the node to be in the listening state, consuming energy unnecessarily. For example, after a data transmission, the node is obliged to fulfill the $99 \times ToA$ restriction time. Also, when the gateway is using non-ideal modes, there is no interest in listening to the medium (with the exception of when requesting a mode change, in *standard*).

Usually, the *obligatory backoff time* is spent in sleeping state and the added time slots are for listening to the medium. There is, however, one specific situation in which this is not true, that is when the backoff is caused by another node sending an IM requesting a mode change. In this scenario, the remaining nodes must keep listening to verify if the mode will be changed or if the request is unanswered, and only then adjust their backoff accordingly.

Like in the channel access diagram, when a node listens to a CM announcing its mode of interest, it must change to this mode of operation, even if it will not be the next to transmit, and then calculate a new backoff time accordingly. Backoff time updates are also necessary when an IM is received and implies an *obligatory backoff time* higher than the nodes' remaining backoff time. Figure 5.6 details the behaviour of nodes in backoff state.

5.2.2.2 Gateway side

Unlike end-nodes, which can spend the majority of their time in sleeping state, the gateway needs to always be listening since at any given moment a node may be ready to transmit data. Interactions between nodes and the gateway always begin with the latest receiving an IM. If this message indicates that a data packet will be transmitted in the current mode, no further action is required and the gateway prepares to receive the information. On the other hand, if another mode is requested, the gateway must first assure that, by sending a CM announcing a new mode, the duty-cycle regulations will not be violated. It also needs to verify if the requested mode is allowed at the time, and if so, a CM is broadcasted and the mode altered

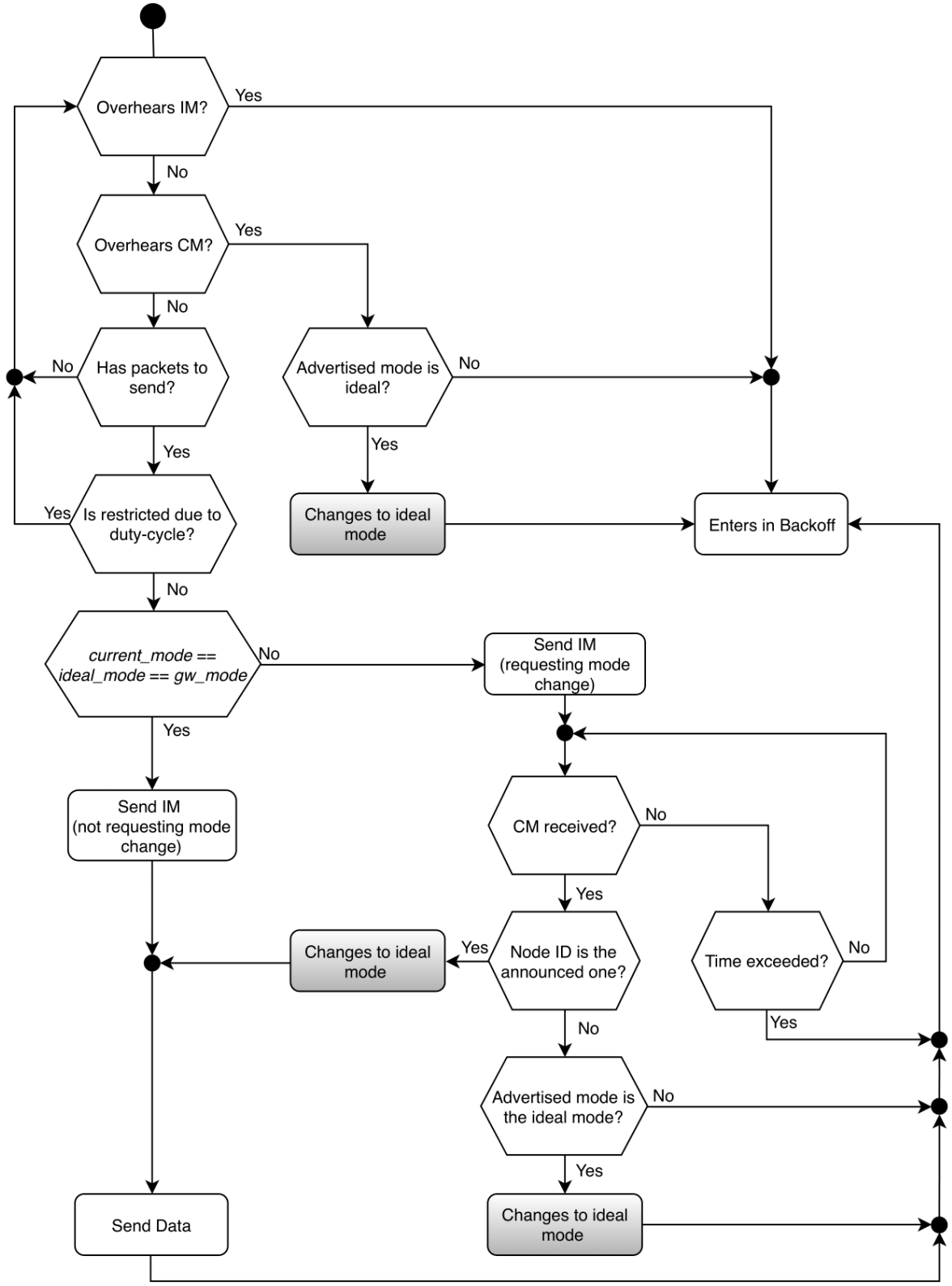

Figure 5.5: Node medium access behaviour.

afterwards. If these conditions are not met, the IM is ignored and the gateway continues using the default mode.

A non-default mode may not be allowed at the time if used too recently, because this would leave a group of devices - that transmit using the other non-default mode - without access opportunities. However, in normal conditions such requests do not occur, as the information presented in CMs allow every end-node to know when they should try to access the channel. This situation happens when CM packets are lost due to connectivity issues. The described

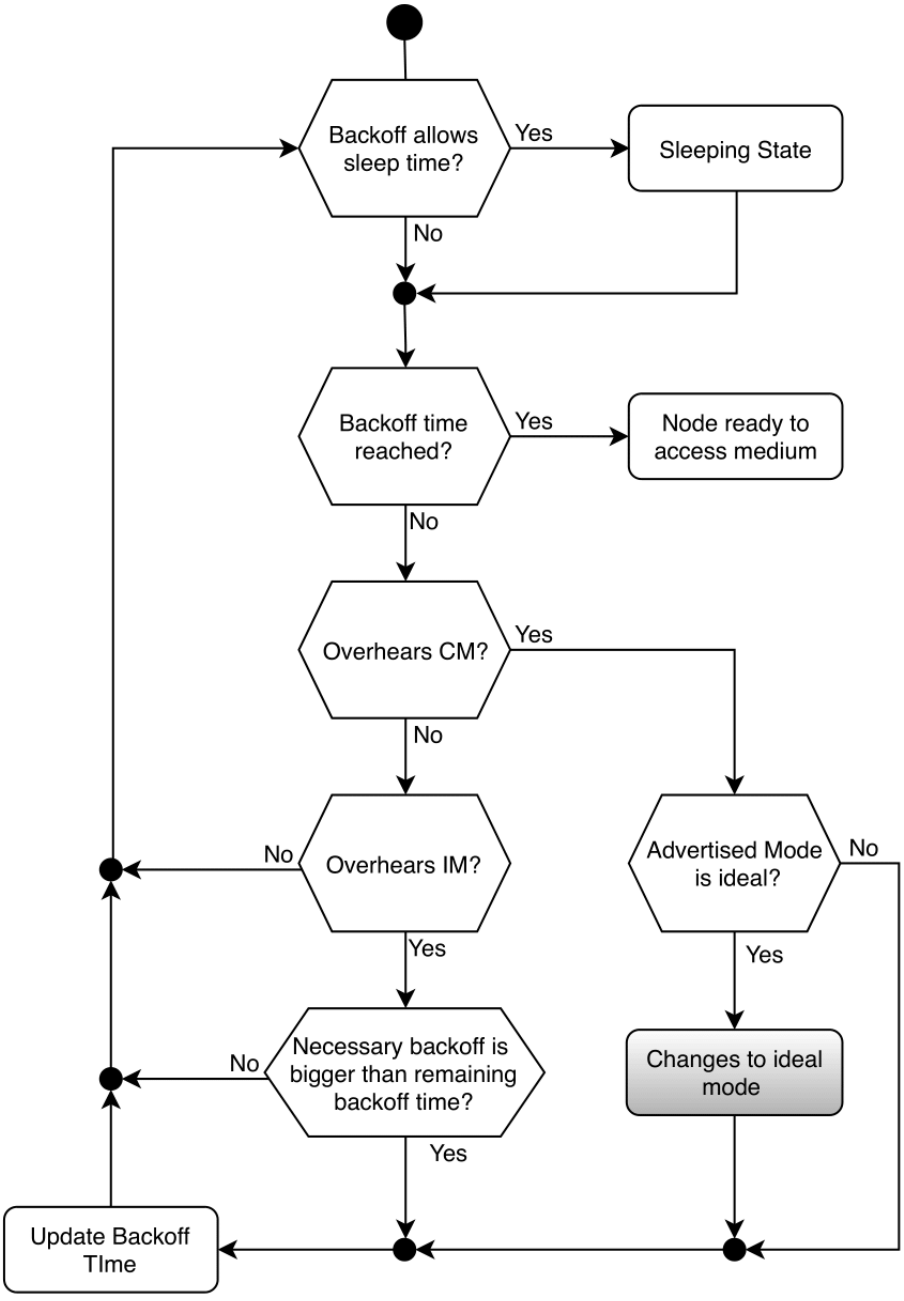

Figure 5.6: Node behaviour during backoff state.

behaviour of the Gateway is shown in Figure 5.7.

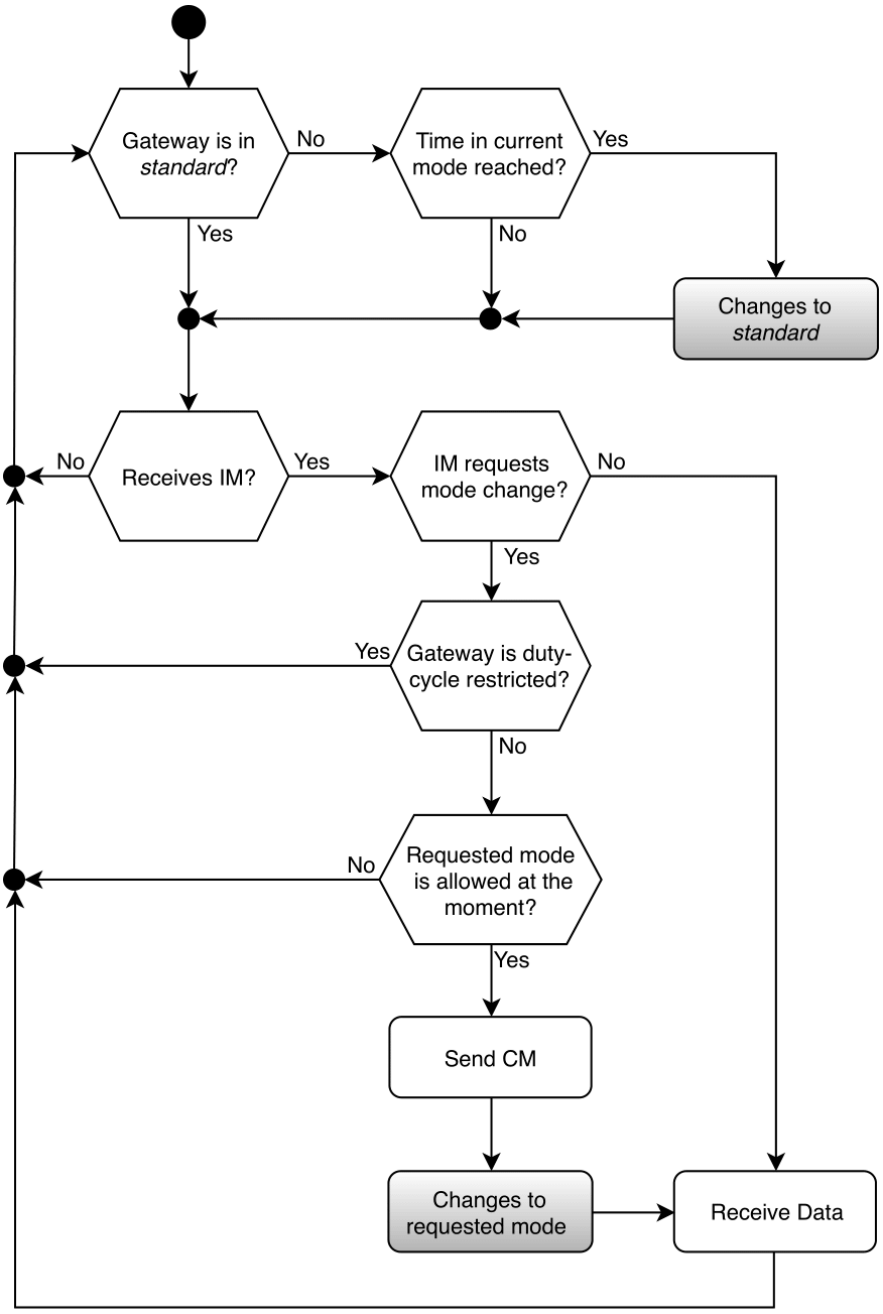

Figure 5.7: Gateway medium access behaviour.

5.3 Operation Mode Selection

LoRa-MAP counts with three distinct modes of operation that are used alternately, with each corresponding to a different configuration of the LoRa physical parameters. Three SX1272 LoRa Module pre-configured modes were utilized, Mode 3 for *standard*, Mode 7 for *mid-rate* and Mode 10 for *fast-rate*.

Since the primary motivation of using a multi-mode scheme is diminishing the packet transmission time as much as possible, for *fast-rate* it was chosen the configuration with the least time-on-air, Mode 10, to be used by nodes in very favorable conditions to communicate with the gateway.

For the opposite situation, when choosing *standard*, it was not followed a similar approach because Modes 1 and 2, although they offer a better sensitivity, imply a much higher time-on-air per transmission. For example, according to the information in [60], the transmission of a 100-byte packet lasts approximately 4.3 seconds in Mode 1 and 2.2 seconds in Mode 2, whilst in Mode 3 a packet with this size can be transmitted in 1.2 seconds. By selecting Mode 3 there is a good tradeoff between time-on-air and sensitivity, offering great connectivity range without highly sacrificing the data-rate.

Lastly, *mid-rate* was selected to be a middle ground between the other two. Mode 7 was chosen, being a compromise in terms of bandwidth, spreading factor and sensitivity.

The information about which specific physical layer parameters are used for each of the modes can be found in Table 5.1.

Table 5.1: SX1272 module operation modes.

Mode	Bandwidth (Hertz)	Coding Rate	Spreading Factor	Sensitivity (dB)	Description
1	125	4/5	12	-134	
2	250	4/5	12	-131	
3	125	4/5	10	-129	*standard*
4	500	4/5	12	-128	
5	250	4/5	10	-126	
6	500	4/5	11	-125.5	
7	250	4/5	9	-123	*mid-rate*
8	500	4/5	9	-120	
9	500	4/5	8	-117	
10	500	4/5	7	-114	*fast-rate*

It is up to the end-node to decide which mode is the best to use at any given time by assessing the strength of the connection to the gateway, measured through the reception of downlink messages. The gateway gathers information from the network, and knowing the ideal configuration for each node, it manages the time distribution.

As tests were performed in order to obtain a relation between packet size and time-on-air for each the 10 SX1272 module operation Modes [68], using expressions (5.2), (5.3) and (5.4) it is possible to estimate the transmission time of the control messages. This information is shown in Table 5.2.

$$ToA(standard) = 10.25 \times \ dataSize(bytes) + 194.3ms. \tag{5.2}$$

$$ToA(mid\text{-}rate) = 2.96 \times \ dataSize(bytes) + 48.88ms. \tag{5.3}$$

$$ToA(\textit{fast-rate}) = 0.54 \times \ dataSize(bytes) + 7.53ms. \tag{5.4}$$

Table 5.2: Time-on-Air and inherent duty-cycle restriction of each control message.

Control Message	**Time-on-Air**	**Restriction period (99*ToA)**
$\text{CM}_{standard}$	307.05ms	30.40s
$\text{IM}_{standard}$	286.55ms	28.37s
$\text{IM}_{mid-rate}$	75.52ms	7.48s
$\text{IM}_{fast-rate}$	12.39ms	1.23s

5.3.1 Ideal Mode of Operation

The process of deciding the ideal mode is of major importance for the good operation of the LoRa Mode Adaptive Protocol. If this mechanism is flawed, end-nodes may end up using a mode that will unnecessarily prolong their transmissions, or worse, mistakenly assume they are in a good condition to use high data-rates, leading to connection loss and not being able to send information to the gateway.

There are many factors that affect the link quality, such as: distance between emitter and receiver, the velocity of both parties during the transmission, difference in altitude, obstacles in the transmission path and environment conditions, such as rain or temperature.

It is possible to predict the impact that these variables have on the RSSI of transmitted packets (*i.e.* the received signal strength decreases more or less linearly when increasing distance between the devices), but since the list of factors affecting the signal strength is long, it becomes hard for a communicating device to predict RSSI based on these metrics.

For the reasons mentioned, it was decided that nodes would calculate their ideal mode based on real RSSI measurements obtained in recent downlink messages. CMs are sent very often by the gateway, meaning that end-nodes do not stay long without updating their ideal mode. If because of the network characteristics the CMs are not as frequent, additional messages are sent just to allow all devices to verify their current connection. This procedure is described in the following subsection.

5.3.1.1 Multi-mode connectivity tests

End-nodes will decide which mode is ideal based on the RSSI of received gateway messages. For this reason, real tests were performed in which two devices start by establishing communication using the *standard* mode, and afterwards its connection is evaluated while using the remaining modes, without changing the transmission conditions.

The equipment and methodology used for the connectivity tests were the same as the ones used in Chapter 3, however with a single transmitter and with the RSSI fixed on specific values. After the setup phase (using the SX1272 module's Mode 3) and without changing the transmission conditions, the remaining Modes were evaluated (7 and 10), registering PDR and average RSSI.

With a total of 50 packets of 100 bytes transmitted for each test, the results obtained are displayed in Table 5.3, where the left column details the RSSI at the setup phase.

Table 5.3: Multi-mode connectivity results.

Mode 3	**Mode 7**		**Mode 10**	
RSSI(dBm)	avgRSSI(dBm)	PDR	avgRSSI(dBm)	PDR
-95	-95	98%	-95	98%
-100	-99	98%	-99	100%
-105	-104	100%	-103	94%
-110	-108	100%	-114	96%
-115	-120	94%	-119	10%
-120	-122	98%	—	0%
-125	-126	24%	—	0%

These results are in line with the specified sensitivity for Modes 7 and 10, -123dBm and -114dBm respectively, since when the RSSI drops beneath these values, most of the packets are lost. It is also noticeable that, as the RSSI value approaches the theoretical sensitivity, the average strength of the transmissions becomes generally worse than when using Mode 3.

As referred before, it is imperative that end-nodes do not end up being too optimistic, operating in modes that are not adequate to their current situation. Furthermore, in the conditions that LoRa-MAP is proposed to operate, it can often happen that the mode calculation is done well in advance of when the data transmission will take place, with a possible decrease in signal quality occurring in the meantime. After analysing the test results, it was considered that a mode is fit for a given RSSI value only when the PDR is close to 100% and the average RSSI measured is not lower than the one registered with Mode 3. The allocation of modes per RSSI of downlink messages in the developed protocol is presented in Table 5.4.

Table 5.4: Adequate mode depending on the RSSI.

Downlink RSSI (dBm)	**Adequate Mode**
$>$ -101	*fast-rate*
[-110,-101]	*mid-rate*
$<$ -110	*standard*

5.3.2 Time allocation per Mode

Most of the complexity of LoRa-MAP is offloaded to the gateway. The end-nodes are only responsible for updating their ideal mode based on the received CMs, without having any knowledge about the remaining end-nodes. The gateway, on the other hand, is responsible for keeping information regarding all devices on the network, in order to calculate how much time should be allocated for each mode. Table 5.5 exemplifies how the end-node list is organized.

In addition to the preferred mode of each device, the gateway keeps the timestamp of the last communication with each node. This way, when performing the calculation of each mode time, the gateway will not take into account inactive devices or devices no longer in range, and only active end-nodes will be considered. The timeout period for an end-node to

Node ID	Last Contact	Ideal Mode
11	1571500449	2 (*mid-rate*)
63	1571481011	1 (*standard*)
5	1570594267	2 (*mid-rate*)
279	1571500347	3 (*fast-rate*)

Table 5.5: End-node list.

be considered out of the network must be carefully selected, since it depends on how often the nodes communicate, as well as other factors such as network size: an active end-node should not be considered inactive simply because it has not been able to access the medium recently.

It it essential for the gateway to know the preferential mode of each device, which is calculated according to the received CMs, as mentioned before. However, this means that before receiving the first downlink message, a device has no information regarding its connection to the gateway, and therefore the *standard* mode is the mode to be selected by default. When this occurs, the transmission of CM (transmitted by the gateway) may not be as frequent, or not happen at all, preventing nodes from updating their optimal mode of operation. For this reason, if a certain time period passes without the emission of a CM, the gateway broadcasts a message with no purpose other than to allow a mode recalculation.

As aforesaid in the protocol description, the gateway does not alternate from *fast-rate* to *mid-rate* (or vice-versa) directly. After spending time using one of these modes, *standard* is the one that follows. This being said, and as the protocol works cyclically, one can divide the gateway's operation period in cycles, where one cycle corresponds to a period in which all modes have been used - with *standard* being used twice - as Figure 5.8 exemplifies.

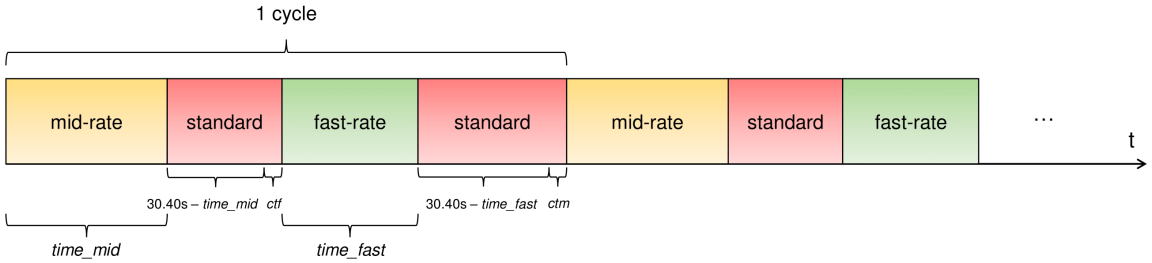

Figure 5.8: LoRa-MAP cycle.

While *time_mid* and *time_fast* are precisely the times calculated by the gateway as the CM is sent, the time spent in *standard* can be unpredictable, since for this mode to be abandoned it is necessary that nodes compete for access, requesting a different mode. Nonetheless, it is possible to calculate its minimum value. Due to the gateway having a $30.4s$ restriction period caused by the use of a CM, *time_standard* depends greatly on the time allocated for the remaining modes: until this interval is fulfilled, all requests for a mode alteration are ignored.

Summarizing, the time spent in *standard* per cycle is given by

$$time\_standard = (CM\_ToA \times 99 - time\_mid) + ctf + (CM\_ToA \times 99 - time\_fast) + ctm, \quad (5.5)$$

where *ct* stands for change time, representing the time it takes for the gateway to change the mode since the restriction period has passed, and *ctf* and *ctm* represents the transition to *fast-rate* and *mid-rate*, respectively. These time periods are highly influenced by network characteristics such as scale and node preference distribution among the operation modes.

5.4 Medium Access Fairness

One of the main objectives of a MAC protocol must be to ensure a fair network, allowing an adequate distribution of accesses for every device. A fairness evaluation method was already referred, the Jain's Fairness Index, with an expression that compares the individual throughput of each end-node. This metric was proposed to evaluate the performance of LoRaWAN and RTS-LoRa, protocols in which all nodes are seen as equal, and all make use of the network resources equally (*i.e.* same configuration, data-rate, energy consumption).

However, this equation fails to capture discrepancies in the end-nodes' behaviour. Due to the different configurations used by different devices to perform data transmissions in LoRa-MAP, some nodes will be consuming a lot more channel time in comparison to those using higher data-rates. For this reason, the JFI was adapted to create a different evaluation metric that takes into account the data-rate of each mode, by replacing x_i with $x_i \times t_i$, where t_i represents the average time spent per transmission of the ith node, which is given by

$$a\jmath(x_1, x_2, ..., x_n) = \frac{(\sum_{i=1}^{n} x_i \times t_i)^2}{n \times \sum_{i=1}^{n} (x_i \times t_i)^2}. \tag{5.6}$$

Similarly to the Jain's Fairness Index, this expression ranges from $\frac{1}{n}$ to 1, but maximum fairness is achieved in a scenario in which every node has the right to the same medium access time (*i.e.* if node A has twice the data-rate of node B, it is fair that it is able to send twice the amount of information).

Using this new metric on single-mode protocols would output exactly the same as JFI, as the transmission time-on-air is similar for every device.

5.5 Chapter Considerations

This chapter focused on the LoRa Mode Adaptive Protocol, the proposed solution to improve the performance of LoRa networks.

First, a discussion is provided as to why a protocol with the characteristics of LoRa-MAP would be beneficial, taking into account the particularities of LoRa technology and the flaws with the currently used scheme. The messages created to support the proposed access scheme are presented, as is the information that each message carries. The operation of the protocol is explained by showing how both the end-nodes and the gateway act during the information exchange process, according to the type of messages received. Experimental results referring to the PDR under different modes of operation and connection strengths are exhibited, justifying the choice of the three configurations used for devices with different characteristics. At last, considerations regarding the fairness of the protocol are made, leading to the creation of a new metric, an adapted Jain's Fairness Index equation that takes into account the bit-rate of the end-nodes.

The next chapter presents an evaluation on all the topics referred throughout this dissertation, via simulation of the three MAC protocols. An optimization for LoRa-MAP is done in order to obtain information on how to better perform the time allocation per mode. In terms of physical layer, different models are considered in order to study the impact the obtained probabilistic collision model has on the medium access, in comparison to other assumptions.

Chapter 6

Evaluation

This chapter describes the evaluation process and results of the three medium access schemes described in the previous two chapters, by considering several LoRa collision models, including the one presented in Chapter 3.

Section 6.1 describes the simulation environment used in the evaluation. Section 6.2 presents the results obtained for LoRaWAN single-channel modeled as a pure-ALOHA scheme, considering different network characteristics. Special attention is given to the performance when considering the probabilistic model obtained. Section 6.3 evaluates the same scenarios considered for LoRaWAN, while including the Ready-to-Send packet in the medium access. LoRaWAN and RTS-LoRa results are analysed and compared afterwards. Section 6.4 presents the network performance with LoRa-MAP, studying the influence of different allocation times for each operation mode. Following the simulation results, a model is derived to estimate the mode distribution times that results in a good tradeoff between fairness and network capacity, valid for any network configuration. Section 6.5 presents a comparison of the three MAC protocols. Finally, Section 6.6 summarizes the chapter.

6.1 Simulation Environment

Most of the work developed throughout this dissertation targets large-scale networks. To evaluate and compare the performance of LoRaWAN single-channel, RTS-LoRa and LoRa-MAP, a MATLAB simulator was developed, allowing the extensive evaluation of situations difficult to perform in a real deployment.

The operation of the three protocols is simulated, modeled as described by the flowcharts from Chapters 4 and 5, and the parameterization of a number of variables is possible, such as:

- ***Number of Nodes*** in the network;
- ***Data Packet Size*** up to a maximum of 256 bytes;
- ***Simulation Time*** measured in slots with $1ms$ precision (slot length);
- ***Physical Layer Configuration*** from the 10 predefined modes of the SX1272 LoRa module;
- ***End-node Distribution*** over the network, to assess different network topologies;

- ***Packet Collision Model*** used, among three possibilities: the probabilistic model obtained via experimentation (characterized in Chapter 3); a collision model that assumes the loss of all colliding packets; and a collision model that enables the packet decoding when a gap of 6dB between transmissions is observed;

- ***Maximum Backoff Time*** calculated in addition to the obligatory restrictions. For LoRaWAN this time is specified in *ms*, while for the other schemes it is given by the number of slots.

To observe the difference between the collision models, the end-nodes have to be associated with different link strengths to the gateway. A network layout like the one shown in Figure 6.1 was adopted, with devices distributed among three different groups. The signal strength of a packet transmission is set to be related with the group that the emitter belongs to, as detailed in Table 6.1. The value is obtained randomly, from the specified range.

To facilitate the comparison between MAC protocols, the RSSI values allocated to one group correspond to the values that lead to the use of each LoRa-MAP operation mode (*i.e.* in the presented network topology all devices from group 3 would prefer *fast-rate*, nodes from group 2 would transmit in *mid-rate*, and the ones from group 1 would need to resort to the slow transmissions from *standard*.)

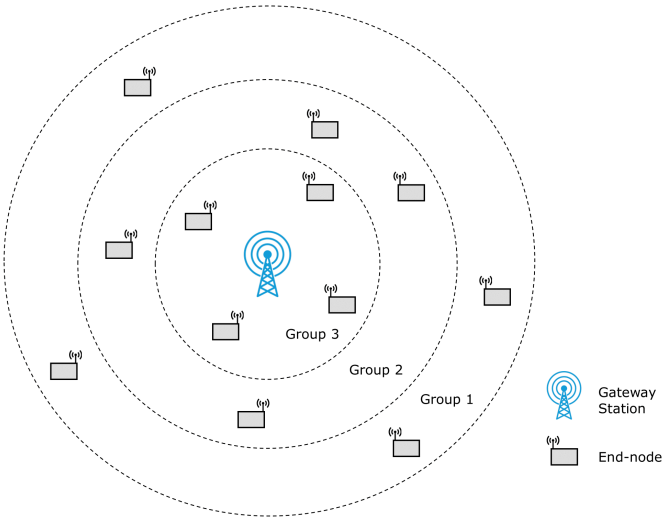

Figure 6.1: Network Layout.

Group	Possible RSSI values
1	[-125,-111]dBm
2	[-110,-101]dBm
3	[-100,-90]dBm

Table 6.1: Range of RSSI values per group.

It is important to note that, with this layout, it is not stated that the RSSI of a transmission is directly related to the distance between emitter and receiver: in fact, it is known that the distance is not the only (or in some situations even the best) metric to predict the signal strength. The insertion of a device into one of the three groups depends only on the RSSI of the transmissions between the device and the gateway, being Figure 6.1 purely illustrative.

To evaluate the performance of the different schemes, each simulation outputs the total network capacity, the network fairness - according to both JFI and the adapted Fairness Indicator, as described in the end of the previous chapter - and the amount of packets delivered by each group separately.

6.2 LoRaWAN Single-Channel

6.2.1 Network Capacity

The simplest of the three protocols, LoRaWAN, is expected to have the smallest capacity due to the uncoordinated medium access performed by the end-nodes, leading to a large number of collisions.

6.2.1.1 Different packet sizes and packet collision models

The evaluation process started with an exhaustive capacity evaluation for LoRaWANs of different scales, from 10 to 1000 end-devices, considering different packet sizes - 10, 25, 50, 75, 100 and 200 bytes - and physical layer models. This analysis, as well as the remaining ones, was performed under saturated conditions. Regarding the end-node disposition, an equitable distribution was followed, with a third of the total number of devices allocated to each group. To ensure that it is possible for the gateway to receive packets from nodes in all three groups, Mode 3 was used, providing a good tradeoff between time-on-air and sensitivity. A simulation time of 10^9 slots was used for every simulation and the maximum backoff time chosen was $15000ms$, in order to privilege large-scale networks. Figure 6.2 presents the obtained results.

It is immediately noticeable that a higher throughput is achieved when larger data packets are transmitted, no matter which model is considered, even if fewer packets are received due to the long duty-cycle restrictions. For the destructive collisions model, the pure-ALOHA behaviour is observed, with the throughput of the network increasing until around the 55 nodes mark. However, as the number of devices increases, the number of collisions results in a lower delivery rate. For more than 400 end-nodes the throughput is negligible, and for

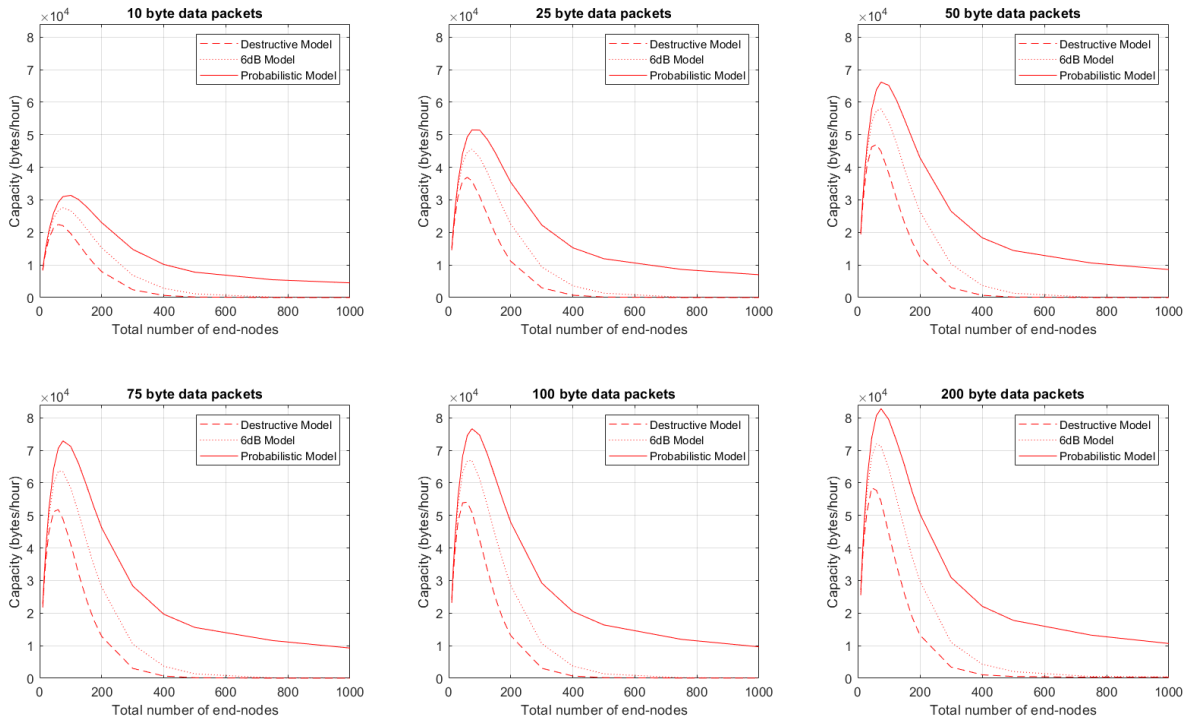

Figure 6.2: LoRaWAN capacity for different data packet lengths and packet collision models.

a total of 750 end-nodes the average number of packets delivered per node throughout the entire simulation ($\approx$ 278 hours) is lower than 1, regardless of the packet size.

When considering the 6dB margin, the network has a higher capacity and its value peaks for a greater number of end-nodes - around 70 - when compared to the destructive model. However, for larger networks, the behaviour observed is quite similar. Using the probabilistic model characterized in Chapter 3, the network capacity is significantly higher than the remaining two models no matter the packet size, but for larger data packets this discrepancy is even higher. The same can be said for the the network size, with this superiority being highly relevant after the 50 end-nodes mark. Following this model the capacity value not only peaks for a higher amount of devices ($\approx$ 80 nodes) but also decreases slowly as the network size increases. With 1000 end-nodes it is still possible for the gateway to receive a considerable amount of packets, being compared to the delivery rate achieved for the other models with around 250 devices.

Considering a -6dB threshold, even if closer to the reality, is shown to be a pessimistic model, specially for large scale networks. Therefore, this collision model will not be considered for the remaining of this chapter.

6.2.1.2 The impact of different end-node distributions

The previous analysis, while it studied the impact of considering colliding packets as delivered according to the probabilistic model, it did not account for the effect of having different network topologies on the network capacity (*i.e.* all evaluated scenarios followed a $\frac{1}{3}$ per group distribution).

Figure 6.3 follows the opposite approach, setting the packet size for 100 bytes and varying the density of nodes across the network, for different combinations of [% group 1, % group 2, % group 3], where group 1 comprises the nodes with the worst connection to the gateway and group 3 the best. Following the destructive model, the end-node distribution is irrelevant, so only one curve is required to represent it. The results for this situation were taken from the previous analysis, namely the [33.3%, 33.3%, 33.3%] scenario.

From the results obtained, it can be concluded that considering the probabilistic model results in a much higher delivery rate regardless of the network layout. When increasing the amount of end-nodes, the impact of the node's distribution on network capacity is virtually indistinguishable, becoming more noticeable for larger networks.

The throughput value is higher when the percentage of nodes in the best transmission conditions is lower. This is explained by the fact that this model highly privileges the connection strength, meaning that in densely populated networks the devices in group 3 are able of, by themselves, nullifying the transmissions coming from the remaining two groups. If many devices are in favorable conditions, not only the ones with a worse connection are impaired, but there are also more collisions among those in group 3, leading to a high number of packet losses.

6.2.2 Channel Access Fairness

To study the impact of the probabilistic model on the network fairness, the well known Jain's Fairness Index (described in Section 4.1.2) was used, considering the end-node distributions from the previous analysis. Figure 6.4 details the obtained results.

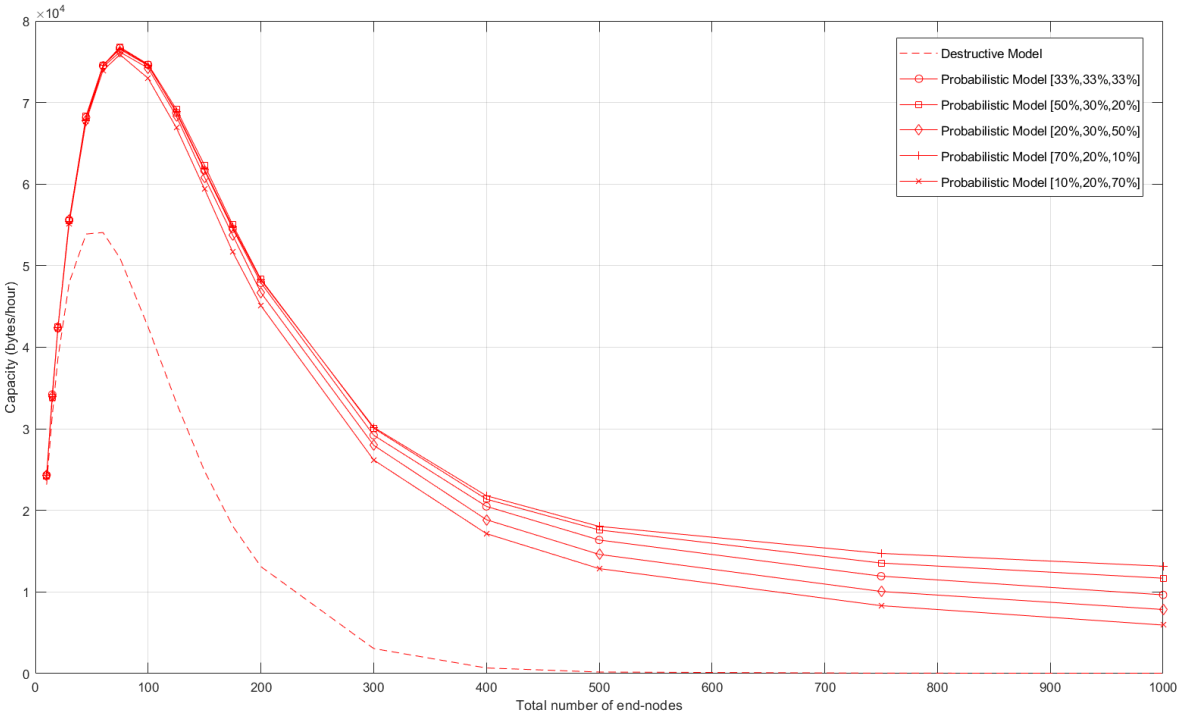

Figure 6.3: LoRaWAN capacity for different network layout and packet collision models.

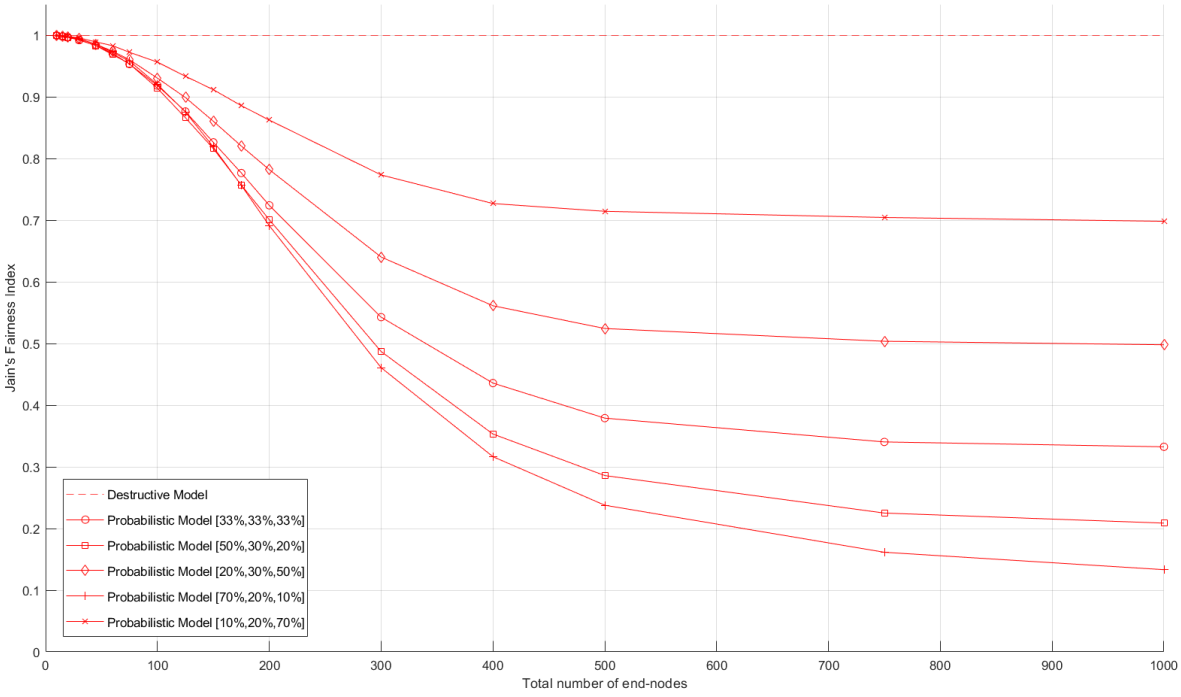

Figure 6.4: Access fairness in LoRaWANs for different network layouts and packet collision models.

With the destructive model, the channel access is considered completely fair since every end-node has the same probability of having a successful transmission, so $\jmath = 1$ is obtained no matter the network scale. When the non-destructive property is considered, the network becomes unfair, and a total of 30 end-devices is sufficient for $\jmath$ to drop from 1 to 0.99. Moreover, the scenarios in which the observed throughput was higher are also the ones with lower fairness, corroborating the idea that, as the scale increases, almost all the extra accesses allowed by the probabilistic model are performed by the end-nodes in group 3. For each of the 5 curves obtained for the probabilistic model, $\jmath$ always tends to $\frac{N_{group3}}{N_{total}}$, which corresponds to a situation in which N_{group3} equally share the access time, and the remaining end-nodes are totally deprived of sending information.

The performed analysis shows that, while the realistic model greatly increases the overall network capacity, essentially only devices capable of high RSSI packet transmissions are benefited, when in comparison to the destructive model.

6.3 RTS-LoRa vs LoRaWAN Single-Channel

The performance analysis done for LoRaWAN will serve as a comparison to verify the advantage of including a simple control package on the medium access of LoRa networks, giving rise to RTS-LoRa. All the same parameter combinations are studied with the exception of the -6dB model.

For simplicity, it is assumed that every Ready-to-Send packet emitted can be received throughout the network (as long as a collision does not occur), considering that all end-nodes are in range of each other.

6.3.1 Network Capacity

It is expected that, due to the existence of an RTS message allowing the adjustment of the access window of the remaining nodes, the number of collisions decreases, consequently increasing throughput.

6.3.1.1 The impact of different packet sizes and packet collision models

Figure 6.5 shows a comparison of the capacity achieved with the RTS-LoRa protocol with that obtained with LoRaWAN, when varying the data packet size and the packet collision model. Other than the protocol used all the remaining simulation parameters were the same as for the LoRaWAN analysis. 50 slots were used for the additional backoff time, since considering 9-byte RTS messages and the time-on-air inherent to Mode 3, this amount of slots results in a maximum wait time of 14.33s, similar to the 15 seconds used for the LoRaWAN evaluation.

Once again no matter the packet size the probabilistic model results in higher throughput. However, the difference between this model and the destructive one is greater for LoRaWAN than RTS-LoRa, since a pure-ALOHA scheme suffers more from collisions than a reservation based protocol. On the other hand, in terms of packet size RTS-LoRa gains more from using larger packets. The use of a broadcast message before each data transmission ensures that it will not be interrupted (as long as the broadcast is successful), and a higher ratio between data size and control message size results in a higher network throughput.

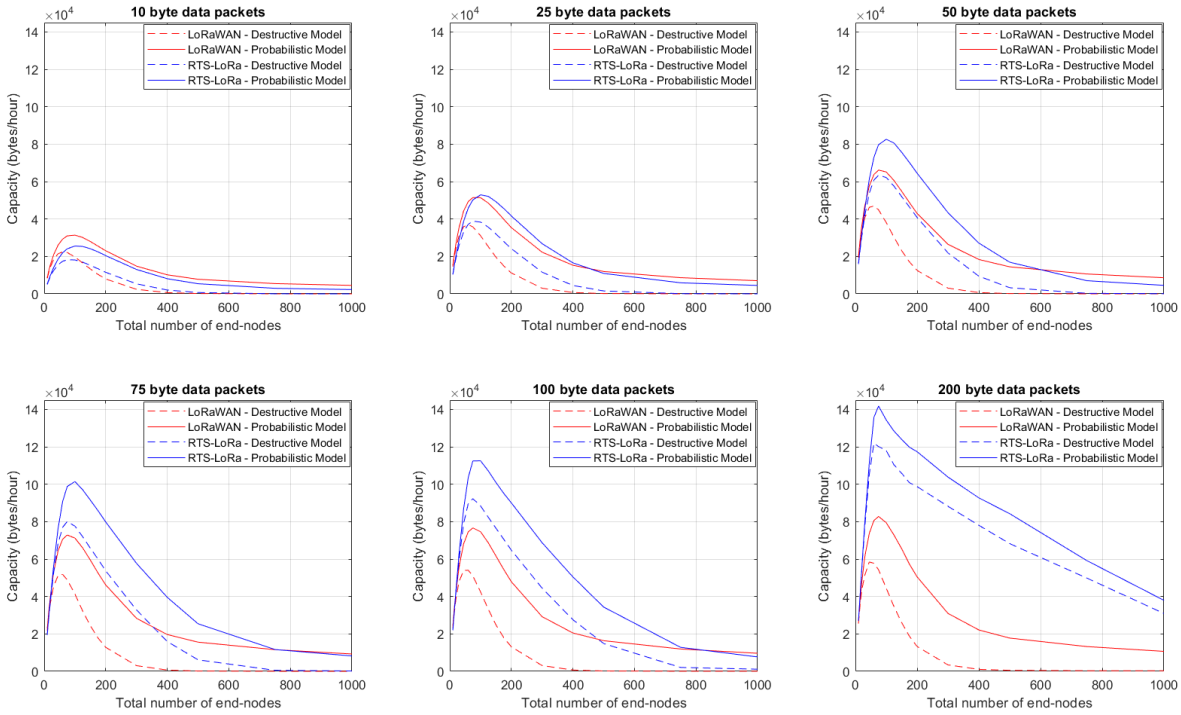

Figure 6.5: RTS-LoRa vs LoRaWAN: network capacity for different data packet lengths and packet collision models.

In general it can be stated that LoRaWAN has the advantage in scenarios with fewer end-nodes - because of little to no packet collisions - and when using smaller packet sizes, but is outperformed by RTS-LoRa in higher-scale networks and large data packets. The peak in terms of throughput is obtained for around 100 end-devices, proving that RTS-LoRa makes use of the duty cycle available to the technology in a more efficient way. However there is an important consideration to be taken from these results: even if RTS-LoRa peaks higher than LoRaWAN (with the exception of the 10-byte packet situation), as the number of nodes increases and RTS collisions become more frequent it is verified a steeper decline in terms of throughput. The data packets must be at least 100-bytes long for RTS-LoRa to surpass LoRaWAN in networks with up to 1000 end-devices.

6.3.1.2 The impact of different end-node distributions

Figure 6.6 illustrates the impact of the network layout on the capacity, in the same scenarios studied for LoRaWAN, using 100-byte data packets. Once again, results show the probabilistic model outcoming a much higher throughput than the destructive model, regardless of the network layout. The difference between the five cases is much less noticeable for RTS-LoRa, since by decreasing the occurrence of collisions the network capacity becomes less affected by the signal strength discrepancy of the end-nodes. In networks with up to 500 nodes it is practically indistinguishable which scenario results in the higher delivery rate, but as the number of devices is further increased it is possible to verify a separation of the five curves, displayed in the same order as for the LoRaWAN protocol.

6.3.2 Channel Access Fairness

The access fairness of the two medium access schemes is shown in Figure 6.7. Again, the destructive model results in a completely fair channel access, and consequently $\jmath = 1$.

As expected, the RTS message contributes positively to the network fairness, allowing that in large-scale networks not only the end-nodes from group 3 can transmit data. Depending on the distributions studied, between 475 and 700 devices are required to lower the $\jmath$ value below 0.9, while for LoRaWAN this happens with around 100 to 200 nodes.

It is expected that, for a larger number of end-nodes, the fairness indicator will inevitably tend to the same values as with LoRaWAN, when RTS collisions become more frequent. However, results show that, not only does RTS-LoRa generally allows a higher network capacity, but also ensures a better channel access distribution across the network.

6.4 LoRa Mode Adaptive Protocol

When performing simulations on networks using LoRa-MAP, other than the aforementioned parameters, there are two more variables to be considered: *time_mid* and *time_fast*, corresponding to the *mid-rate* and *fast-rate* distribution times per cycle, respectively. The time spent in *standard* does not have to be specified since, as explained before, it is calculated depending on the time spent in the non-default modes due to the duty-cycle restriction.

6.4.1 The impact of different channel time distributions

Let us start with a network with an equal distribution of devices per group, [33.3%, 33.3%, 33.3%], with different combinations of *time_fast* and *time_mid* durations per cycle. It is important that every combination allows for transmissions in every mode. Thus, the minimum values considered were $7.50s$ for *time_mid* and $5s$ for *time_fast*. Since the gateway is restricted for $30.4s$ after sending a CM, by selecting $22.5s$ and $20s$ for the maximum time in the non-default modes, at least $18.3s$ are guaranteed to be spent in the *standard* mode ($2 \times 30.4s - (22.5s + 20s)$). Altogether 16 [*time_mid*, *time_fast*] combinations were tested, in intervals of 2.5 seconds.

Like in the previous evaluations, the total number of devices ranged from 10 to 1000, and a simulation time of 10^9 slots was used. The only physical layer model used was the probabilistic along with the data packet size of 100 bytes. Similarly to as in the RTS-LoRa evaluation, the maximum number of backoff slots used was 50. Figures 6.8 and 6.9 show the results obtained in terms of network capacity and fairness, the last according to two metrics: Jain's Fairness Index ($\jmath$), and an alternative version, referred to as adapted-JFI (or $a\jmath$), to consider the discrepancies in the data-rate of each node.

From the first figure, it can be observed that there is a great distinction in the obtained throughput depending on the time attributed to each mode of operation, specially for large-scale networks. Generally the delivery rate is much higher when less time is spent by the gateway in *standard* - when the sum value of *time_mid* and *time_fast* is bigger - since this mode forces to a much higher time-on-air than the remaining two. For the same reason the network capacity is higher when more time is assigned to fast-rate than to mid-rate (*i.e.* comparing the combinations $[20, 17.5]s$ and $[22.5, 15]s$ or other pairs of scenarios in which the time sum is equal).

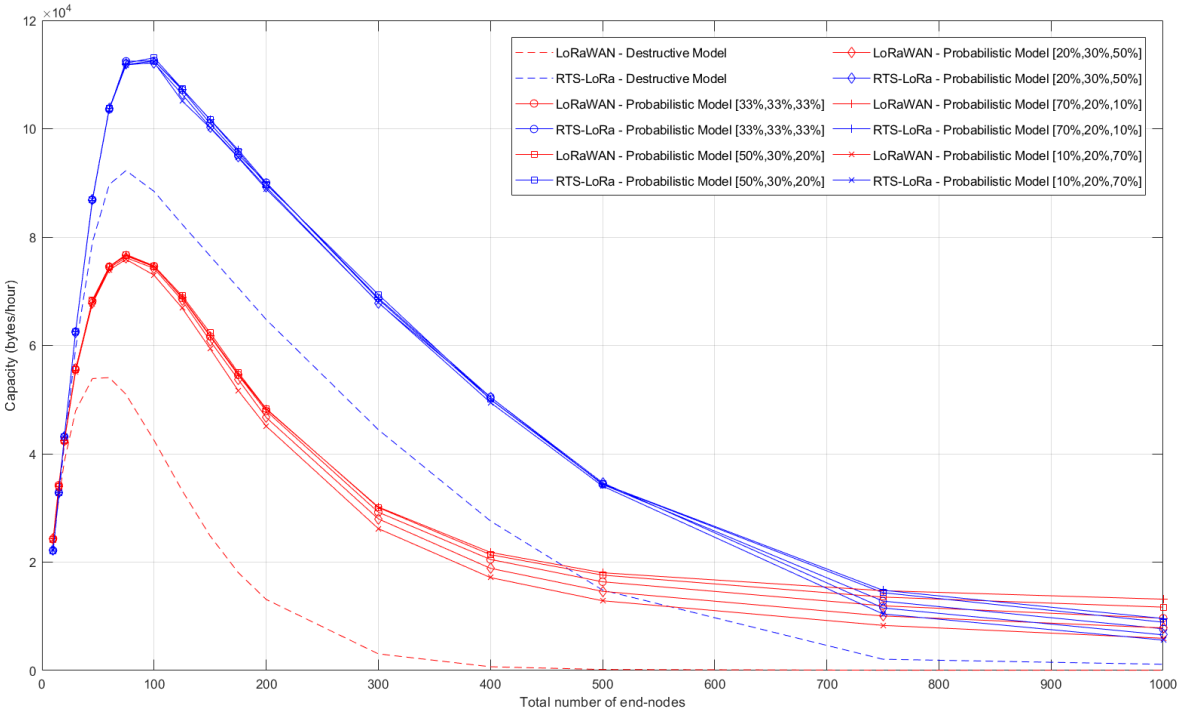

Figure 6.6: RTS-LoRa vs LoRaWAN: network capacity for different network layouts and packet collision models.

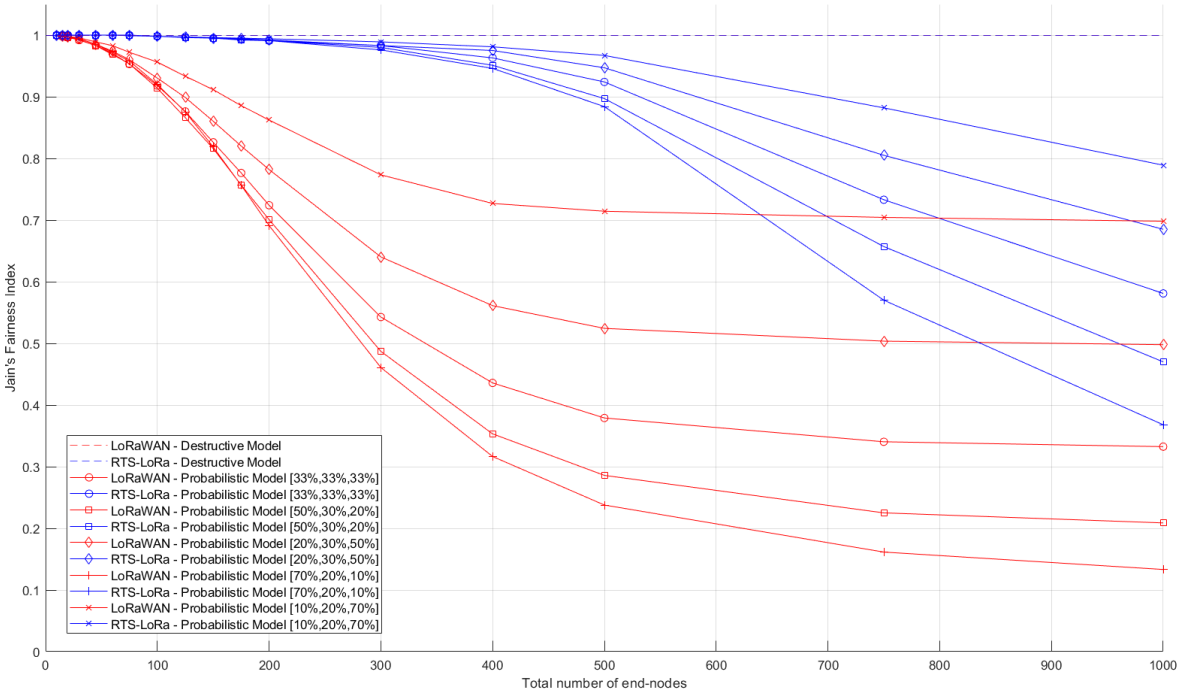

Figure 6.7: RTS-LoRa vs LoRaWAN: access fairness for different network layouts.

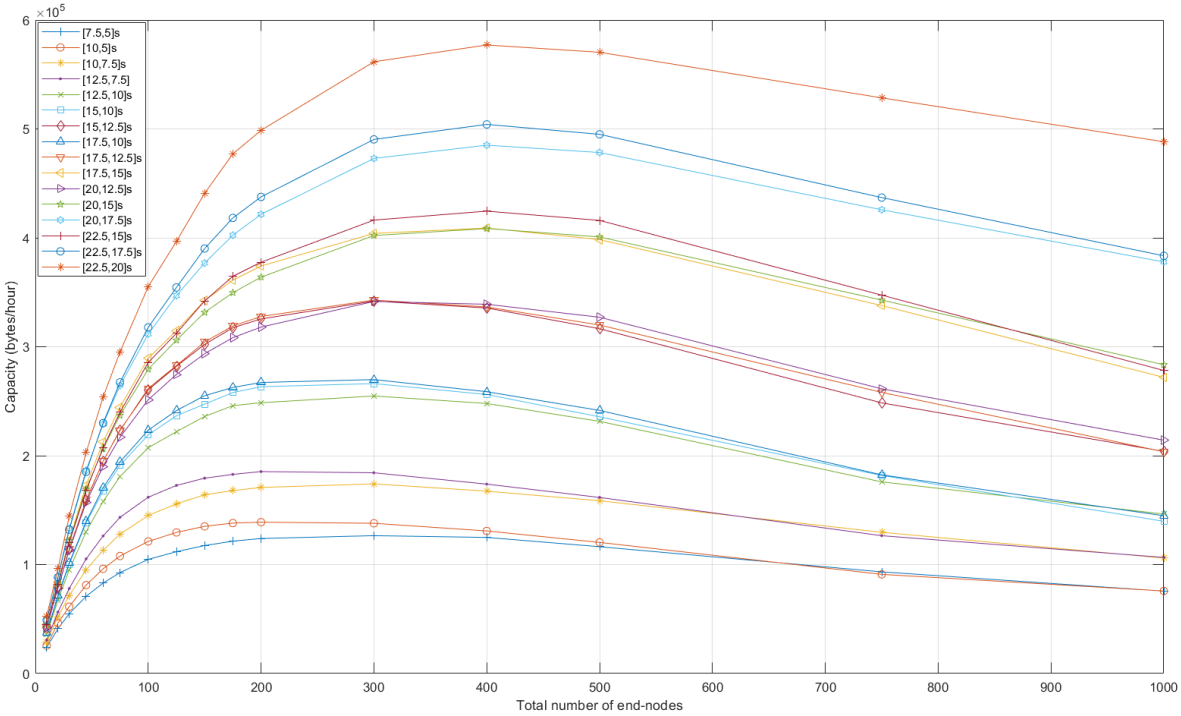

Figure 6.8: LoRa-MAP capacity depending on time allocation per mode for networks with a [33.3%, 33.3%, 33.3%] distribution.

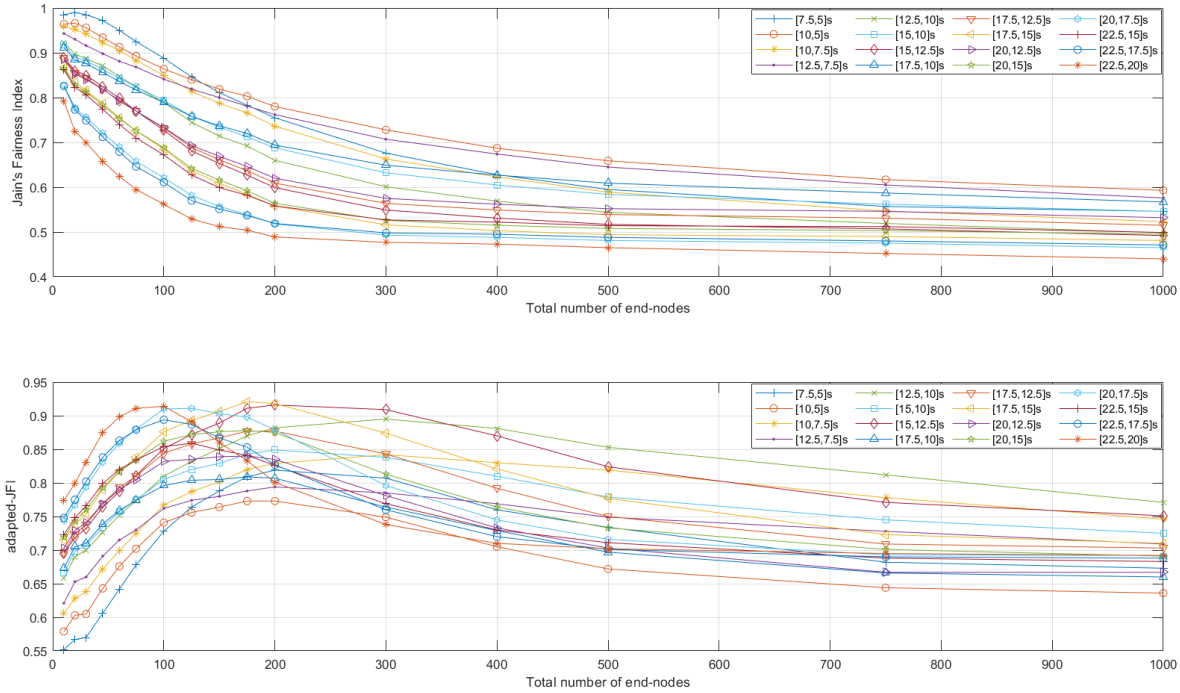

Figure 6.9: LoRa-MAP access fairness depending on time allocation per mode for networks with a [33.3%, 33.3%, 33.3%] distribution.

At a first glance, the relationship between the capacity and the time combinations seems to be the same no matter the number of devices, with $[22.5, 20]s$ resulting in the higher value, $[22.5, 17.5]s$ the second highest, and so on. However, an important aspect from this analysis is that, even though the end-node distribution is always $\frac{1}{3}$ in each group, as the network scale increases there are curves that surpass others. For example, until the 300 end-nodes mark the $[17.5, 12.5]s$ curve is above the $[20, 12.5]s$ one, but after this point the latest goes up. This happens because the transmissions in *fast-rate* are much faster than the ones in *mid-rate*, and with a similar increase in the number of devices in each group the network benefits - in terms of throughput - from spending more time in *mid-rate* per cycle. This allows to conclude that, when anticipating the best combination of times, not only the distribution ratio of end-nodes per mode is important, but also the specific amount.

Concerning the fairness assessment according to Jain's Fairness Index, the results follow an inverse behavior than the ones presented in the network capacity, with the shortest times corresponding to the higher values. As this metric considers maximum fairness when every device has equal channel access opportunities, due to the low bit-rate from group 1, $\jmath$ is typically higher for the lower values of *time_fast* and *time_mid*. Since the ToA in *fast-rate* is shorter than of those in *mid-rate* (*i.e.* about $\frac{1}{5}$ of the time when considering 100-byte packets), a larger value of *time_mid* over *time_fast* is expected to contribute positively to this index. This explains why combinations like $[7.5, 5]s$ and $[10, 7.5]s$ result in some of the higher $\jmath$ values for small-scale networks, but this value rapidly drops as the total number of end-nodes increases.

When measuring the fairness according to the adapted-JFI the results are much different, with the $a\jmath$ value growing rapidly until a certain amount of end-devices is reached and then decreasing slowly, much like the network capacity results. This increase is justified by the fact that this metric encourages a much higher throughput from group 2 and 3 than from group 1. With this packet size, the maximum fairness is obtained if, by each data packet received by the gateway from group 1, approximately 3.5 packets are received from group 2 nodes, and 20 packets from group 3. As the number of devices per group increases, packet delivery by groups with shorter ToA will undergo a larger increase, which contributes positively to the network fairness. However, as the network scales, this scheme starts to favor in an exaggerated way the groups with lower bit-rates, and the packet delivery per group starts do deviate from the ideal ratio. This is corroborated by the fact that $a\jmath$ has a peak with less end-nodes for scenarios that have more time allocated for the non-default modes, while more balanced combinations such as $[15, 12.5]s$ and $[12.5, 10]s$ achieve better fairness values in large-scale networks. On the other hand, using shorter time values like $[7.5, 5]s$ result in low fairness regardless of the number of end-nodes, since it is assigned a great deal of time to *standard* (*i.e.* $2 \times 30.4s - (7.5s + 5s) = 48.3s$).

The performed evaluation was repeated for networks with different combinations of end-nodes per group. Figures 6.10, 6.11 and 6.12 present the results for networks with distributions of [50%, 30%, 20%], [20%, 30%, 50%] and [25%, 50%, 25%] respectively, featuring only five time combinations.

The graph of the network capacity seems to be the least subject to change as the end-node distribution varies. Nonetheless, it is possible to observe that the scenario with half of the devices belonging to group 3 can achieve higher throughput, while the one where 50% is from group 1 achieves the lowest peak values, justified by the data-rate inherent to each mode. On the other hand, despite achieving the highest values, networks that have most of the end-nodes using *fast-rate* also suffer the biggest reduction in the global capacity as its size

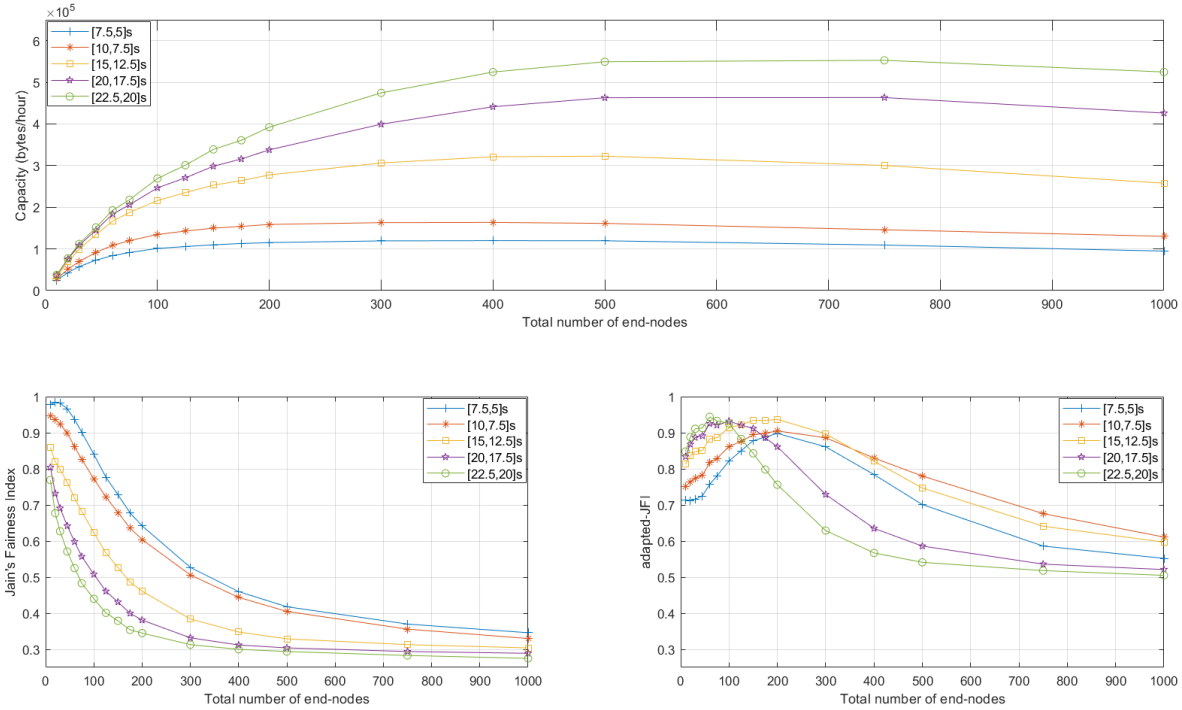

Figure 6.10: LoRa-MAP evaluation for networks with an end-node distribution of [50%, 30%, 20%].

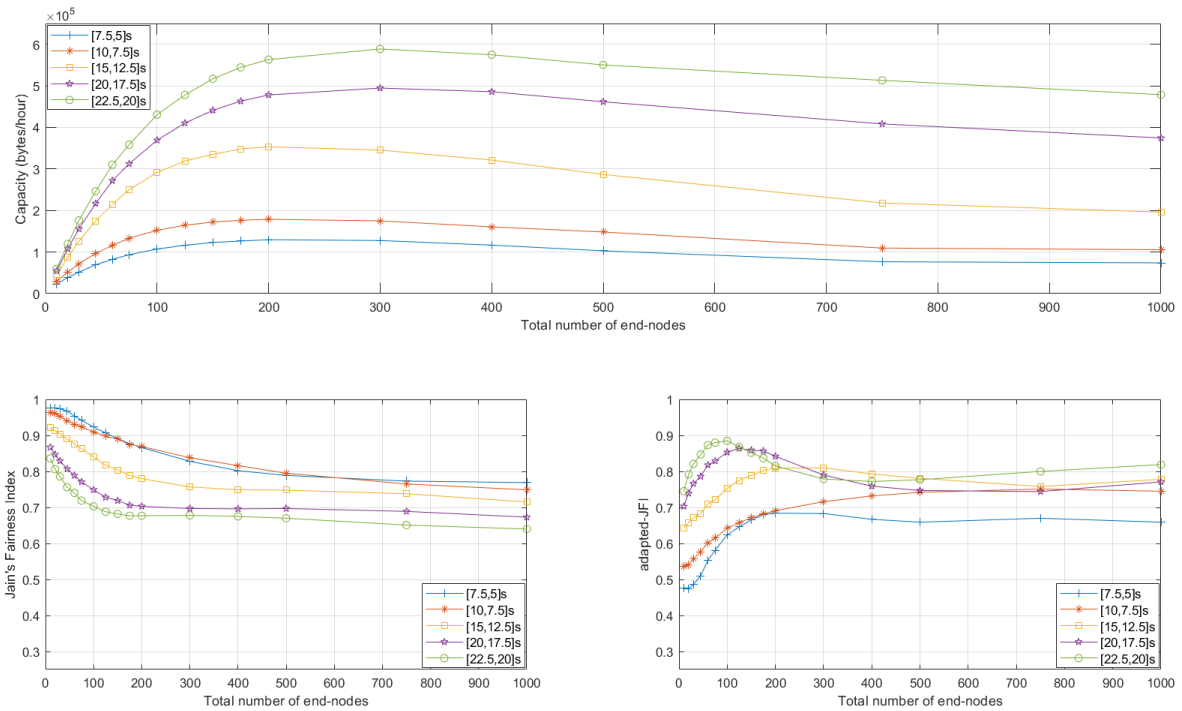

Figure 6.11: LoRa-MAP evaluation for networks with an end-node distribution of [20%, 30%, 50%].

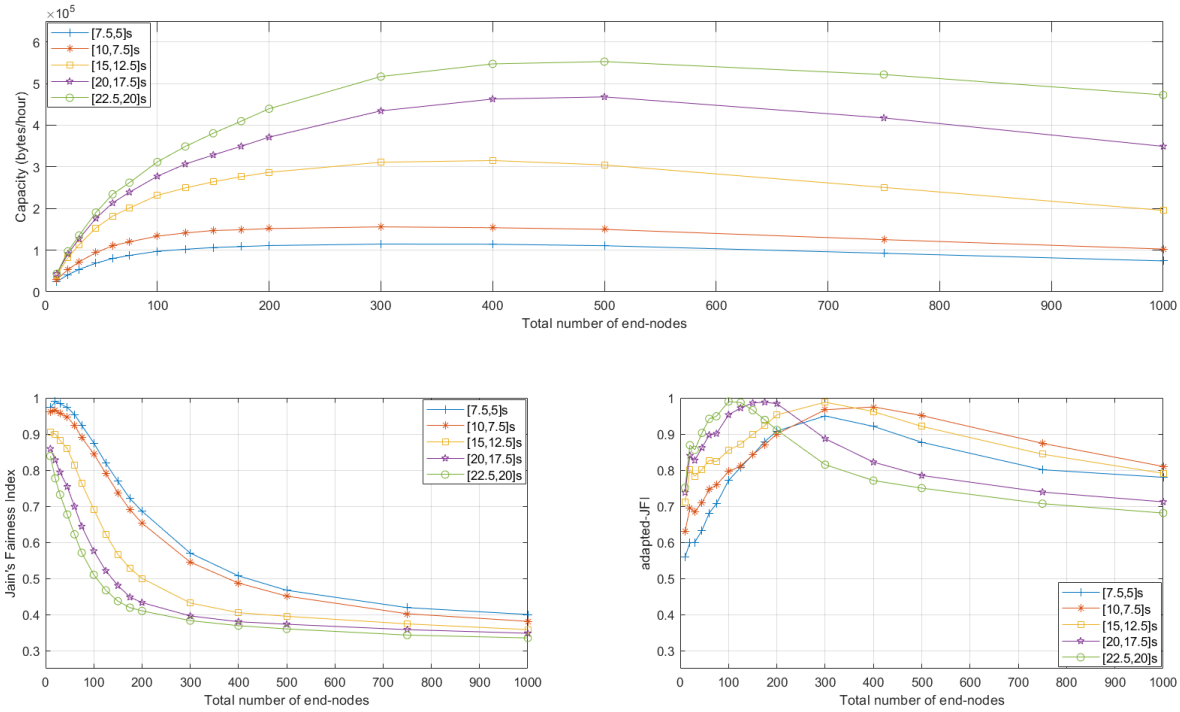

Figure 6.12: LoRa-MAP evaluation for networks with an end-node distribution of [25%, 50%, 25%].

increases mainly due to packet collisions. While packet losses occur to devices in the three groups, collisions from devices in group 3 have more impact on the global throughput, since they are the ones which contribute the most to it.

Regarding the fairness assessment, the distribution of devices per groups has a significant impact. In the [50%, 30%, 20%] scenario, $\jmath$ drops faster and to lower values when compared to an equal end-node distribution, since the number of devices using slow transmissions is higher. Low data-rates and a lot of channel access competition justify this behaviour, and also explains how $a\jmath$ has a peak with very few end-nodes. Using a distribution of [20%, 30%, 50%], it is easier to obtain good results considering both fairness indexes. As there are less end-nodes transmitting in *standard*, fewer time using this mode is required, and a lower discrepancy in $\jmath$ is observed when choosing different time combinations. It is also the only scenario in which using a longer *time_fast* and *time_mid* results in the highest $a\jmath$ values in densely populated networks. The last scenario presented, [25%, 50%, 25%], is the one closest to the equitable distribution, only with a few more devices belonging to group 2 instead of the remaining two. This distribution density benefits the $a\jmath$ value obtained in comparison to the last scenario, since there are less devices included in group 3, whose delivery rate will be higher because there is less competition for medium access.

6.4.2 Calculating the duration of each mode

In LoRa-MAP the gateway must be able to, based on the amount of end-devices and their connectivity, decide the ideal duration for each mode. As there is a huge amount of possible network layouts, it is not feasible to perform simulations on all of them in order to discover

the best time combination for every given situation. Thus, the evaluation performed in the previous subsection was extended to consider the following network sizes {10, 20, 30, 45, 60, 75, 100, 125, 150, 175, 200, 300, 400, 500, 750 and 1000}, and different network distributions, namely {[70%, 20%, 10%], [10%, 20%, 70%], [15%, 70%, 15%]}. This results in a total of 112 different scenarios that were evaluated in terms of network capacity, $\jmath$ and $a\jmath$, using the 16 combinations of [*time_mid*, *time_fast*] shown in Figure 6.8. The packet size was set to 100 bytes.

For each scenario, it is considered ideal a combination that achieves good throughput without greatly sacrificing the access fairness. Naturally, as previously observed, allowing an extensive amount of time per cycle to modes with low ToA results in a very high capacity, but it impairs the network fairness.

6.4.2.1 Fairness Indicator

The two metrics used to assess fairness so far are very discordant, as they associate totally different situations with maximum fairness. For this reason, a new indicator is created, that takes both aspects into consideration. This new evaluation metric, referred to as Fairness Indicator (FI), is calculated as follows:

$$FI = \frac{\jmath + a\jmath}{(1-\jmath)^2 + (1-a\jmath)^2}. \tag{6.1}$$

The FI is higher when the sum of the two values ($\jmath$ and $a\jmath$) is greater and when there is a good compromise between the two (*i.e.* the FI value is greatly harmed if one of the two metrics has a low value even if the other is close to 1). This way, it is assured that the disparity in access opportunities among the groups is not exceedingly high, while encouraging that certain groups are privileged according to a ratio that makes sense, based on the ToA per transmission. Table 6.2 shows an example of FI values obtained for different $\jmath$ and $a\jmath$ values, for a specific scenario of 75 end-nodes, 25 on each group. The results show that, in scenarios in which one of the fairness index is very close to 1, the other is considerably low, resulting in small values of FI. According to this method the fairest option for a network with these characteristics would be to assign 10 seconds per cycle to *fast_rate* and 15 seconds to *mid_rate*.

[*time_mid*, *time_fast*]	[7.5, 5]s	[10, 5]s	[10, 7.5]s	[12.5, 7.5]s	[12.5, 10]s	[15, 10]s	[15, 12.5]s	[17.5,10]s
$\jmath$	0.925	0.893	0.883	0.868	0.824	0.824	0.770	0.817
a$\jmath$	0.678	0.702	0.725	0.730	0.773	0.775	0.811	0.774
FI	14.7	15.9	18.0	17.7	19.4	19.6	17.8	18.8
[*time_mid*, *time_fast*]	[17.5, 12.5]s	[17.5, 15]s	[20, 12.5]s	[20, 15]s	[20, 17.5]s	[22.5, 15]s	[22.5, 17.5]s	[22.5,20]s
$\jmath$	0.770	0.726	0.770	0.726	0.658	0.710	0.646	0.595
a$\jmath$	0.810	0.838	0.805	0.834	0.880	0.834	0.879	0.911
FI	17.8	15.4	17.3	15.2	11.7	13.8	10.9	8.76

Table 6.2: Fairness assessment in a 75 end-nodes network with equitable group distribution.

6.4.2.2 Choosing the *best* combination

The process of determining the best *time_mid* and *time_fast* for each of the 112 networks started by calculating the FI for each time combination. The three combinations with the

higher FI are selected, and the one in which it is verified the highest network capacity is considered the ideal combination. Using the scenario from Table 6.2 as an example, 10 seconds per cycle is considered the best choice for *fast_rate*, and depending on the throughput obtained in each simulation, a value between 12.5 and 17.5 seconds will be considered ideal for *time_mid*.

This method allows for a compromise between fairness and network capacity, privileging the first, since it immediately rules out time combinations that lead to very low $\jmath$ and $a\jmath$ values regardless of the throughput they grant. From the 112 network different scenarios, Figure 6.13 expresses the best time allocated for *mid_rate* and Figure 6.14 the one appropriate for *fast_rate*, depending on the number of devices using *standard* (N_s), *mid-rate* (N_m) and *fast-rate* (N_f) modes.

From both figures it should be noted that each of the 3 variables is essential when it comes to predict the ideal time distribution. Shorter times are adequate when nodes that transmit in *standard* prevail over the other two groups, while values such as 20 or 22.5 seconds are appointed only when the majority of the network transmits in the faster modes. Near the origin, the ideal values indicate that, for small-scale networks, even subtle changes in the group distribution can lead to very different time combination choices. As the amount of end-nodes increases the division becomes clear, enabling the estimation of when certain times would be more suitable than others.

The achieved results were used to obtain a model that can estimate the ideal *time_fast* and *time_mid* used for a LoRa-MAP network based on the values of N_s, N_m and N_f. To execute this, it was used multinomial logistic regression, a classification method that performs a predictive analysis on problems with more than two possible discrete outcomes (multiclass problems). For this specific case there are 6 classes for *time_mid*: {10s, 12.5s, 15s, 17.5s, 20s, 22.5s} and also 6 for *time_fast*: {7.5s, 10s, 12.5s, 15s, 17.5s, 20s}, and are used three features - or independent variables -, the number of devices per group. This allows for the prediction of the ideal time combination for endless scenarios without recurring to simulations. In Figures 6.15 and 6.16 can be observed the values that the model obtains as ideal for *time_mid* and *time_fast*, respectively.

It is important to note that for scenarios with higher density, it is expected that the model deviates from the expected values due to the lack of information from the simulations performed (*i.e.* only a total of 3 scenarios were considered in which a group had 700 end-nodes, and this was the maximum quantity considered).

6.4.2.3 Model validation

To validate the estimation model, three completely new scenarios were tested. For each scenario, the ideal duration for each mode was estimated, to evaluate the network performance with the supposedly ideal time periods and compare these results to the ones obtained when using different combinations.

For the first validation scenario, a network with 25 end-devices was used, with 10 belonging to group 1, 7 to group 2 and the remaining 8 to group 3 (distribution of [40%, 28%, 32%]). Table 6.3 presents the results obtained from the simulations considering the 16 different *time-mid* and *time-fast* combinations.

The model outputs $[20.5, 12.5]s$ as the ideal option for this network, and the table shows that this combination is, along with $[17.5, 10]s$, the one with the highest FI. While using longer times for both non-default modes would result in a higher throughput, this would

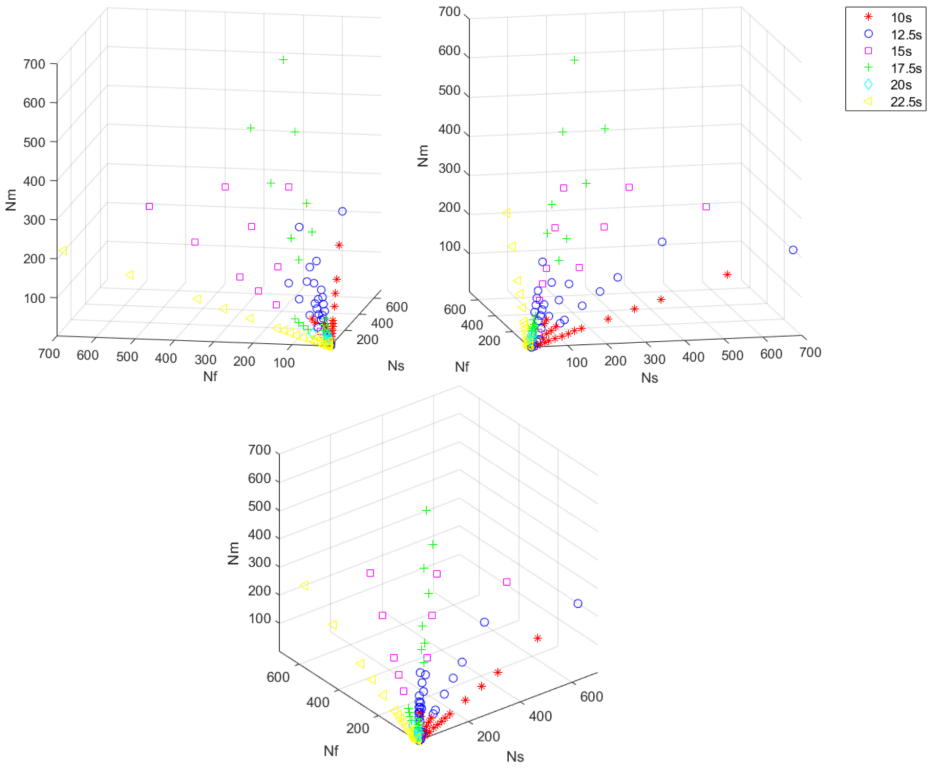

Figure 6.13: Best *time_mid* for the several network scenarios.

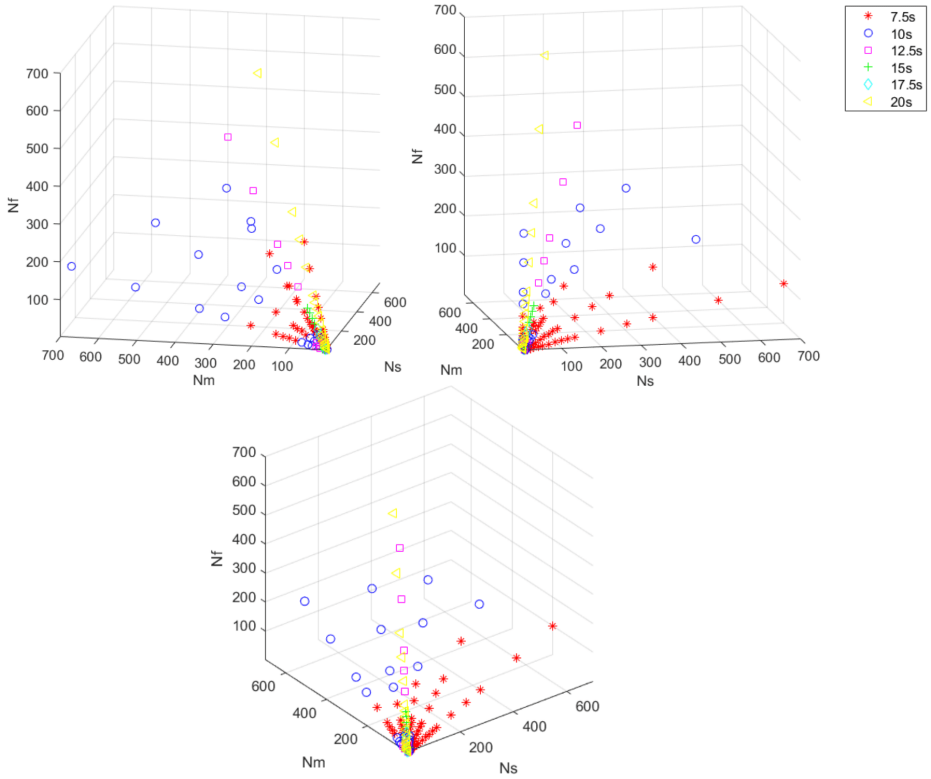

Figure 6.14: Best *time_fast* for the several network scenarios.

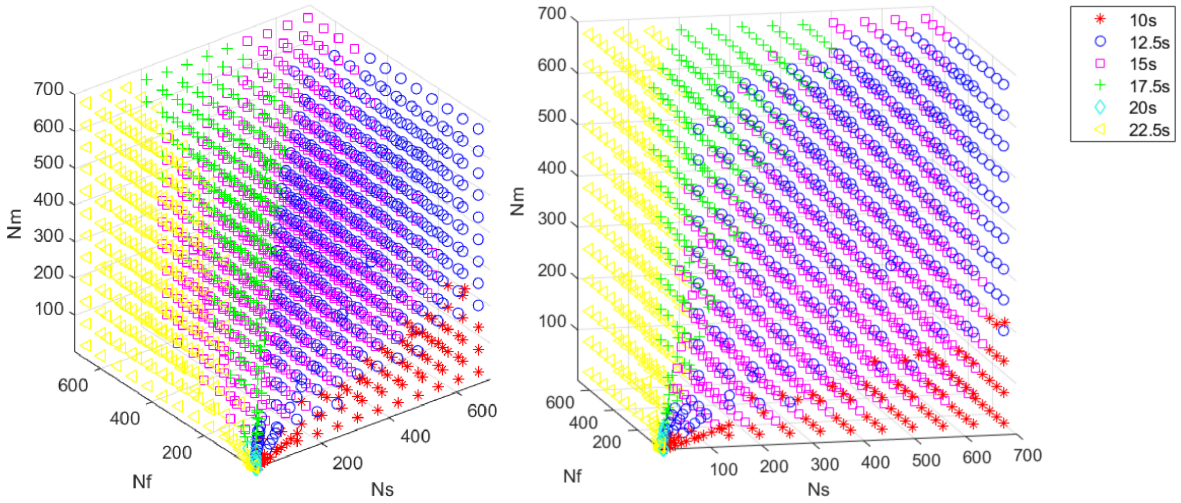

Figure 6.15: Estimated ideal *time_mid* for non-evaluated scenarios (two different perspectives).

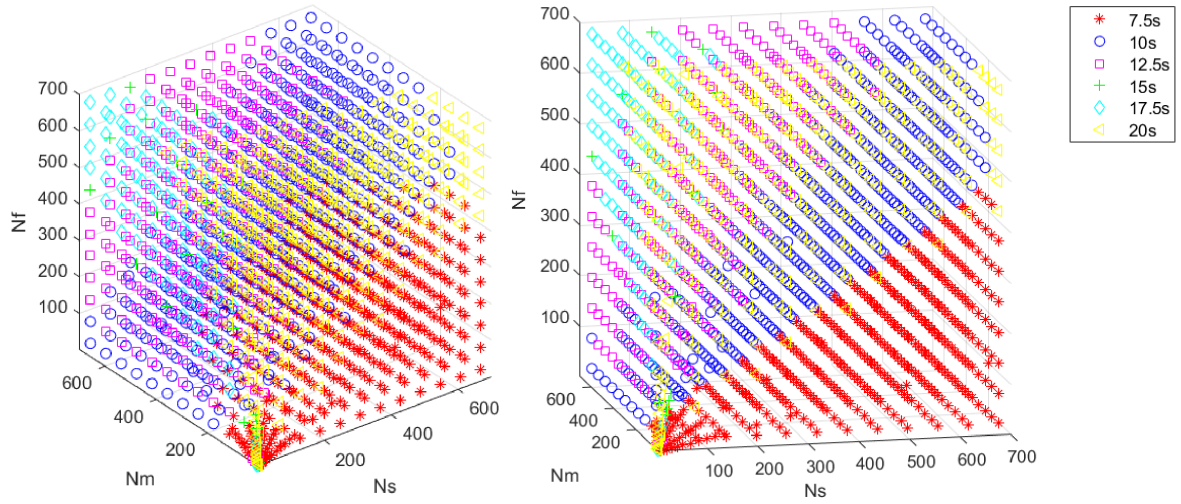

Figure 6.16: Estimated ideal *time_fast* for non-evaluated scenarios (two different perspectives).

[*t_mid*, *t_fast*]	$\jmath$	a$\jmath$	FI	Network throughput (B/h)
[7.5, 5]s	0.984	0.623	11.29	4.88×10^4
[10, 5]s	0.955	0.653	13.13	5.34×10^4
[10, 7.5]s	0.939	0.681	15.36	6.12×10^4
[12.5, 7.5]s	0.915	0.700	16.61	6.53×10^4
[12.5, 10]s	0.880	0.735	19.08	7.84×10^4
[15, 10]s	0.867	0.746	19.62	8.22×10^4
[15, 12.5]s	0.832	0.770	19.75	9.24×10^4
[17.5, 10]s	0.860	0.752	19.88	8.26×10^4
[17.5, 12.5]s	0.827	0.774	19.76	9.28×10^4
[17.5, 15]s	0.794	0.793	18.61	10.3×10^4
[20, 12.5]s	0.822	0.779	19.88	9.21×10^4
[20, 15]s	0.791	0.797	18.71	9.83×10^4
[20, 17.5]s	0.734	0.826	15.44	10.8×10^4
[22.5, 15]s	0.785	0.803	18.68	9.72×10^4
[22.5, 17.5]s	0.733	0.830	15.60	10.6×10^4
[22.5, 20]s	0.682	0.861	12.81	11.7×10^4

Table 6.3: Scenario 1 network performance.

come at the cost of losing fairness, mainly due to the value of the Jain's Fairness Index, since group 1 devices, which make up 40% of the network, would be able to transmit much less. Thus, in this scenario the model performs well when it comes to giving preference to fairness over capacity, while also ensuring a good value from the latest.

For the second scenario, it was a considered a network with 10 times the size - 250 end-nodes - disposed according to a distribution of [15%, 40%, 45%], which results in 38 nodes in group 1, 100 in group 2 and 112 in group 3. The predicted ideal combination is 17.5s for *mid-rate* and 12.5s for *fast-rate*, as highlighted in the results from Table 6.4.

[*t_mid*, *t_fast*]	$\jmath$	a$\jmath$	FI	Network throughput (B/h)
[7.5, 5]s	0.835	0.785	22.06	7.09×10^4
[10, 5]s	0.885	0.722	17.76	7.68×10^4
[10, 7.5]s	0.826	0.795	22.42	9.65×10^4
[12.5, 7.5]s	0.874	0.749	20.58	10.2×10^4
[12.5, 10]s	0.762	0.855	20.82	14.3×10^4
[15, 10]s	0.800	0.825	23.01	14.8×10^4
[15, 12.5]s	0.708	0.916	17.59	19.1×10^4
[17.5, 10]s	0.822	0.790	21.27	15.2×10^4
[17.5, 12.5]s	0.725	0.890	18.41	19.3×10^4
[17.5, 15]s	0.668	0.942	14.17	23.1×10^4
[20, 12.5]s	0.741	0.849	17.69	19.4×10^4
[20, 15]s	0.683	0.907	14.57	22.9×10^4
[20, 17.5]s	0.647	0.919	11.94	27.2×10^4
[22.5, 15]s	0.686	0.880	13.86	23.8×10^4
[22.5, 17.5]s	0.655	0.890	11.78	28.1×10^4
[22.5, 20]s	0.629	0.887	10.08	32.1×10^4

Table 6.4: Scenario 2 network performance.

Unlike in scenario 1, the pair of values calculated by the model for a network with these characteristics do not result in the maximum fairness possible, as there are 6 other combinations in which the FI is higher. It is however important to point out that, in this situation, there is still a good compromise between fairness and capacity, as there is no other combination in which the performance of both aspects is superior, and a higher throughput is only possible when using times that cause a substantial $\jmath$ decrease.

The network considered in the third scenario counts with a total of 500 end-nodes that follow a distribution of [35%, 35%, 30%] with 175 devices in groups 1 and 2, and the remaining 150 in group 3, a very alike situation to the one used to train the model: the same amount of devices but equitable distribution. In this previous scenario the ideal durations were $15s$ for *mid_rate* mode and $10s$ for the *fast_rate* mode.

[*t_mid*, *t_fast*]	$\jmath$	a$\jmath$	FI	Network throughput (B/h)
[7.5, 5]s	0.554	0.743	4.90	1.18×10^5
[10, 5]s	0.619	0.699	5.58	1.22×10^5
[10, 7.5]s	0.543	0.841	5.90	1.59×10^5
[12.5, 7.5]s	0.602	0.773	6.54	1.62×10^5
[12.5, 10]s	0.499	0.878	5.18	2.33×10^5
[15, 10]s	0.537	0.810	5.38	2.39×10^5
[15, 12.5]s	0.471	0.845	4.33	3.21×10^5
[17.5, 10]s	0.563	0.724	4.80	2.47×10^5
[17.5, 12.5]s	0.493	0.768	4.05	3.25×10^5
[17.5, 15]s	0.451	0.783	3.54	3.95×10^5
[20, 12.5]s	0.508	0.721	3.85	3.27×10^5
[20, 15]s	0.464	0.741	3.40	4.00×10^5
[20, 17.5]s	0.439	0.716	2.92	4.83×10^5
[22.5, 15]s	0.471	0.715	3.28	4.12×10^5
[22.5, 17.5]s	0.445	0.703	2.90	4.95×10^5
[22.5, 20]s	0.423	0.692	2.61	5.71×10^5

Table 6.5: Scenario 3 network performance.

Following, the model $[15, 10]s$ is also envisioned as the ideal combination. Despite the similar nodes' distribution with a previous scenario, the results in Table 6.5 show that this combination should not be selected since there are 3 other pairs of values that allow a higher FI. Nonetheless, although not ideal according to the initial standards, with $[15, 10]s$ a good compromise is attained once again in terms of capacity and fairness.

The results obtained from this validation show that, while it is possible to predict time combinations that take into account both the fairness and the throughput of the network, the used model fails to generalize to scenarios with higher network density, mostly justified by the scenarios used to feed the model.

6.5 Protocol Comparison

The final step in the evaluation process is to compare the performance of LoRa-MAP, LoRa-RTS and LoRaWAN. It was considered a much higher density of devices in the group that has the best connectivity to the gateway. Such a scenario tries to simulate a real urban deployment, considering that the gateway is located in an advantageous location and many

devices are capable of performing transmissions with RSSIs larger than -100dBm. A distribution of [20%, 30%, 50%] was chosen, with the total number of end-nodes ranging from 10 to 1000. The data packet size used was 100 bytes, and the simulation time was set to 10^9 slots. Only the probabilistic packet collision model was considered.

Regarding the LoRa-MAP curve, for each network size, the gateway allocates the ideal time for *fast-rate* and *mid-rate*, according to the procedure described in Section 6.4.2. When the network has 60 or less end-nodes, the ideal combination is $[22.5, 20]s$. For 75 end-nodes the ideal *fast-time* decreases to 17.5s, and with 100 devices the *mid-rate* decreases to 20s. With 125 nodes both ideal times decrease 2.5s, resulting in the $[17.5, 15]s$ combination. These values are used when the total number of devices is between 125 and 300. For more populated networks the selected combination is $[15, 12.5]s$.

Figure 6.17 compares the network capacity for the three MAC protocols, and Figure 6.18 presents a fairness analysis, presenting the values of $\jmath$ and $a\jmath$ (for LoRaWAN and RTS-LoRa there is no difference between the two since all transmissions are of equal ToA). For LoRa-MAP, it is also shown the network performance when using a single combination throughout all network sizes, for the 5 combinations that are deemed as ideal at least once, for a certain amount of end-nodes.

Regarding the network capacity, LoRa-MAP outperforms the remaining two protocols no matter the network size, even when using time combinations that do not highly favor the modes with higher bit-rate. Due to dealing with a shorter ToA, the devices are capable of delivering a much higher amount of packets, and separating the medium access phase into three groups diminishes the competition and allows for a more efficient use of the duty-cycle available to the technology.

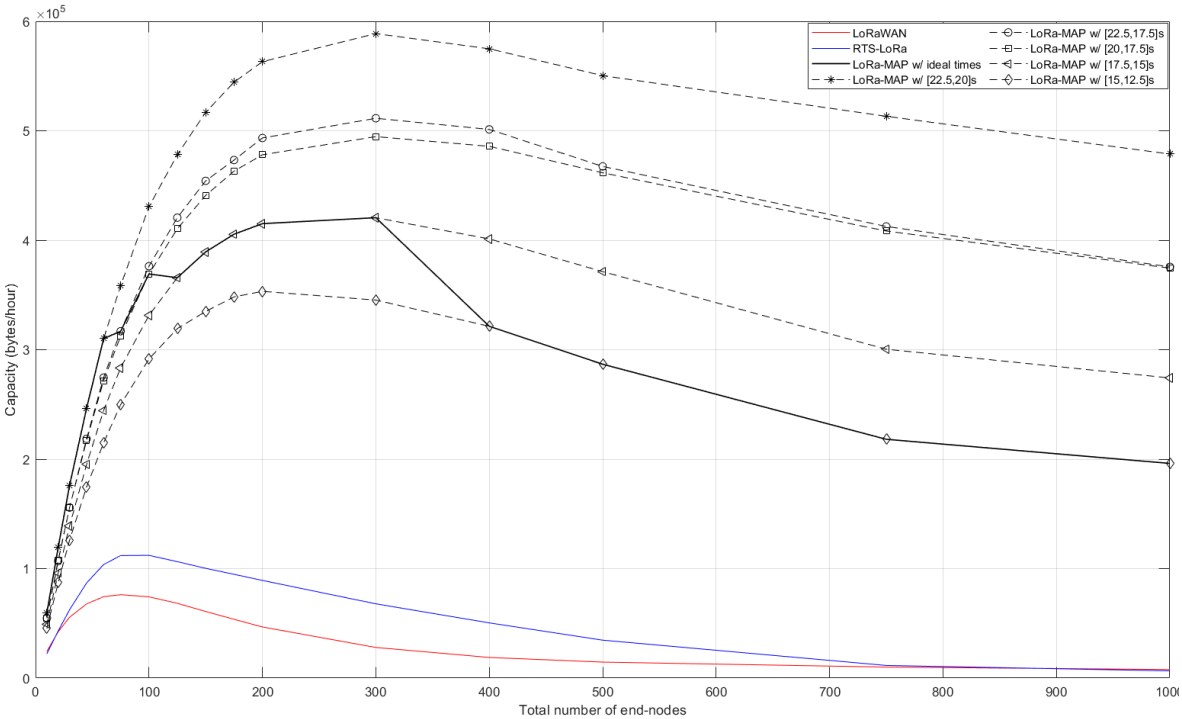

Figure 6.17: LoRa-MAP, RTS-LoRa and LoRaWAN: network capacity analysis.

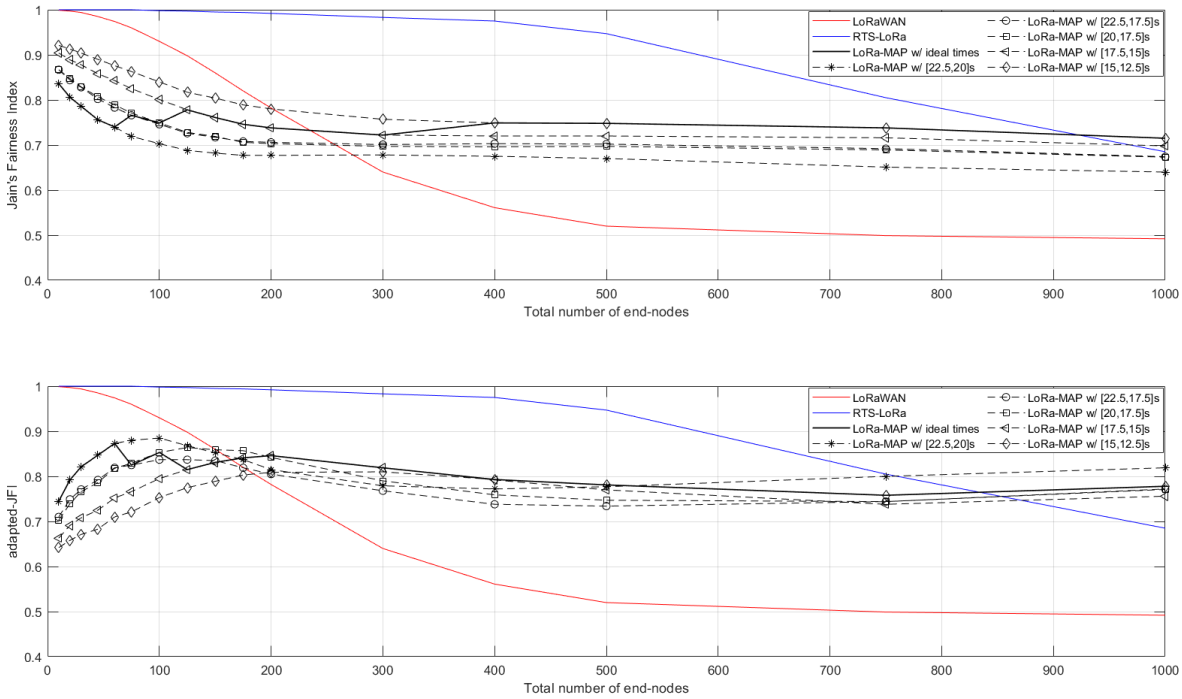

Figure 6.18: LoRa-MAP, RTS-LoRa, LoRaWAN: access fairness assessment.

Analysing the fairness results, RTS-LoRa has the edge on both metrics, as it allows for the more even distribution of access opportunities across the three protocols. However, these results can be misleading, giving the idea that using this protocol will immensely benefit the devices with worse signal strength. The lower fairness values obtained for LoRa-MAP are largely due to the discrepancy among the groups and not necessarily because of the nodes in group 1 having lower throughput. Table 6.6 presents the average throughput per node for group 1.

This analysis shows that RTS-LoRa generally allows the higher packet delivery in group 1 devices. Although LoRaWAN has the advantage for the 10 nodes scenario, as the scale increases the random access scheme causes the throughput value to drop rapidly. When using LoRa-MAP, the amount of packets delivered by group 1 nodes is lower than with RTS-LoRa in most occasions, but as the number of nodes grows, the gap between the two starts to shrink and LoRa-MAP takes the lead around the 500 nodes.

Protocol \ Network size	10	20	30	45	60	75	100	125
LoRaWAN	2345 b/h	1971 b/h	1651 b/h	1232 b/h	948 b/h	726 b/h	468 b/h	302 b/h
RTS-LoRa	2220 b/h	2154 b/h	2078 b/h	1915 b/h	1708 b/h	1444 b/h	1066 b/h	786 b/h
LoRa-MAP	1733 b/h	1413 b/h	1192 b/h	895 b/h	648 b/h	567 b/h	454 b/h	428 b/h
Protocol \ Network size	150	175	200	300	400	500	750	1000
LoRaWAN	190 b/h	125 b/h	79 b/h	13 b/h	3 b/h	1 b/h	$\approx$ 0b/h	$\approx$ 0b/h
RTS-LoRa	609 b/h	494 b/h	403 b/h	192 b/h	104 b/h	51 b/h	8 b/h	2 b/h
LoRa-MAP	322 b/h	257 b/h	209 b/h	94 b/h	70 b/h	45 b/h	18 b/h	11 b/h

Table 6.6: Average throughput per node in group 1.

In RTS-LoRa, nodes from group 1 should be able to have the same channel allocation as the remaining nodes for the network to be considered fair, since all nodes operate under the same access conditions. However, for LoRa-MAP, one can argue that there is no problem in communicating less, since they waste more channel access time. The decrease in the throughput of group 1 - when using LoRa-MAP instead of RTS-LoRa - is justified by the very high increase in the average throughput of nodes from group 2 and 3, represented in Tables 6.7 and 6.8, respectively.

Protocol \ Network size	10	20	30	45	60	75	100	125
LoRaWAN	2409 b/h	2052 b/h	1771 b/h	1402 b/h	1110 b/h	880 b/h	596 b/h	414 b/h
RTS-LoRa	2217 b/h	2159 b/h	2084 b/h	1931 b/h	1719 b/h	1487 b/h	1094 b/h	831 b/h
LoRa-MAP	4750 b/h	4459 b/h	4187 b/h	3676 b/h	3316 b/h	3089 b/h	2500 b/h	2218 b/h
Protocol \ Network size	150	175	200	300	400	500	750	1000
LoRaWAN	284 b/h	194 b/h	134 b/h	31 b/h	8 b/h	2 b/h	1 b/h	$\approx$ 0b/h
RTS-LoRa	648 b/h	514 b/h	422 b/h	207 b/h	112 b/h	57 b/h	9 b/h	3 b/h
LoRa-MAP	1872 b/h	1591 b/h	1386 b/h	914 b/h	589 b/h	423 b/h	21 b/h	13 b/h

Table 6.7: Average throughput per node in group 2.

Protocol \ Network size	10	20	30	45	60	75	100	125
LoRaWAN	2484 b/h	2224 b/h	1985 b/h	1684 b/h	1434 b/h	1218 b/h	940 b/h	727 b/h
RTS-LoRa	2219 b/h	2160 b/h	2081 b/h	1936 b/h	1743 b/h	1515 b/h	1160 b/h	889 b/h
LoRa-MAP	8402 b/h	8748 b/h	8714 b/h	8498 b/h	8089 b/h	6415 b/h	5701 b/h	4367 b/h
Protocol \ Network size	150	175	200	300	400	500	750	1000
LoRaWAN	565 b/h	449 b/h	355 b/h	163 b/h	89 b/h	57 b/h	27 b/h	16 b/h
RTS-LoRa	705 b/h	578 b/h	478 b/h	252 b/h	144 b/h	84 b/h	22 b/h	10 b/h
LoRa-MAP	3940 b/h	3587 b/h	3236 b/h	2218 b/h	1226 b/h	875 b/h	448 b/h	311 b/h

Table 6.8: Average throughput per node in group 3.

As expected, with LoRa-MAP, devices from groups 2 and 3 are capable of a much higher throughput than the one RTS-LoRa allows, since nodes in good conditions are not forced to use unnecessarily slow transmissions. Sacrificing group 1 is the price to pay in order to make the network more scalable and viable in scenarios with a few hundreds of end-nodes. It is also important to note that, while it limits the access opportunities of group 1, this medium access scheme also ensures that a great deal of time per cycle is reserved solely for these end-nodes to transmit, meaning that as the network grows, nodes in the worst conditions benefit more from LoRa-MAP than from RTS-LoRa (*i.e* with 750 and 1000, the throughput from group 1 is superior for LoRa-MAP).

Finally, another aspect of LoRa-MAP is that it allows flexibility in optimizing the network performance. For the evaluation carried out in this chapter, preference was given to the channel access fairness giving equal importance to the balance between throughput equality ($\jmath$) and channel occupation time equality ($a\jmath$). Nevertheless, a different method of deciding the combination of [*mid-time*,*fast-time*] durations can be used depending on the application and desired outcome.

6.6 Chapter Considerations

This chapter presented the evaluation in terms of medium access and network capacity, of the three MAC protocols discussed throughout this dissertation. Also, the probabilistic packet collision model was tested and compared to common assumptions widely used in the literature.

First, it was modeled the performance of single-channel LoRaWANs using different packet sizes, end-node distributions and considering different packet collision models. It was concluded that the purely destructive model grossly underestimates the network capacity, and the -6dB model, while closer to reality, is still very pessimistic.

Then, for the same scenarios used, an evaluation was conducted on RTS-LoRa in order to study the impact of including an uplink control packet in the channel access. A general improvement was verified in terms of capacity and access fairness, specially for large scale networks and when using bigger data packets.

Afterwards, it was displayed an extensive analysis on the performance of LoRa-MAP, evaluating the outcome of distributing the channel allocation time in different proportions among the three operation modes. A method for estimating the ideal time combination was proposed, reaching a compromise between the capacity and access fairness. Using this estimation technique, it was shown that, even privileging fairness, LoRa-MAP is still capable of achieving massive capacity and scalability in comparison to the other two protocols.

The results have shown that LoRa-MAP is a great MAC candidate for IoT networks with a massive amount of devices, while also not falling short in smaller scale situations.

Chapter 7

Conclusions and Future Work

The main goal of this dissertation consisted on studying the performance of LoRa, one of the most prominent LPWAN technologies, to be used as the solution for information exchange in networks with a massive amount of devices, as the IoT paradigm envisions. The developed work can be broadly divided into the characterization of LoRa's non-destructive property, and the proposal and evaluation of different MAC protocols.

The characterization of the non-destructive property - carried out in a controlled environment - focused in the gray area of 6-dB margin where frequently it is affirmed that a minimum gap of 6dB is required for the successful reception of one transmission over interference. Through real experimentation, the likelihood of decoding one out of two or three concurrent LoRa transmissions was associated with different levels of SIR, and the results obtained allowed the achievement of a probabilistic model capable of estimating the probability of packet reception in the event of concurrent interference. Employing this model has shown the non-destructive property to be very relevant in the subject of medium access, especially for densely populated scenarios, as it deeply affects the network performance when data collisions are frequent.

Insights on how LoRa's capture effect behaves allowed to verify that, generally, the capacity of LoRaWANs is highly underestimated, by considering purely destructive collisions or a -6dB threshold model. However, while it is verified an increase in capacity, another problem arose when acknowledging the capture effect, regarding channel access fairness. An analysis on the drawbacks of using an ALOHA-based scheme like LoRaWAN has led to the proposal of two reservation-based MAC protocols:

RTS-LoRa, a simple improvement to LoRaWAN, has shown that the addition of a control packet without any other major changes to the scheme used can greatly reduce the occurrence of collisions, benefiting the network primarily in terms of access fairness.

LoRa-MAP, a protocol designed to make a good use of the strengths of the technology while dealing in the best way possible with its weaknesses, resorting to adapt the physical layer parameters as necessary in order to provide the most adequate connection between gateway and end-node.

Regarding LoRa-MAP, using a system in which the gateway switches between three operation modes - instead of restricting itself to one that allows long range - grants: i) faster data transmissions and duty-cycle restricted periods; ii) less energy drain per transmission,

as faster modes consume less battery; iii) network fragmentation into groups, reducing access competition and consequently decreasing packet collisions.

With this work, it is possible to conclude that a dynamic approach to Medium Access Control is ideal to get the most out of large-scale LoRa networks. By not adapting the physical layer parameters according to each connection, devices in good transmisson conditions are highly harmed, considering the throughput they could otherwise achieve. Having into account the short time periods in which LoRa devices are allowed to operate, it is beneficial to shorten the duration of data transmissions, enabling more devices to use the channel. LoRa-MAP remains a viable solution even as the network scale reaches a thousand end-devices. It is arguable whether or not this solution is indicated for networks with fewer devices (around a few dozen), since the additional network overhead and overall protocol complexity do not grant a performance improvement as rewarding, even if higher network capacity is achieved.

Several aspects of the work developed could be either improved or further advanced. This way, some suggestions for future work are presented:

Probabilistic model extension Improve the probabilistic collision model by extending the characterization, performing the same tests for different packet sizes and with asynchronous transmissions;

LoRa-MAP scalability Study the proposed MAC protocol scalability by implementing LoRa-MAP in a large number of devices and performing tests over real environments;

LoRa-MAP mathematical model Develop a mathematical model that characterizes the capacity of a LoRa-MAP network based on the time allocated for each of the operation modes, and compare it with the behaviour verified in the simulations. A good starting point would be perceiving how the characteristics of the network affect the amount of time spent in *standard* mode, since so far it is only possible to predict the minimum time period in which that mode is used per cycle, but not its entirety. This aspect, while addressed in this dissertation, was not explored;

LoRa-MAP predictive model Improve the time allocation predictive model with results obtained from testing in real environments rather than solely recurring to simulations. The decision process should also be extended to consider aspects such as different packet sizes and frequency of medium access attempts. The ultimate goal is to have the gateway continuously optimizing the time allocation based on previous experiments, instead of focusing on deterministic values from generic tests;

Energy consumption tests Perform energy consumption tests with the different MAC protocols to verify the viability in making each solution available for battery-driven devices;

Multi-gateway adaptation Adapt LoRa-MAP to work in scenarios with multiple gateways to provide an even wider coverage. Having multiple gateways connected to a common network server allows them to communicate seamlessly without dealing with duty-cycle restrictions. This enables constant information sharing regarding the network characteristics, that can be used to decide, for example, the ideal gateway for each end-node to communicate with, or the current configuration of each gateway (*i.e.* having different access points receiving packets in distinct operation modes, instead of a cyclic process in a single gateway). Such a system is expected to greatly improve the scalability aspect of the protocol.

Bibliography

[1] International Telecommunication Union. "ITU Internet Report 2005: The Internet of Things". `https://www.itu.int/net/wsis/tunis/newsroom/stats/The-Internet-of-Things-2005.pdf`, 2005.

[2] `https://www.i-scoop.eu/internet-of-things-guide/`. Accessed: 07-08-2019.

[3] R. Fernandes, R. Oliveira, M. Luís, and S. Sargento. On the Real Capacity of LoRa Networks: the Impact of Non-destructive Communications. *IEEE Communications Letters*, Early Access, 2019.

[4] W. Ayoub, A. E. Samhat, F. Nouvel, M. Mroue, and J. Prvotet. "Internet of Mobile Things: Overview of LoRaWAN, DASH7, and NB-IoT in LPWANs standards and Supported Mobility". *IEEE Communications Surveys Tutorials*, 21(2):1561–1581, Oct. 2018.

[5] J. Bardyn, T. Melly, O. Seller, and N. Sornin. "IoT: The era of LPWAN is starting now". In *ESSCIRC Conference 2016: 42nd European Solid-State Circuits Conference*, pages 25–30, Sep. 2016.

[6] A. Boulogeorgos, P. Diamantoulakis, and G. Karagiannidis. Low Power Wide Area Networks (LPWANs) for Internet of Things (IoT) Applications: Research Challenges and Future Trends. *CoRR*, abs/1611.07449, 2016.

[7] L. Vangelista, A. Zanella, and M. Zorzi. "Long-range IoT technologies: The dawn of LoRa". In *Future Access Enablers of Ubiquitous and Intelligent Infrastructures*, pages 51–58. Springer, Sep. 2015.

[8] D. Ismail, M. Rahman, and A. Saifullah. "Low-power Wide-area Networks: Opportunities, Challenges, and Directions". In *Proceedings of the Workshop Program of the 19th International Conference on Distributed Computing and Networking*, Workshops ICDCN '18, pages 1–6. ACM, Jan. 2018.

[9] M. Andersson. "Short range low power wireless devices and Internet of Things (IoT)". In *Wireless Congress*, 2013.

[10] `https://www.helpnetsecurity.com/2019/05/23/connected-devices-growth/`. Accessed: 17-08-2019.

[11] `https://www.ericsson.com/en/mobility-report/internet-of-things-forecast`. Accessed: 15-08-2019.

[12] https://www.zdnet.com/article/iot-to-drive-growth-in-connected-devices-through-2022-cisco. Accessed: 17-08-2019.

[13] J. Petajajarvi, K. Mikhaylov, A. Roivainen, T. Hanninen, and M. Pettissalo. "On the coverage of LPWANs: range evaluation and channel attenuation model for LoRa technology". In *2015 14th International Conference on ITS Telecommunications (ITST)*, pages 55–59, Dec 2015.

[14] R. Sharan Sinha, Y.Wei, and S. Hwang. "A survey on LPWA technology: LoRa and NB-IoT". *ICT Express*, 3(1):14–21, Mar 2017.

[15] A. Saifullah, M. Rahman, D. Ismail, Dali, C. Lu, J. Liu, and R. Chandra. "Enabling Reliable, Asynchronous, and Bidirectional Communication in Sensor Networks over White Spaces". pages 1–14. SenSys, ACM, Nov. 2017.

[16] R. Ratasuk, N. Mangalvedhe, Y. Zhang, M. Robert, and J. Koskinen. "Overview of Narrowband IoT in LTE Rel-13". In *Standards for Communications and Networking(CSCN), 2016 IEEE International Conference on*. IEEE, Nov. 2016.

[17] K. Mekki, E. Bajic, F. Chaxel, and F. Meyer. "A comparative study of LPWAN technologies for large-scale IoT deployment". *ICT Express*, 5:1–7, Mar. 2019.

[18] Nokia. "White paper: Optimizing LTE for the Internet of Things". `https://novotech.com/docs/default-source/default-document-library/lte-m-optimizing-lte-for-the-internet-of-things.pdf?sfvrsn=0`, May. 2015. Accessed: 24-04-2019.

[19] H. Mroue, A. Nasser, S. Hamrioui, B. Parrein, E. Motta-Cruz, and G. Rouyer. "MAC layer-based evaluation of IoT technologies: LoRa, SigFox and NB-IoT". In *Middle East and North Africa Communications Conference (MENACOMM), IEEE*, pages 1–5. IEEE, 2018.

[20] SigFox. "White paper: SIGFOX: M2M and IoT redefined through cost effective and energy optimized connectivity". `https://lafibre.info/images/3g/201302_sigfox_whitepaper.pdf`. Accessed: 2018-11-25.

[21] Weightless Special Interest Group. `http://www.weightless.org/about/what-is-weightless`. Accessed: 2018-11-25.

[22] R. Sanchez-Iborra and M. Cano. "State of the art in LP-WAN solutions for industrial IoT services". *Sensors*, 16(5):708, 2016.

[23] T. Myers, D. Werner, K. Sinsuan, J. Wilson, S. Reuland, and P. Singlerand M. Huovila. "Light monitoring system using a random phase multiple access system", July 2 2013. US Patent 8,477,830.

[24] Ingenu. `https://www.ingenu.com/`. Accessed: 2018-01-26.

[25] DASH7. `http://www.dash7-alliance.org`. Accessed: 2018-11-25.

[26] A. Saifullah, M. Rahman, D. Ismail, C. Lu, R. Chandra, and J. Liu. "SNOW: Sensor network over white spaces". In *Proceedings of the 14th ACM Conference on Embedded Network Sensor Systems*, pages 272–285. ACM, 2016.

[27] Telensa. https://www.telensa.com/. Accessed: 2018-11-25.

[28] LoRa Alliance. https://www.lora-alliance.org/. Accessed: 22-04-2019.

[29] SemTech. https://www.semtech.com/uploads/documents/sx1272.pdf. Accessed: 2018-11-25.

[30] M. Bor, J. Vidler, and U. Roedig. "LoRa for the Internet of Things.". *International Conference on Embedded Wireless Systems and Networks*, pages 361–366, Fev. 2016.

[31] SemTech. "Application Note: AN1200.22 - LoRa Modulation Basics". https://www.semtech.com/uploads/documents/an1200.22.pdf. Accessed: 2018-11-25.

[32] M. Bor, U. Roedig, T. Voigt, and J. Alonso. Do LoRa Low-Power Wide-Area Networks Scale? In *Proceedings of the 19th ACM International Conference on Modeling, Analysis and Simulation of Wireless and Mobile Systems*, MSWiM '16, pages 59–67, 2016.

[33] U. Noreen, A. Bounceur, and L. Clavier. "A study of LoRa low power and wide area network technology". In *Advanced Technologies for Signal and Image Processing (ATSIP), 2017 International Conference on*, pages 1–6. IEEE, 2017.

[34] A. Augustin, J. Yi, T. Clausen, and W. Townsley. "A study of LoRa: Long range & low power networks for the internet of things". *Sensors*, 16(9):1466, 2016.

[35] LoRa Alliance. White paper: LoRaWAN: What is it? A technical overview of LoRa and LoRaWAN, 2018. Accessed: 2018-11-25.

[36] P.Cheong, J. Bergs, C. Hawinkel, and J. Famaey. "Comparison of LoRaWAN classes and their power consumption". In *Symposium on Communications and Vehicular Technology (SCVT), 2017 IEEE*, pages 1–6. IEEE, 2017.

[37] F. Adelantado, X. Vilajosana, P. Tuset-Peiro, B. Martinez, J. Melia-Segui, and T. Watteyne. "Understanding the Limits of LoRaWAN". *IEEE Communications Magazine*, 55(9):34–40, Sep. 2017.

[38] R. Oliveira, L. Guardalben, M. Luís, and S. Sargento. "Long range communications in urban and rural environments". *IEEE Symposium on Computers and Communications*, pages 810–817, Jul. 2017.

[39] M. Andrei, L. Radoi, and D. Tudose. "Measurement of node mobility for the LoRa protocol". In *Networking in Education and Research (RoEduNet), 2017 16th International Conference on*, Sep. 2017.

[40] R. Sanchez-Iborra, J. Sanchez-Gomez, J. Ballesta-Viñas, M. Cano, and A. Skarmeta. "Performance Evaluation of LoRa Considering Scenario Conditions". *Sensors*, 18(3):772, Mar. 2018.

[41] O. Georgiou and U. Raza. Low Power Wide Area Network Analysis: Can LoRa Scale? *IEEE Wireless Communications Letters*, 6(2):162–165, Apr. 2017.

[42] F. Van Den Abeele, J. Haxhibeqiri, I. Moerman, and J. Hoebeke. "Scalability Analysis of Large-Scale LoRaWAN Networks in ns-3". *IEEE Internet of Things Journal*, pages 2186–2198, Dec 2017.

[43] T. Elshabrawy and J. Robert. "Analysis of BER and Coverage Performance of LoRa Modulation under Same Spreading Factor Interference". In *IEEE 29th Annual International Symposium on Personal, Indoor and Mobile Radio Communications (PIMRC)*, pages 1–6, Sep. 2018.

[44] O. Afisiadis, M.Cotting, A. Burg, and A. Balatsoukas-Stimming. "On the Error Rate of the LoRa Modulation with Interference". *arXiv e-prints*, page arXiv:1905.11252, May 2019.

[45] J. Haxhibeqiri, F. Van den Abeele, I. Moerman, and J. Hoebeke. "LoRa scalability: a simulation model based on interference measurements". *SENSORS*, 17(6):1193:1–1193:25, 2017.

[46] K. Chan, L. Yeung, and W. Shao. "Contention-based MAC protocols with erasure coding for wireless data networks". *Ad Hoc Networks*, 3(4):495–506, Jul.

[47] G. Hassan and H. Hassanein. "MoT: A Deterministic Latency MAC Protocol for Mission-Critical IoT Applications.". *International Wireless Communications Mobile Computing Conference (IWCMC)*, 14(2):588–593, 2018.

[48] G. Hassan, M. Elmaradny, M. Ibrahim, A. Rashwan, and H. Hassanein. "Energy Efficiency Analysis of Centralized-Synchronous LoRa-based MAC Protocols". *International Wireless Communications Mobile Computing Conference (IWCMC)*, 14:999–1004, 2018.

[49] R. Oliveira, L. Guardalben, M. Luís, and S. Sargento. "Multi-Technology Data Collection: Short and Long Range Communications". In *Vehicular Technology Conference (VTC-Fall), 2017 IEEE 86th*, pages 1–6, Sep. 2017.

[50] T. Deng, J. Zhu, and Z. Nie. "An Improved LoRaWAN protocol based on adaptive duty cycle". *IEEE Information Technology and Mechatronics Engineering Conference*, (3), Jan. 2017.

[51] M. Bor and U. Roedig. "LoRa Transmission Parameter Selection". In *2017 13th International Conference on Distributed Computing in Sensor Systems (DCOSS)*, pages 27–34, June 2017.

[52] M. Slabicki, G. Premsankar, and M. Francesco. "Adaptive Configuration of LoRa Networks for Dense IoT Deployments". *NOMS 2018 - 2018 IEEE/IFIP Network Operations and Management Symposium*, pages 1–9, 2018.

[53] B. Reynders, Q. Wang, P. Tuset-Peiro, X. Vilajosana, and S. Pollin. "Improving Reliability and Scalability of LoRaWANs Through Lightweight Scheduling". *IEEE Internet of Things Journal*, 5(3):1830–1842, Jun 2018.

[54] B. Sartori, S. Thielemans, M. Bezunartea, A. Braeken, and K. Steenhaut. "Enabling RPL multihop communications based on LoRa". In *2017 IEEE 13th International Conference on Wireless and Mobile Computing, Networking and Communications (WiMob)*, pages 1–8, Oct. 2017.

[55] O. Iova, P. Picco, T. Istomin, and C. Kiraly. "RPL: The Routing Standard for the Internet of Things... Or Is It?". *IEEE Communications Magazine*, 54(12):16–22, Dec. 2016.

[56] J. Lee and W. Jeong. "A Scheduling Algorithm for Improving Scalability of LoRaWAN". *Information and Communication Technology Convergence (ICTC)*, pages 1383–1388, 2018.

[57] T. Polonelli, D. Brunelli, A. Marzocchi, and L. Benini. "Slotted ALOHA on LoRaWAN-Design, Analysis, and Deployment". *Sensors*, 19(4):838, Feb. 2019.

[58] D. Croce, M. Gucciardo, S. Mangione, G. Santaromita, and I. Tinnirello. "Impact of LoRa Imperfect Orthogonality: Analysis of Link-Level Performance". *IEEE Communications Letters*, 22(4):796–799, Apr. 2018.

[59] D. Croce, M. Gucciardo, I. Tinnirello, D. Garlisi, and S. Mangione. "Impact of Spreading Factor Imperfect Orthogonality in LoRa Communications". In *International Tyrrhenian Workshop on Digital Communication*, pages 165–179. Springer, Sep. 2017.

[60] Libelium. `http://www.libelium.com/development/waspmote/documentation/waspmote-lora-868mhz-915mhz-sx1272-networking-guide/`. Accessed: 22-04-2019.

[61] Raspberry Pi Foundation. `https://www.raspberrypi.org/products/raspberry-pi-3-model-b-plus/`. Accessed: 05-08-2019.

[62] T. Petrić, M. Goessens, L. Nuaymi, L. Toutain, and A. Pelov. "Measurements, performance and analysis of LoRa FABIAN, a real-world implementation of LPWAN". *IEEE International Symposium on Personal, Indoor and Mobile Radio Communications, PIMRC*, Sep. 2016.

[63] C. Goursaud and J. Gorce. "Dedicated networks for IoT: PHY / MAC state of the art and challenges". *EAI Endorsed Transactions on Internet of Things*, 15(1), Oct. 2015.

[64] A. Rahmadhani and F. Kuipers. "When LoRaWAN Frames Collide". In *12th International Workshop on Wireless Network Testbeds, Experimental Evaluation Characterization (WiNTECH18)*, pages 89–97, Oct. 2018.

[65] LoRa Alliance. "LoRaWAN Specification V1.0". `https://www.rs-online.com/designspark/rel-assets/ds-assets/uploads/knowledge-items/application-notes-for-the-internet-of-things/`. Accessed: 20-04-2019.

[66] R. Jain, D. Chiu, and W. Hawe. "A quantitative measure of fairness and discrimination". *Eastern Research Laboratory, Digital Equipment Corporation, Hudson, MA*, Jan. 1998.

[67] A. Jayasuriya, S. Perreau, A. Dadej, and S. Gordon. "Hidden vs . Exposed Terminal Problem in Ad hoc Networks". *Proceedings of the Australian Telecommunication Networks and Applications Conference*, Jan. 2004.

[68] C. Pham. "QoS for Long-range wireless sensors under duty-cycle regulations with shared activity time usage". *ACM Transactions on Sensor Networks*, 12(4):1–31, 2016.

[69] S. Li, U. Raza, and A. Khan. "How Agile is the Adaptive Data Rate Mechanism of LoRaWAN?". *2018 IEEE Global Communications Conference, GLOBECOM 2018 - Proceedings*, Dec. 2018.